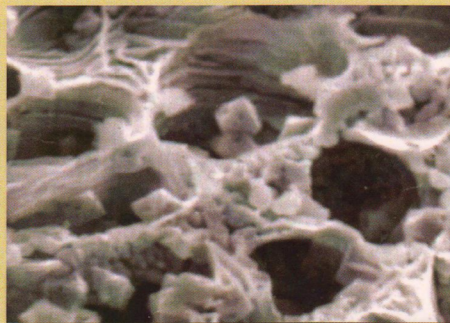
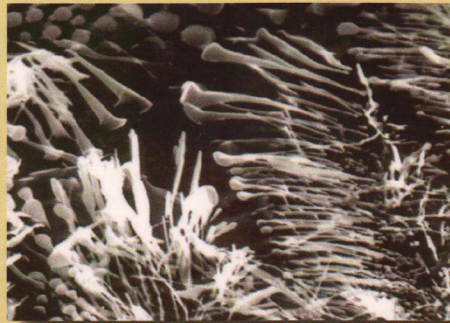
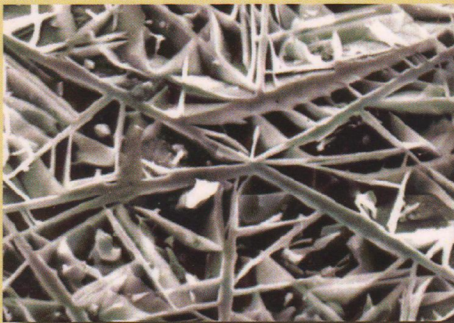




# Theoretical fundamentals and technologies of deposition of wear resistant eutectic coatings

*edited by*  
*Paszeczko Mychajło*  
*Myroslav Kindrachuk*



MONOGRAPHIE

# Theoretical fundamentals and technologies of deposition of wear resistant eutectic coatings

# Monografie – Politechnika Lubelska



Politechnika Lubelska  
Wydział Podstaw Techniki  
ul. Nadbystrzycka 38  
20-618 LUBLIN

# Theoretical fundamentals and technologies of deposition of wear resistant eutectic coatings

edited by  
Paszeczko Mychajło  
Myroslav Kindrachuk



Lublin University of Technology  
Lublin 2017

Reviewer:

prof. dr hab. inż. Antoni Świć, Lublin University of Technology

Authors:

Myroslav Kindrachuk

Mykhaylo Pashechko

Klaudiusz Lenik

Valentyn Panarin

Marcin Barszcz

Oleksandr Tisov

Anatolii Kornienko

Oleksandr Dukhota

Edition and DTP: Marcin Barszcz

Publication approved by the Rector of Lublin University of Technology

© Copyright by Lublin University of Technology 2017

ISBN: 978-83-7947-292-5

Publisher: Lublin University of Technology  
ul. Nadbystrzycka 38D, 20-618 Lublin, Poland

Realization: Lublin University of Technology Library  
ul. Nadbystrzycka 36A, 20-618 Lublin, Poland  
tel. (81) 538-46-59, email: wydawca@pollub.pl  
[www.biblioteka.pollub.pl](http://www.biblioteka.pollub.pl)

Printed by: TOP Agencja Reklamowa Agnieszka Łuczak  
[www.agencjatorp.pl](http://www.agencjatorp.pl)

---

The digital version is available at the Digital Library of Lublin University of Technology: [www.bc.pollub.pl](http://www.bc.pollub.pl)  
Circulation: 100 copies

## **CONTENTS**

INTRODUCTION.....	7
1. BACKGROUND, STRUCTURE AND PROPERTIES OF CAST EUTECTIC METAL ALLOYS WITH interstitial phases.....	9
1.1. The basic scientific idea of the work.....	9
1.2. The scientific approach of the proposed work.....	9
1.3. Phase equilibrium in systems ‘transition metal – interstitial phase’....	12
1.4. Structure of cast eutectic alloys .....	17
1.5. Properties of cast eutectic metal alloys with the interstitial phases ..	20
Conclusions on section #1 .....	23
2. METASTABLE EUTECTIC iron BASED COATINGS WITH REFRACTORY INTERSTITIAL PHASES.....	24
2.1. Objectives to investigate non-equilibrium states of eutectics .....	24
2.2. Impact of cooling rate on the crystallization mechanism of eutectics....	28
2.3. The growth of rapidly cooled eutectics .....	31
2.4. Annealing of eutectic coatings.....	35
2.5. Eutectic coating with composite structure.....	41
Conclusions on section #2.....	46
3. DEVELOPMENT OF INDUSTRIAL TECHNOLOGIES OF EUTECTIC COATINGS DEPOSITION.....	47
3.1. Formation of structure and tribological properties of eutectic coatings.....	47
3.1.1. Coatings deposited with use of concentrated energy aflows....	47
3.1.1.1. Methods of cladding .....	47
3.1.1.3. Plasma cladding.....	55
3.1.1.5. Treatment of plasma coatings by laser remelting and thermosycling .....	59
3.1.1.6. Wear resistance of laser treated plasma coatings ....	61
3.1.1.7. Bilayer coatings .....	64
3.1.1.8. Tribological properties of bilayer coatings .....	66
3.1.1.9. Cavitation resistance of eutectic coatings .....	68
3.2. Technological deposition processes and industrial testing of eutectic coatings.....	71
3.3. Performance and economic output of developed materials and coatings.....	79
Conclusions on section #3 .....	81

4. POWDER EUTECTIC MATERIALS OF FE-MN-C-B SYSTEM FOR COATINGS OF INCREASED ABRASIVE WEAR.....	82
4.1. Materials and methods .....	82
4.2. Examination and analysis of $\text{Fe}_3\text{C}$ – $\text{Fe}_3\text{B}$ –‘ $\text{Fe}_3\text{Mn}$ ’ quasi-ternary intersection .....	90
4.3. Examination and analysis of ‘ $\text{Fe}_2\text{C}$ ’– $\text{Fe}_2\text{B}$ –‘ $\text{Fe}_2\text{Mn}$ ’ quasi-ternary intersection .....	92
4.4. Examination and analysis of $\text{Fe}_3\text{C}$ - $\text{Fe}_3\text{B}$ -‘ $\text{Fe}_{1.2}\text{Mn}$ ’ quasi-ternary intersection .....	95
4.5. Examination and analysis of ‘ $\text{Fe}_{23}\text{C}_6$ ’–‘ $\text{Fe}_{23}\text{B}_6$ ’–‘ $\text{Fe}_{23}\text{Mn}_6$ ’ quasi-ternary intersection .....	97
Conclusions on section #4 .....	101
References .....	103

# INTRODUCTION

Ukraine is one of the countries in the world having complete aircraft manufacturing industry, spacecraft designing, manufacturing and maintenance organizations. It also supplies its equipment, aerospace engineering products to its consumers to Europe, America, Asia, and Africa. These enterprises also provide a service and repair of their products. Ukraine also has its own minerals, oil and gas industries, which include explorations, mining and extraction, refining and transportation. A very important part of national economy is devoted to power generation, manufacturing of nuclear, gas and oil power equipment. Successful functioning and development of these crucial industries requires a strong scientific background. First of all it requires institutions capable to design and produce heavy manufacturing equipment, to upgrade, recover or modify existing production capacities.

New facilities and engineering products should possess a set of continuously rising properties: reliability, serviceability, service live etc. At the same time, beared loads also increase. So, this requires design and development of new materials, which will meet growing requirements. The future materials should be stronger, more stable, and more efficient compared to now existing ones. "Just materials" of the past now became a masterpiece of engineering thought. The variety of available materials is just amazing! The capabilities of materials engineering nowadays allow designing a material for a particular application, to predict its mechanical and chemical behavior.

Aerospace industry is reasonably considered to be one of the main consumers of novel materials. Those metals and alloys which were the best one or two decades ago now can not be used (as like many steels, early super alloys and composites). Especially this is an issue for aerospace jet engines manufacturers. Rising requirements to noise, CO and NO<sub>x</sub> emissions, fuel efficiency force them to increase the fuel combustion temperature, what imposes additional stresses to engine elements. New materials should combine strength, heat resistance, wear resistance. The metal temperature often exceeds 1000 °C, while working ambient temperature may reach 1500 °C. A particular problem is high temperature wear resistance of materials. More then 70% of all rejected engine parts have impermissible level of wear damages.

In this work we propose a new view to natural composite materials – multicomponent eutectic alloys, which may be used for broad variety of applications – manufacturing and recovery of turbine blades, stator vanes, metallurgical furnaces, quick closing equipment, cutting tools etc. Among them are 12Cr18Ni9Ti-TiB<sub>2</sub> (TiNi alloys), 12Cr18Ni9Ti-TiB<sub>2</sub>-CrB<sub>2</sub> (CrTiNi) and 12Cr18Ni9Ti-TiB<sub>2</sub>-BC (VTiNi). The metal matrix of alloys has chemical composition of austenitic steel 12Cr18Ni9Ti, which contains strengthening

borides and/or carbides. These wear resistant materials may be used for manufacturing or modification of heavy duty components, so significant part of current work is devoted to overview and development of efficient coating deposition technologies – plasma and gas spray, laser alloying and surface engineering. We also evaluate the effects of deposition processes parameters on microstructures, mechanical properties and wear resistance of coatings being investigated.

The monograph deals with:

- Theoretical fundamentals of production of eutectic alloys with hard interstitial phases, which have high performance and may be used for high temperature applications;
- Development of industrial technologies of eutectic coatings deposition, including iron-based materials with refractory interstitial phases;
- Development of directionally solidifying eutectic alloys strengthened by borides – a new generation of hard high temperature composite materials of multifunctional purpose;
- Post treatment of eutectic coatings by laser and evaluation of its effect on microstructure and wear properties;
- Examples of industrial realization of proposed eutectic alloys, coatings testing results.

The monograph may be used by scientific and engineering staff in the field of metallurgy, engineering technology, gas turbine engines and power equipment manufacturing and maintenance.

# **1. BACKGROUND, STRUCTURE AND PROPERTIES OF CAST EUTECTIC METAL ALLOYS WITH INTERSTITIAL PHASES**

## **1.1. The basic scientific idea of the work**

Basic scientific idea of the work is formulated by material scientist academician V. Trefilov and consists of the theory of new alloys making using the principle of natural composites, i.e. integrally combining phases with dissimilar properties. The eutectic transition is the indispensable condition for thermodynamically stable existence of these alloys and their phase components. Eutectic crystallization reaction expects no chemical interaction on the phase boundaries that provides thus keeping their initial properties. As the main components forming eutectic alloys V. Trefilov suggested combining transition metals and interstitial phases (carbides, borides, nitrides, oxides etc) having very dissimilar physical, mechanical, thermodynamic and chemical properties. The combination of a metal matrix and interstitial phases in one alloy gives them extraordinary complex of characteristics due to formation of specific structures during eutectic crystallization reaction. The given theoretical approach enables to create a large range of new alloys with unique properties that are used to solve a number of problems in the industry which arise during research and development of modern technological processes, extending the durability and reliability of machines and allows cutting expenses for wear and corrosion issues.

## **1.2. The scientific approach of the proposed work**

Properties of metal alloys which are used for manufacturing of a variety of modern machines and mechanisms are determined by their phase composition, structure and degree of thermodynamic equilibrium of the alloy components as a thermodynamic system. There are several theoretical approaches to create structural and functional alloys, one of which is to predict the behavior of the alloy in specific operating conditions, based on the theoretical justification of interaction of its phases under the action of external destructive factors/ This includes rise of internal energy of the alloy by supplying additional energy (friction, heat, irradiation, and plastic deformation), penetration of foreign harder particles, chemical interactions etc. Alloy external destructive factors lead to developing of atom diffusion processes, initiate the diffusionless processes, change amount of lattice imperfections and electronic alloy structure that result in changing the metallographic structure, phase composition and, consequently alters alloy's performance.

Nowadays there are two fundamentally different approaches in development of new structural alloys: a) creation of alloys with predetermined properties, stable structure and phase composition – when we know the structure and chemical composition impact on their properties; b) induction of non-equilibrium states of the alloy. Moving alloy to thermodynamically unstable state changes its structure and phase composition as a respond to external factors. The second approach can be called as “the ability of alloys to adapt their properties to operating conditions by changing the structural-phase composition”, and extending the service life of a component. The alloy thus diminishes the destructive action of external factors by changing its structural and phase composition.

From the point of view of given above considerations, the approach that combines both courses is very promising for creation of new promising structural alloys for modern engineering products. This approach may be realized using the eutectic transition. The eutectic transition has a characteristic feature – in eutectic alloy either thermodynamic stable phase and structural states or non-equilibrium states may be formed. This depends on the crystallization conditions while keeping initial chemical composition of alloy. Thus the eutectic alloys have great potential to meet the complex designer’s demands towards their mechanical, wear and other properties by creating different crystallization conditions, i.e. the possibility of combining these two (equilibrium and non-equilibrium) states.

A promising use of eutectic alloys to solve complex practical materials science tasks is derived from the possibility to combine these two states simultaneously, in a single portion of metal. Theoretically, an alloy with the same composition may be used as a thermodynamically stable material with predetermined properties, but it also may be used in non-equilibrium state formed under non-equilibrium crystallization conditions (fast cooling) with its properties self-optimized under the action of external forces during wear, abrasion, oxidation etc.

A particular interest is devoted to engineering of modern materials using eutectic transition. This allows to combine phases with significantly different properties in case of their thermodynamic compatibility. Each of the phases gives to alloy its intrinsic properties. The properties of resultant composition is usually significantly differs from properties of each of constituents. In our work, taking this principle into consideration, we have developed eutectic alloys based on transition metals with refractory interstitial phases (chemical compounds of refractory metals of IV–VI groups with interstitial elements – carbon, boron, nitrogen, oxygen) – carbides and borides.

The task of the work was to create a new class of structural materials with high rate of properties. For this we focused on alloys which combine interstitial phases with refractory metals what is achieved by means of eutectic transition and metallurgical interaction between dissimilar phases. It is well known that the

interstitial phases have high hardness, strength, high temperature strength, melting point, thermodynamic stability, chemical stability. Their significant drawback is high brittleness caused by their electronic structure, in particular high amount of polar covalent atomic bonds. This is a reason of their limited range of use pure form. The most common practice is to use the interstitial phases as coatings – by means of nitriding, carburizing, borating and various combinations of these and other methods. They also may be used in combination with metals as cemented carbides (tungsten carbide, titanium carbide are bonded with cobalt binder). In hard alloys cobalt serves as a matrix between carbide crystals. Chemical interaction between binder and carbides is not unwelcomed, because it will change (usually worsen) initial carbides properties.

Transition metals (iron, cobalt, nickel) are known for their high ductility, strength, relatively low hardness, moderate melting point, low modulus of elasticity, the ability to chemically interact with other metals and interstitial elements. With interstitial atoms they form chemical compounds, which are resistant to high temperatures and have quite high mechanical properties, resistant to abrasion. The use of eutectic crystallization reaction between these metals and interstitial phases would allow to use above mentioned features and to form alloys with new properties inherent in some ratio to each of metals and interstitial phases since the equilibrium eutectic transition does not involve chemical interaction between the phases. The last remark is a key to keeping the initial properties of phases which form eutectic alloy.

In the work it was experimentally proven that the eutectic alloy should consist of transition metals (about 75% of its volume). Interstitial phases (carbides, nitrides and borides) effectively strengthen metallic matrix, providing a eutectic alloy with new properties. On one hand for the investigated alloys were obtained thermodynamically stable states of dissimilar phases and was shown that the properties of these alloys remain stable under the action of external destructive forces. On the other hand the possibility of transition of these eutectics to a non-equilibrium state opens opportunities to adapt their structural and phase state to better response to the action of external factors.

The long-term work of equilibrium phase diagrams constructing was devoted to searching the thermodynamic equilibrium states of systems consisting of transition metals and interstitial phases forming eutectic. A graphic representation of the phase equilibrium is possible only for ternary alloys (for quaternary – only in some cases). That is why in the beginning of the work a model (simplified) systems were investigated. They were presented in a form of polythermal intersections between transition metals and interstitial phases. The task was to discover the presence of eutectic crystallization reaction. The successive complication of systems by alloying with other metals and taking into account the interstitial phases interaction led to the development of

multicomponent alloys, but the initial idea of forming a eutectic had been certainly kept.

### **1.3. Phase equilibrium in systems ‘transition metal – interstitial phase’**

The investigation of thermodynamic equilibrium between phases during alloy development is fundamental issue. This approach was used in our work to produce new metallic eutectic alloys with interstitial phases.

As it was mentioned above, the stability of alloy properties, especially at elevated temperatures, is provided only through providing thermodynamic compatibility between the interstitial phases (reinforcing crystals) and the alloy metal matrix. With regard to this requirement, large amount of phase equilibriums of transition metals alloys and interstitial phases having a natural eutectic transition have been investigated initially. In these systems, due to the eutectic transformation a transition metal and an interstitial phase were in the thermodynamic equilibrium. Dozens of corresponding phase diagrams have been built [1–12]. Mostly they were ternary phase diagrams: a transition metal + a metal forming the interstitial phase + interstitial element (carbon, boron, nitrogen, or oxygen). In addition, a significant part of the work was devoted to studying of phase equilibriums in four-component and more complex systems.

It has been experimentally found that in these complex quasi-binary and quasi-ternary systems there are eutectic type polythermal sections between solid solutions based on a transition metal and an interstitial phase.

The experimental data made it possible to establish certain regularities of the equilibrium eutectic phase formation between transition metals and carbides, borides, nitrides and metal oxides, which allowed us to reasonably choose optimal ways for an experimental search for the presence of eutectic transition in predefined multicomponent systems. It should be noted that experimental construction of the indicated phase diagrams is very large scope of work, which requires involvement of a large number of highly skilled researchers, unique research equipment, a lot of time and funding. Therefore, established regularities played a very important role in accelerating the work, cutting time and financial expenses, while maintaining a high level of results reliability, what was proven by their further practical application in the development of new grades of eutectic alloys.

Experimental and literary data [1, 11–13] made it possible to develop the classification of ternary phase diagrams. This classification breaks them into four groups depending on the interaction nature between transition metal and interstitial phases. More than a half, namely 266 of 506 well-known diagrams in literature belong to the group, where a transition metal is in thermodynamic equilibrium with interstitial phase. That is why in most of triple systems there is a thermodynamic

equilibrium between the metal and the interstitial phase. That opens the possibility of metal strengthening by interstitial phases. Thus TiC, ZrC, HfC carbides may be successfully used to strengthen such metals as: Fe, Co, Ni, Cr, Mo, W, V, Re, Mn, Al, Mg, etc.; VC, NbC, TaC – for Fe, Co, Ni, Mn, Al, Re and others; boride TiB<sub>2</sub> – for Fe, Al, Mn, W, Re; borides ZrB<sub>2</sub>, HfB<sub>2</sub> – for Fe, Al, V, Mn, Cr, W, Re; nitrides TiN, ZrN, HfN – for Fe, Co, Ni, V, Nb, Cr, Mo, U, etc. This established regularity has allowed us to substantially narrow the experimental search for the necessary thermodynamic equilibrium between the interstitial phases and transition metals, and thus significantly accelerated the work and reduced required costs.

The phase equilibrium between interstitial phase and metal matrix is determined using polythermal intersections of the corresponding ternary phase diagrams, called quasi-binary diagrams, which, as we have experimentally established, are of eutectic type in the systems of a certain group. The analysis of these eutectic quasi-binary systems has revealed some regularities regarding the composition and the melting points of eutectic alloys [13–17]. These regularities are shown in Fig. 1.1, indicate the relation of the eutectic alloy (transition metal + carbides) composition ( $C_{ec}$ ) on the difference between the melting points of the carbide and the metal ( $\Delta T_c$ ). Based on these relations we can conclude that to increase the carbide concentration in the eutectic it is necessary to reduce the difference of melting points between the metal and the carbide. For example, if a new eutectic alloy is to be developed, then in order to provide high tribotechnical properties, it will be necessary to choose the strengthening carbide with relatively low melting points. Thus, the melting points difference is minimal, and the carbide concentration in the eutectic alloy will be significant compared to more refractory carbides. To ensure high strength, carbide content may be less than it is necessary for formation of high tribotechnical properties, and then you can choose more refractory carbide for strengthening the metal matrix. If it is necessary to provide high-temperature strength, you should choose more refractory metal and strengthen it with the most refractory carbide, but taking into account that increasing the difference in the melting points between the carbide and the metal will reduce the carbide concentration in eutectic.

The established relations made it possible to manage the most effective metallurgical interaction of metals with carbides to provide the developed eutectic alloys with complex of necessary mechanical, tribotechnical, technological, operational and economic properties.

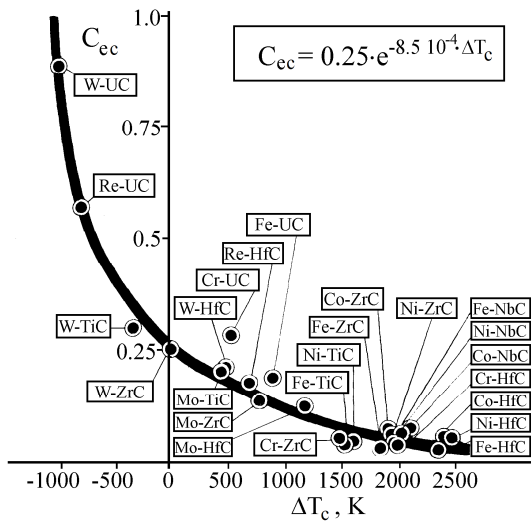


Fig. 1.1. The dependence of quasi-binary metal-carbide eutectic alloys composition ( $C_{cc}$ ) on the difference between the melting points of the carbide and the metal matrix ( $\Delta T_c$ )

Similar experimental dependences have been established for alloys of metals with borides, nitrides and oxides (Fig. 1.2), which indicate their objective character and wide use for a number of interstitial phases. The established regularities have been used for development of new eutectic alloys with multicomponent composition.

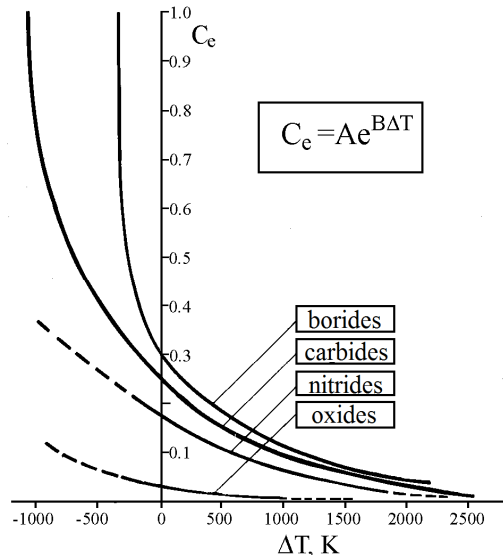


Fig. 1.2. The dependence of the quasi-binary metal-interstitial phase eutectic alloys composition ( $C_e$ ) on the difference between the melting points of interstitial phase and the metal matrix ( $\Delta T$ )

The analysis of experimental data and literature has revealed the dependence of melting point of developed eutectic alloys ( $T_e$ ) on the melting point difference between the metal and the interstitial phase ( $\Delta T$ ) (Fig. 1.3). These dependencies may be presented in a following form:

$$C_e = Ae^{B\Delta T}, T_e = T_m (1 - Ee^{F\Delta T}),$$

where  $T_e$  is the quasi-binary eutectic melting point,  $T_m$  is the metal matrix melting point, A, B, E, F are the coefficients for metal alloy carbides, nitrides, borides and oxides.

Using these dependences to find the optimal composition of strengthening carbides for the new high temperature eutectic alloys allows to significantly reduce costs required for long high-temperature tests in the study of their properties.

The researches of thermodynamic equilibrium of eutectic systems formed by transition metals and interstitial phases have shown that the mutual maximum solubility of the alloy components in the solid state is negligible [14–17]. Another important conclusion has been made as the result of the literature data analysis – a small amount of metal is usually solid solved in interstitial phases. On one hand, this allows expecting the stability of alloy phases' properties, and on the other hand offers the possibility to alter the eutectic properties by alloying both metal matrix and interstitial phases

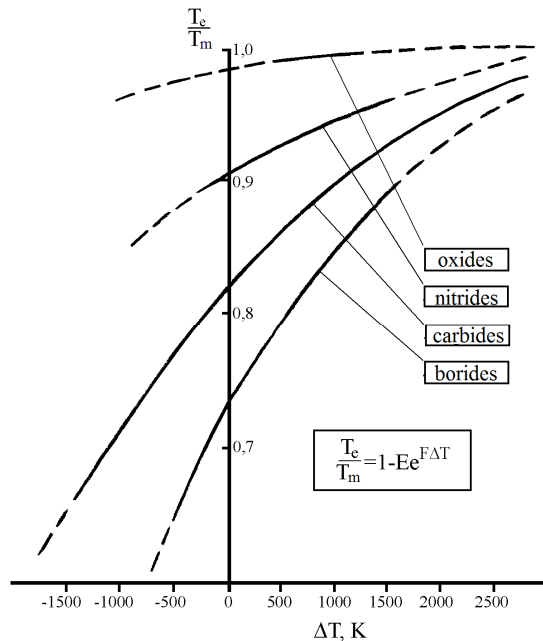


Fig. 1.3. The dependence of the quasi-binary metal-interstitial phase eutectic alloys melting point on the difference between the melting points of interstitial phase and the metal matrix

This finding has been widely used in further development of new eutectic alloys, including providing them with high corrosion properties to work in chemically active environments or at high temperatures in the air. Also the metal eutectic matrix alloying made it possible to influence on oxidation process during friction especially at high temperatures, when wear depends on the ability of the metal matrix of alloy to form the protective oxide films with balanced composition, structure, thickness and adhesion to the substrate. The oxide films reduce tangential force and adhesive interaction of friction couple contiguous surfaces.

By studying the phase equilibriums [1, 14–17] in three- and four-component alloy systems the regularities of interstitial phase maximum solubility in alloy metal matrix depending on alloy content (basically on content of matrix metal and of the metal forming interstitial phase) have been developed. The solubility regularities of alloying elements in matrix metal in the presence of interstitial phase have been also developed. Based on this, the possibility of producing multicomponent eutectic alloys with equilibrium interstitial phase embedded to metallic matrix containing several alloying admixtures has been discovered.

Thus, studying of phase equilibriums of transition metals with interstitial phases have led to the following conclusions about future developments of wear- and heat resistant alloys:

1. The general regularities of eutectic point location on the quasi-binary and quasi-ternary eutectic phase diagrams of multicomponent systems formed transition metals and interstitial phases depending on their melting points have been established. These regularities allow optimizing selection of strengthening interstitial phases during development of eutectic alloys with high heat resistance and/or tribological properties.

2. It was experimentally examined and found: in which multicomponent systems based on transition metals with interstitial phases polythermal sections of the eutectic type exist; phases that are in thermodynamic equilibrium in these stretches; location of the eutectic point on the phase diagram; the limiting solid solubility of the interstitial phases in a solid solution (matrix material) has been established.

3. The experimental data analysis of the phase equilibriums of investigated systems and using the developed empirical dependences it is possible to estimate (with reasonable reliability) the eutectic composition (i.e. the amount of interstitial phases in the alloy) and its melting point.

4. The possibility of altering of investigated eutectic alloys properties by alloying metal matrix has been found. This opens ways for producing alloys with high strength and excellent tribotechnical properties.

## 1.4. Structure of cast eutectic alloys

The structure of eutectic alloys during the crystallization from the melt is formed by three mechanisms depending on the cooling rate [36]. At very low cooling rates ( $<0.1$  °C/min), and correspondingly small degrees of supercooling, interstitial phase crystals grow independently. These crystals are usually very coarse. Such eutectics have low strength and ductility and therefore have no practical use. In very wide range of cooling rates (from  $\sim 0.1$  °C/min to about  $\sim 10$  °C/sec) that actually occur during cooling of large castings at production or small drops (during the spraying of molten alloys) there are no conditions (diffusion is partially restricted) to grow large crystals. The low values of the atoms diffusion coefficient are determined by the high degree of the liquid supercooling in which the mobility of atoms is negligible. In this case, the crystallization is carried out by the cooperative crystal growth of the eutectic phases when fine crystals of both phases (in this case, the interstitial phase and the metal phase) grow simultaneously. The mutual growth of the phases involves a relatively small diffusion distance of atoms from the liquid to the crystallization front that does not require large diffusion coefficient values. So the eutectic grains growing in these conditions contain a long dendrite crystal of interstitial phase (a stem crystal, and many branches growing out of it) [18, 19].

The space between such highly branched crystals, which are formed during alloy crystallization, is filled with crystals of another phase – matrix metal. Microstructure examinations of the eutectics showed that for all systems the leading (solidifies first) phase is the interstitial phase, and the secondary phase is the metal component. This structure is colonial. The eutectic grains can combine several eutectic colonies. The disorientation angle of the metallic phase inside of the grain, in case of considered eutectics, is relatively low. On this borders of neighboring zones with low angular disorientation the defects and impurities concentration is low and weakening of eutectic alloy due to this is not significant. The disorientation angle of the metallic phase between the grains is much larger, it accumulates more defects and uncontrolled impurities in the process of crystallization and such borders become the weakest place of the eutectic alloy.

In Fig. 1.4 the examples of the structures of the quasi-binary eutectic alloy obtained by crystallization from the melt with cooling rate about  $20$  °C/min are shown. These fine crystals, located in the monocrystal metallic matrix in the form of fibers, films or plates, are micro reinforcing elements that provide composite strengthening [20]. Thus between the crystal lattices of both phases the most stable crystallographic ratios are set. The fine crystals of interstitial phases contain no dislocations and therefore have very high strength, hardness, and wear resistant properties. Consequently, they also cause the dispersion strengthening of the alloy simultaneously with the composite strengthening.

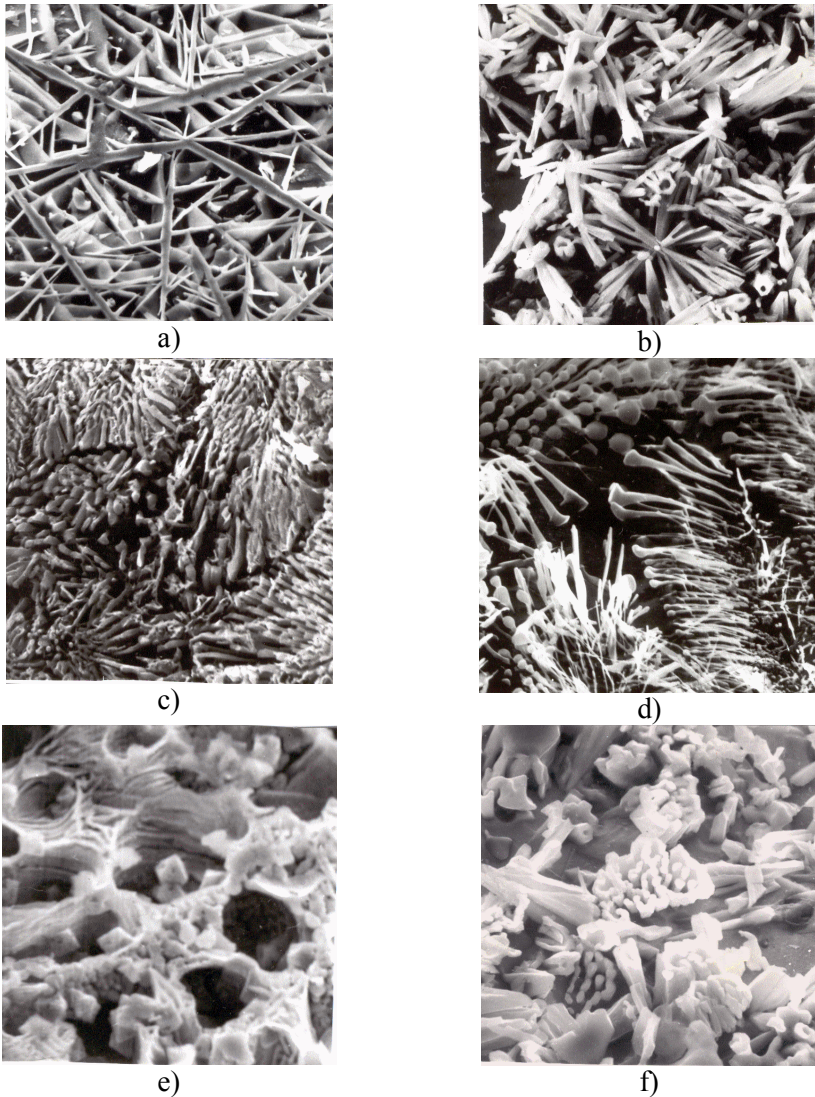


Fig. 1.4. The quasi-binary eutectic alloys colonial structures due to the cooperative phases growth. Scanning electron microscopy. a) Fe-ZrB<sub>2</sub>, x 500; b) Fe-TiB<sub>2</sub>, x 1500; c) Fe-VC, x 3000; d) Mo-TiN, x 3000; e) the iron-based alloy VTiNi, x 2000; f) Fe-TiC-TiB<sub>2</sub>, x 1500

Due to stable crystal orientation ratio of both phases the quasi-binary eutectic alloys retain the fine structure by heating to a temperature  $0.93T_e$  for up to 275 hours. For this reason, these alloys are stable in the process of thermocycling.

The cooling of the quasi-binary eutectic melt at rates greater than 10 °C/sec ( $10^5$  °C/sec) causes colonial structures disappearing and the structure turns to a fine conglomeration of phases with very small sized interstitial crystals.

As mentioned above the eutectic alloy properties are determined by the forming phases properties based on their proportion and structure

The hardness of the quasi-binary eutectic alloys of the considered systems is much higher than the hardness of matrix metals alone due to the presence of interstitial phases. Experimentally we have found that the high-temperature annealing reduces the hardness of the eutectics insignificantly and to less extent than it reduces the hardness of matrix metals [21].

This slowing of hardness drop takes place due to the presence of reinforcing frame built of interstitial phase crystals with good high temperature creep resistance. With increasing of interstitial phase's content the eutectic alloy's strength has two peaks at low and high temperatures (Fig. 1.5): in the solid solution area and the eutectic composition. Almost all examined polythermal intersections of phase diagrams have the strength maximum in the eutectic area and this strength is significantly higher than it is in the area of solid solution. This fact shows that the composite strengthening by interstitial phase frame is more effective than the dispersion strengthening that occurs in the solid solution area. This effect is especially evident during examinations for high temperature creep resistance since the interstitial phases are resistant to continuous stress action at high temperatures.

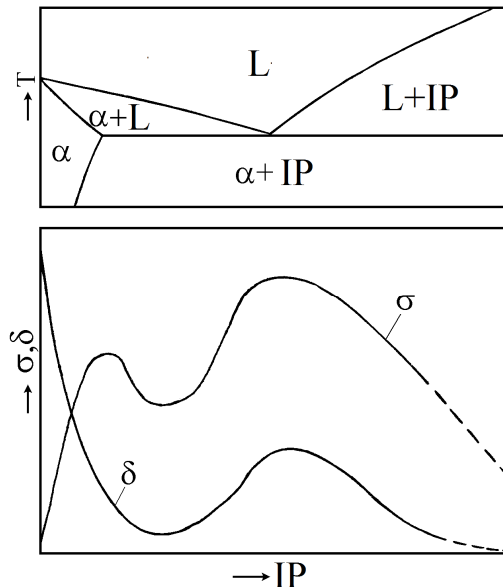


Fig. 1.5. Dependence of the alloys strength ( $\sigma$ ) and ductility ( $\delta$ ) vs. interstitial phase content (IP)

Based on structural examinations we have found that in all examined eutectic systems the interstitial phase is always the leading crystallization phase. The interstitial phase forms reinforcing frame that carries most of the load, and metal matrix transfers and redistributes stresses between individual branches of the reinforcing frame. Thus in the investigated cast eutectics the composite strengthening mechanism is commonly found.

### 1.5. Properties of cast eutectic metal alloys with the interstitial phases

The examinations have shown that ductility of cast eutectic alloys with colonial structure has its maximum condition for alloys with eutectic composition. This indicates that ductility of the investigated eutectics is mainly determined by the interstitial phase structures, which, as shown above, are highly brittle in the initial state. Due to the regular structure eutectic composition alloys have good ratio of strength and ductility [22, 23]. As a result of this, alloys with composite strengthening mechanism (including quasi-binary eutectic alloys) have lower strength drop with increasing temperature than pure metals and alloys with other strengthening mechanisms. On Fig. 1.6 generalized temperature dependences of the strength of pure metal ( $\sigma_m$ ), alloys ( $\sigma_a$ ) and quasi-binary eutectic alloys with interstitial phases ( $\sigma_e$ ) (having the same basic metal) are shown.

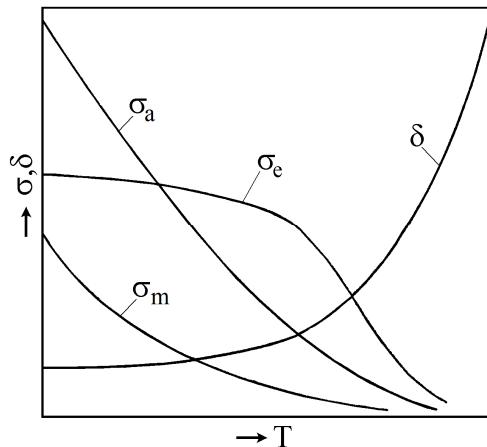


Fig. 1.6. Dependences of metal strength ( $\sigma_m$ ), metal based alloys ( $\sigma_a$ ) and quasi-binary eutectic alloys with interstitial phases ( $\sigma_e$ ) (with the same basic metal) vs. temperature

For all three types of alloys ductility ( $\delta$ ) increases steadily as temperature rises. As it is shown in the figure at high temperatures the colonial structure eutectic alloys have superior strength.

Some of developed eutectic alloys with composition (i.e. colonial) structure in the cast state have high creep resistance especially at high temperatures [24]. However, they are not prone to superplasticity at temperatures up to  $0.8 T_{\text{melt}}$ , which is a characteristic feature of the eutectic alloys without interstitial phases. For example, the eutectic alloy Mo-ZrC has very high strength ( $\sigma = 590$  MPa,  $\delta = 7\%$  at  $1500$  °C) at temperatures up to  $1800$  °C that made it possible to successfully use it as the material of press-moulds for optical ceramics which are processed at  $1500$  °C (used for various applications, including aerospace engineering products).

The eutectic alloys with the interstitial phases, including carbides and borides, are characterized by high wear resistance at different wear conditions. This property is caused by a combination of a metal matrix (which serves as a solid lubricant) with very hard carbides or borides that serve as micro strengtheners at friction. This also is promoted by structure regularity and crystal reinforcing effects [25]. Depending on the content of interstitial phase crystals in the quasi-binary alloys the wear rate of the alloy ( $J_a$ ), and the counterface ( $J_{cb}$ ) have minimum values at the eutectic composition [26, 27] (Fig. 1.7). The Co-WC cemented carbides (grade BK-2) or high chromium content cast iron were used as the wear-resistant counterface materials. Similar dependences are found in other developed eutectic systems, so the diagram (Fig. 1.7) has generalized qualitative view.

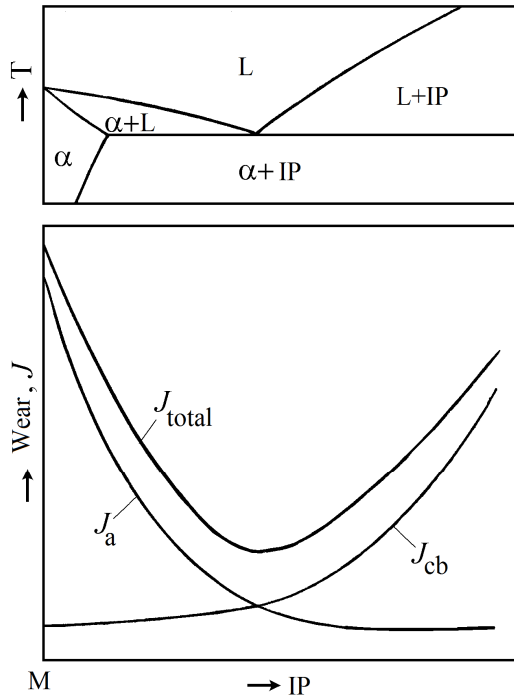


Fig. 1.7. Dependence of the alloy wear loss versus interstitial phase content (IP).  $J_a$  – alloy wear loss,  $J_{cb}$  – counterface wear loss,  $J_{total}$  – total wear loss of friction couple

The established regularity is valid in case of alloying the metal matrix with other metals [28–31]. For example, by alloying the quasi-binary eutectic alloy Fe-TiB<sub>2</sub> with chromium, nickel and titanium up to composition when previously iron matrix changes to austenitic steel 12Cr18Ni9Ti. The wear resistance of obtained alloy becomes superior to wear resistance of austenitic steel itself in order of 20–200 magnitudes depending on the nature of friction. The corrosion resistance of the alloy remains on the same level.

It should be noted that the decrease in wear resistance of hypereutectic alloys is caused by structural factor merely, i.e. the appearing of large primary interstitial phase crystals. These crystals have many structural defects that arise during their growth. As it was mentioned above, the interstitial phases are brittle, and interstitial crystals of these phases are also highly imperfect, they have low fatigue strength. That is why they are easily broken and worn away due to variable loads at abrasive wear or sliding friction. Therefore, the transition into region of hypereutectic alloys to improve their tribotechnical properties requires the development of the technologies that will help to reduce the size of primary interstitial phase crystals and amount their structural imperfections.

Compared to the quasi-binary alloys the increasing of a wear resistance can be achieved in quasi-ternary eutectic alloys where strengthening is provided with

two dissimilar interstitial phases. For example, multicomponent alloy, containing the following three phases: the matrix – austenitic steel 12Cr18Ni9Ti – and eutectic crystals of VC and TiB<sub>2</sub>, combines high wear resistance, sufficiently high corrosion resistance and good casting and machining properties. [32]

Alloying of Fe-TiB<sub>2</sub> alloy with chromium, nickel, aluminum and silicon significantly increases its heat resistance while wear resistance is retained. VC considerably increases abrasive wear resistance of steel 120Mn13 [33]. Alloying of Fe-VC alloy with chromium significantly increases wear resistance in hydrogen atmosphere and in environments containing hydrogen [34, 35].

Practical application of the quasi-binary eutectic alloys is facilitated by their good manufacturing properties, provided by a low melting point, good casting properties (low shrinkage, ease of melting, ease of spraying to obtain a fine powder), and high adhesion strength of coatings applied by cladding, detonation and plasma spraying, electrospark alloying etc.

Consequently, based on comprehensive examination of phase equilibriums, structure and properties of metal alloys containing interstitial phases it has been found that eutectic alloys of this type have important properties for practical application: wear resistance, high temperature strength and manufacturing properties. Obtained results reveal broad prospects for development of the iron, cobalt and others eutectic alloys for various engineering tasks.

## **Conclusions on section #1**

1. For the eutectic alloys of ‘transition metal-refractory interstitial phase’ type the general regularities of the melting point and eutectic concentration dependence on melting point of alloy components have been found. These regularities made it possible to establish the most appropriate way of choosing the metal-based systems with the refractory interstitial phases and the eutectic transition as foundation for the further development of alloys with predefined set of properties.

2. It has been proven that in all investigated eutectic systems the interstitial phase is always the leading crystallization phase. The interstitial phase forms highly branched (dendrite) reinforcing frame, and metallic matrix solidifies in its spaces. This frame – is a main load carrying element of the eutectic alloy, and matrix material serves for proper loads distribution between its individual branches. Thus in the examined cast eutectics the composite strengthening mechanism is commonly found.

3. The structure of examined model eutectic alloys and interstitial phases content allow to recommend these alloys as a base for development of multicomponent alloys with high strength, high temperature strength, tribotechnical characteristics at room and elevated temperatures, good casting properties and other characteristic features of alloys with composition strengthening.

## 2. METASTABLE EUTECTIC IRON BASED COATINGS WITH REFRACTORY INTERSTITIAL PHASES

### 2.1. Objectives to investigate non-equilibrium states of eutectics

Based on the main idea set forth in the fundamental part of Section 1, let us dwell more closely on the theory of eutectic crystallization. According to the theory, firstly proposed by A. Bochvar, and further developed in the works of the Dnipro metallurgical school under the guidance of academician Yu. Taranzhovnir, any eutectic alloy can have three types of structures that correspond to three crystallization mechanisms depending on the cooling rate [36]:

**a. With very low supercooling** (low cooling rate) there is a simultaneous and independent nucleation and subsequent independent growth of phases forming eutectic. The phase growing sites are located apart from each other, since their amount in the supercooled liquid is small that leads to the formation of a coarse structure – large polyhedrons or poorly branched dendrites. This type of structure A. Bochvar called "the structure of a coarse phase conglomeration". In pure metal alloys with eutectic composition such structures appearing is complicated [37]. The introduction of insoluble impurities leads to their accumulation at the front of growing crystals and prevents the simultaneous origin and growth of eutectic phases, and results in formation of coarse phase conglomeration.

**b. In a large region of supercooling** (a broad spectrum of cooling rates), both the origin and growth of phase's crystals forming the eutectic occur simultaneously. The change in the crystallization mechanism is due to the restriction of atoms diffusion in liquid afore the crystallization front. A cooperative growth of the eutectic phase becomes more advantageous energetically. As a result of common growth eutectic colonies are formed. In each particular system, one of the phases becomes a basis for the colony origin, and it is leading in the process of further simultaneous growth. In the eutectics such of 'solid solution – intermetallic compound' (or interstitial phases such as carbides, oxides, borides, nitrides), the intermediate phase (or interstitial phase) serves as the base. The base phase is also characterized by higher melting entropy and greater tendency to develop the flat forms of growth. Their elemental composition is much different from eutectic, and the surface tension at the boundary with the melt is relatively large. This causes the need for greater liquid supercooling for the appearance of base phase crystals and determines the ability of this phase to initiate the origin of the colony. The colony takes the shape of the base crystal, because the substrate formation of the eutectic colony is carried out by solidification of secondary phase along the surface of the base crystal. The growth of the colony on substrate is a process of cooperative growth of eutectic

crystals. In this case, the particles of the base phase grow into a liquid and lead to the crystallization of the second phase.

The most important feature of the cooperative growth of eutectic crystals is the fine branching of eutectics. This leads to a characteristic eutectic appearance in a light metallographic microscope – their virtually fine-granular structure, but in reality they are big intensively branched crystals.

The co-operative growth of eutectic crystals is determined by high gradient concentrations that arise at small interatomic distances in the crystallization front. This, in its turn, leads to a high rate of components separation in the melt afore the crystallization front and prevents the nucleation of new crystals.

**c. The supercooling below a certain critical temperature** (the highest cooling rate and supercooling) at even greater cooling rates causes the eutectic crystallization mechanism changing again: finely dispersed structure is to be formed. The rapid deceleration of diffusion processes inhibits the phases growth, the dimensions of growth sites is strongly reduced, and their amount substantially increased if compared with the mechanism of eutectic crystallization. Under these conditions colonial eutectic crystallization becomes impossible, and fine-grained phase mixtures are formed. This much dispersed structure was named by A. Bochvar "fine phases conglomeration" [38].

In Fig. 2.1 the regions of existence of three types eutectic structures are illustrated schematically.

In addition, another equally important feature of eutectics with structure of fine phases conglomeration should be noted. This structural state is characterized by a greater degree of deviation from the equilibrium state than the cast state. The higher the cooling rate, the greater the eutectic, as the thermodynamic system, deviates from the equilibrium state. At the same time, the energy required for the structural transformations beginning decreases. It is one of the most important factors characterizing the tendency of a material to adapt to external conditions of friction.

This idea was first formulated in the works of B. Kostetskii, L. Bershatsky, I. Kragelsky [39, 40]. It can be expected that the use of rapidly cooled eutectic alloys of the considered systems as tribotechnical materials will provide good characteristics of the friction couple capable to self adaptation.

The state of the eutectic with a structure of fine phases conglomeration differs significantly from that of colonial structures. In particular, for developing of iron based alloys with refractory carbides and borides, an iron-based solid solution should form a metal matrix with the fine-grained crystals of the interstitial phase in the process of rapid cooling. Such an alloy is strengthened mainly by the mechanism of dispersion strengthening, in contrast to the colonial structures of these alloys with a characteristic composition strengthening mechanism. Such change in the structure and mechanism of strengthening leads to a change in properties, namely, ductility is increased in comparison with the cast state, since

the metal matrix is more plastic than the frame of the interstitial phases. The corrosive properties and the propensity to high-temperature oxidation are determined by the metal matrix composition mainly that opens up the prospect of a deliberate change in such properties, for example, by its alloying. Also, the additional possibilities of the metal matrix strengthening by alloying and plastic deformation methods are opened up.

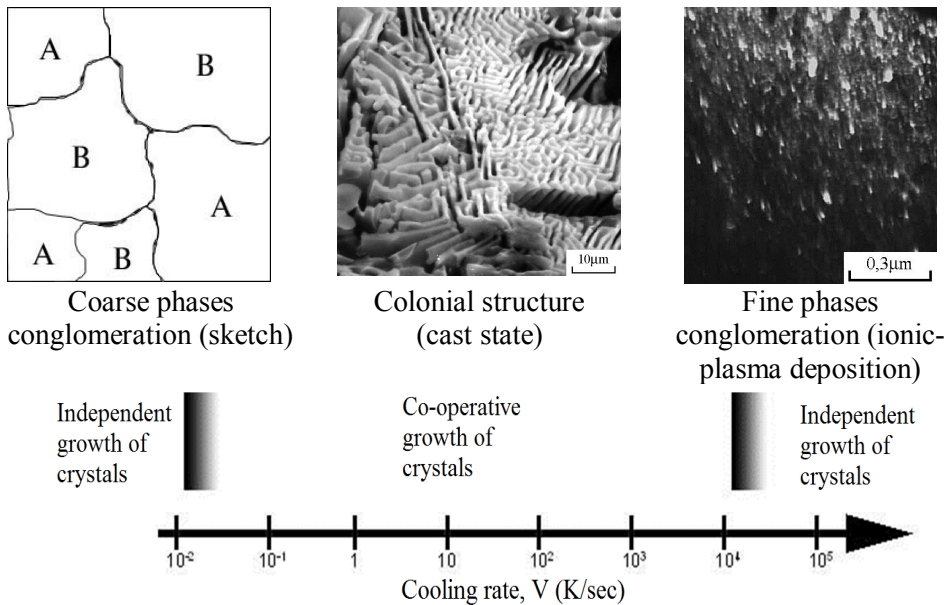


Fig. 2.1. Schematic representation of the three mechanisms of eutectic crystallization depending on the cooling rate of VTiNi alloy and the corresponding structures (in accordance with A. Bochvar)

Thus, the realizing of non-equilibrium states in examined eutectic alloys opens up wide possibilities for solving a number of practical problems related to the optimization of the friction couples of machines and mechanisms, the extension of service life, the increase of corrosion resistance and improvement of other important characteristics.

It is important to note the potential possibility of a deliberate change in the properties of non-equilibrium states of the investigated eutectic systems. This feature follows from the ability to hold the intermediate states which the eutectic as a system passes from a highly non-equilibrium state to a more or completely equilibrium state. Since each intermediate state has its own characteristic properties, it is possible to induce a particular state by controlling cooling rate and subsequent reheating (tempering) of the eutectic.

For practical use of non-equilibrium states of the investigated systems it was suggested an idea of coatings formation using laser, spraying techniques and other methods [41–47]. High power discharge over a short period of time allows an eutectic alloy to be heated quickly to high temperatures, and in case of rapid subsequent cooling makes it possible to produce non-equilibrium states in this alloy.

The properties of some eutectic alloys can be improved by plasma spraying at high speeds of liquid-to-solid transition [48]. Rapid cooling of these alloys results in the formation of metastable structures, including the formation of supersaturated solid solutions and the appearance of intermediate phases. Thus high cooling rate has a major impact on their properties [49, 50].

In this work we used the following deposition techniques: plasma spraying (hereinafter – plasma coating) and detonation thermal spraying process (hereinafter – detonation coating). Characteristic feature of these methods is that each particle of the material falling on the substrate undergoes a very fast temperature-time cycle, schematically represented on Fig. 2.2. This temperature-time cycle allows obtaining highly non-equilibrium states in the process of eutectic coatings crystallization that means to produce non-equilibrium structures and phases. The heating of spray particles occurs as a result of their contact with an energy carrier. For the gas-thermal methods gas is heated to plasma state by electric arc (plasma method) [41] or by the energy of gas mixture explosion (detonation method) [42, 45].

A characteristic feature of these methods is very short time of heating, melt existence and subsequent cooling of each sprayed particle. The short time of these processes imposes restrictions that play a very important role in the spraying of eutectic alloy coatings, since a lot of the diffusion processes during heating and cooling strongly depend on the temperature change rate. Schematically these processes are illustrated on Fig. 2.2, where the dimension of time in *ms* emphasizes small order of magnitudes. The contact time of sprayed particle with the energy carrier for the plasma method is about  $2 \times 10^{-3}$  sec [43, 44], for the detonation method is about  $3 \times 10^{-3}$  sec [45]. During the contact time the solid particle is heated and melted (partial melting). Thus, the melting time is even shorter than the time of contact with the energy carrier.

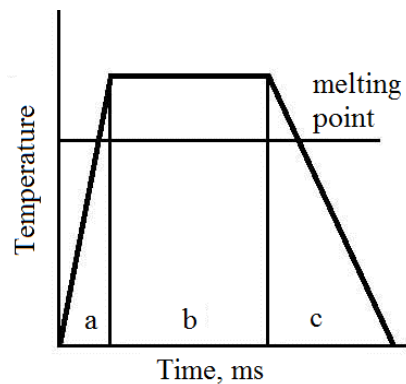


Fig. 2.2. Qualitative diagram of temperature-time influence on eutectic particles sprayed in the form of a coating: a – heating, b – melting, c – cooling

The short time of a liquid existence imposes restrictions on the diffusion processes running, in particular, the diffusion distribution of atoms ahead of the crystallization front. Just as in case of the liquid metal spraying by an inert gas current (a short time of a liquid existence), the spraying of the coating should have the same characteristic features of crystallization process. First of all, this is the existence of stable groups of atoms (clusters) in a liquid, which leads to additional restriction in the diffusion mobility of atoms ahead of the crystallization front during subsequent cooling [46, 47]. Since the rate of superheating of a melt for the used methods is not measured and virtually uncontrolled, it is impossible to quantify its influence on the processes of subsequent solidification. One can only assume that fluctuations in the rate of superheating, caused by different particle sizes, the time of their contact with the energy carrier and the spreading of the temperature field values, cannot significantly affect the behavior of the groups of atoms in the liquid. It follows that the origin, composition and number of equilibrium and non-equilibrium phases formed in the eutectic coating during crystallization should not differ significantly from the case of their formation when the powder is formed by the inert gas spraying. Further investigations have confirmed this assumption.

## **2.2. Impact of cooling rate on the crystallization mechanism of eutectics**

For the metal coatings spraying by plasma and detonation methods, the feedstock material should be in the form of powder. In addition, the metal powder can be used for manufacturing of products by powder metallurgy methods or for deposition of coatings by other methods (laser cladding, HVOF, high frequency currents aided techniques etc). Therefore, one of the tasks of this work was to develop high-performance technology for the production of eutectic powdery feedstock material.

With the variety of existing methods for metal powders production [52] the method of molten metal spraying in a vacuum by an inert gas was chosen was selected. It is widely used in industrial method and many enterprises already have required production capacities.

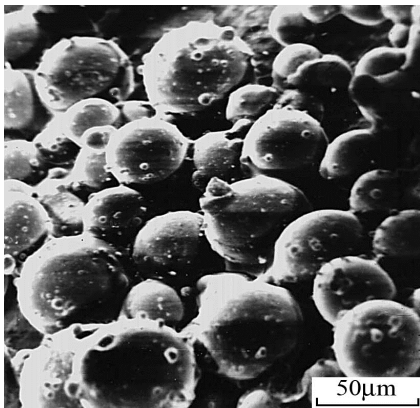
The spraying rate of eutectic alloys of all compositions was not more than 12 kg/min. The suitable powder output was 2/3 of the initial charge weight. The granulometric composition of obtained eutectic powders is given in the table 2.1.

The developed technology for the production of eutectic powders by the method of spraying with an inert gas flow (argon, nitrogen) was confirmed and approved. The appearance, metallographic structure, and dependence of the structure on the cooling rate of the eutectic powders formed by spraying with argon and nitrogen are shown in Fig. 2.3. The critical cooling rate is  $V_{cr} = (4-5.3) \times 10^5$  K/sec.

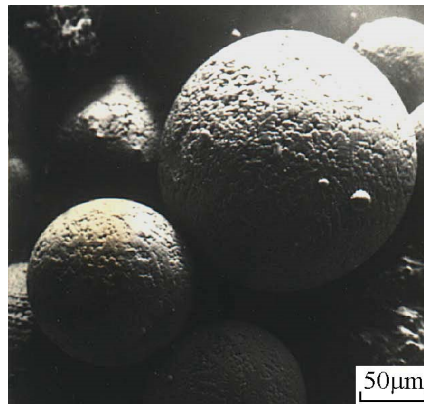
Table 2.1. Granulometric composition of the obtained eutectic powders

Alloy grade	Rremainder on a sieve by weight, %									Density, g/cm <sup>3</sup>
	0315	0280	0180	0160	0140	0100	0056	0045	0045	
VTiNi	1.8	1.6	4.2	5.2	5.2	19.2	–	31.0	22.5	4.2
CrTiNi	21.7	3.6	26.0	13.2	4.6	4.5	–	22.3	0.6	3.8
CrVC <sub>3</sub>	–	25.6	29.4	9.0	3.8	15.4	2.2	1.0	3.6	4.5
CrVC <sub>7</sub>	6.4	3.6	21.2	7.2	8.0	20.4	25.0	4.0	4.2	4.5
NiB	13.8	4.0	26.8	12.5	7.5	20.5	21.4	0.4	1.6	4.4

We have developed a set of alloys and the laboratory technology of plasma spraying and cladding to form powder protective coatings of iron based eutectic alloys with refractory carbides and borides over low-carbon, medium-carbon, low-alloyed, and stainless steel substrates, as well as on the surface of copper, aluminum, titanium and their alloys. The technological parameters of the process of spraying and cladding have allowed recommending the coatings for further research and practical use.



a)



b)

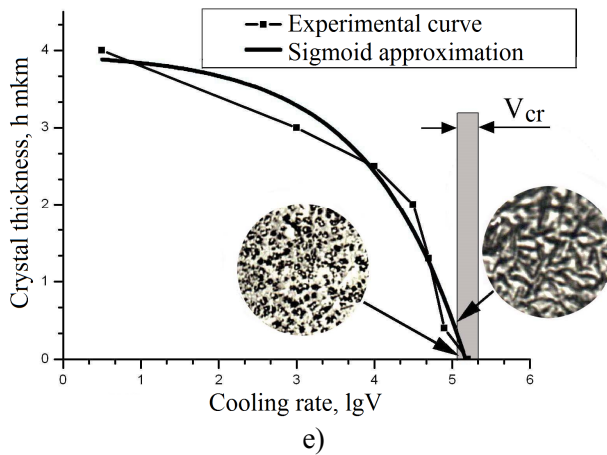
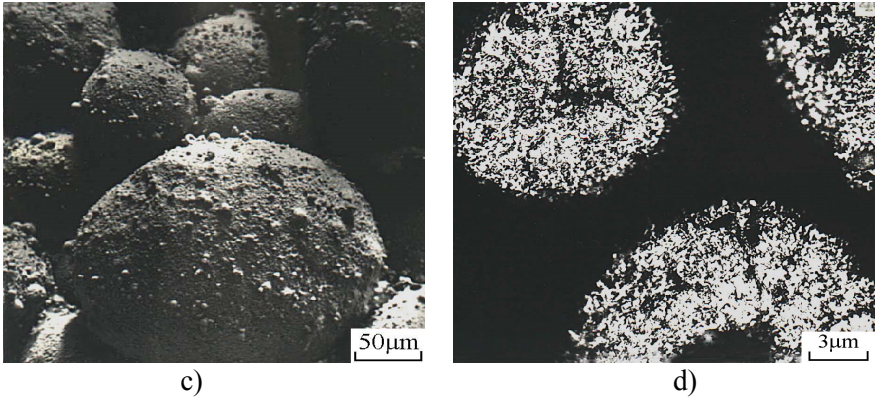


Fig. 2.3. The appearance of the eutectic powders formed by spraying with argon and nitrogen and the dependence of the structure on the cooling rate (e): a) VTiNi, argon; b) CrVC, nitrogen; c) VTiN, nitrogen; d) VTiN, argon

The conducted examinations of structure and composition of the developed coatings have shown that in the process of plasma spraying a change in the mechanism of eutectic crystallization occurs with the formation of regions of fine phase conglomeration (Fig. 2.4), which have major impact on the properties of these coatings. On micrographs, this fine conglomeration is visible like light not etched areas (hereinafter – light areas)

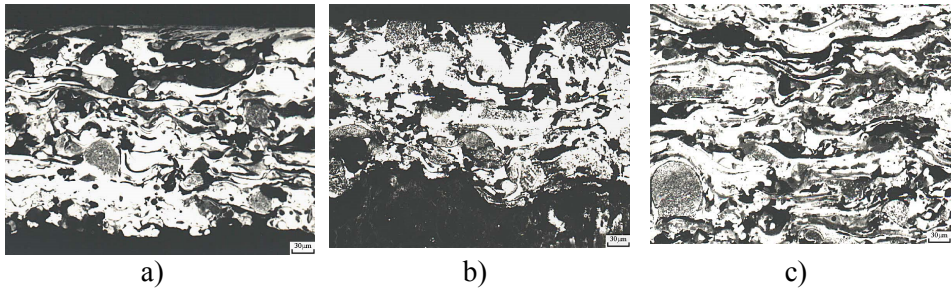


Fig. 2.4. Structures of plasma eutectic coatings (cross sections): a) VTiNi; b) CrTiNi; c) CrVC

X-ray diffraction examinations have shown that the main phase of produced eutectic coatings is iron-based solid solution, which exists in the form of two polymorphic modifications ( $\alpha$ ,  $\gamma$ ), as well as their varieties with an increased period of the lattice ( $\alpha'$ ,  $\gamma'$ ) (Table 2.2). Their ratio depends on the cooling rate of the substrate. The additional effects are associated with the melt state and existence time.

Table 2.2. Phase composition of sprayed plasma eutectic coatings

Grade	Phase composition	Lattice distance, nm				
		$\alpha$	$\alpha'$	$\gamma$	$\gamma'$	VC
CrTiNi (as-deposited)	$\underline{\alpha}' + \gamma + X(?)$	–	0.2881	0.3589	–	–
CrVC (as-deposited)	$\underline{\alpha} + \gamma' + \gamma + \text{Cr}_3\text{C}_2$	0.2873	–	0.3565	0.3618	–
VTiNi (as-deposited)	$\underline{\alpha}' + \gamma' + \text{TiC}$	–	0.2864	–	0.3594	–

The coating strengthening interstitial phases exist in two states: part of them are in equilibrium state, others – in non-equilibrium state. Their amount in the coating depend on both cooling rate and melt conditions.

### 2.3. The growth of rapidly cooled eutectics

It has been found that during plasma spraying or melting of a sprayed plasma eutectic coating with the formation of a liquid phase in the process of subsequent crystallization on the substrate, the colonial structure of the casting state is restored, which determines the properties of the sprayed (melted) coating. This is explained by a lower cooling rate compared to the initial sprayed condition.

The examination of tribotechnical properties of sprayed eutectic plasma coatings in conditions of dry friction showed that they have high wear resistance (Fig. 2.5) and corrosion resistance (Fig. 2.6) simultaneously. This fact makes it possible to recommend them for further investigations for practical problems

solution arising in friction units that operate dry conditions, in conditions of lubricant starvation, in aggressive environments or in the air.

Research of tribotechnical, corrosive and micromechanical properties of the investigated plasma eutectic coatings showed that they are determined by the degree of deviation from the thermodynamic equilibrium state, which forms preconditions for the conscious usage of these properties.

The industrial technology of detonation spraying of the investigated eutectic alloys on various substrates: steel 1030, steel 1045, alloy 12Cr18Ni9, aluminum alloys Al+Mg+Mn, Al+Mg+Zn, AlCu4Mg2, copper, titanium alloy Ti6Al3.3Mo0.3Si have been developed. Thickness of the coatings, depending on the spraying mode, can be ranged from 50  $\mu\text{m}$  to 1500  $\mu\text{m}$ .

It has been shown that the detonation method, as well as the plasma method, changes the eutectic crystallization mechanism of the investigated eutectic coatings due to high cooling rates, resulting in the formation of the fine phases conglomeration. In coating the areas of the fine phases conglomeration (light areas) are formed (Fig. 2.7). The bulk content of the light areas in the detonation coating depends on the parameters of spraying and may be 40–48% and 82–85% for the CrTiNi and VTiNi eutectics respectively. Just as in the case of plasma spraying, the coating properties are mainly determined by these areas.

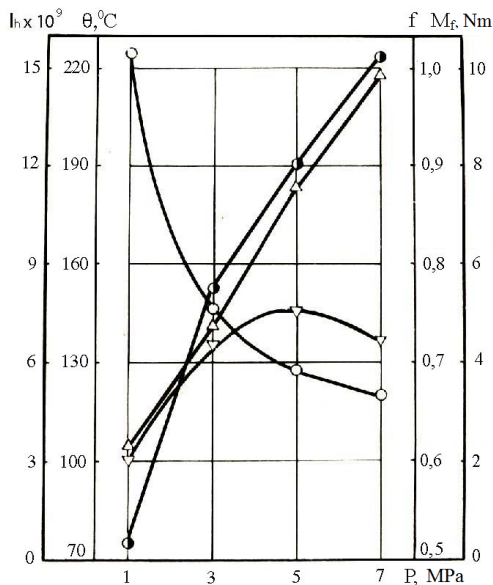


Fig. 2.5. Dependence of linear wear rate,  $I_h$  (▽); maximum temperature in contact,  $\theta$  ( $^\circ\text{C}$ ); friction factor,  $f$  (○), and friction moment,  $M_f$  (△) on the specific load. Material – plasma eutectic coating VTiNi (load conditions:  $V = 0,25$  m/sec, counterface – hardened steel 1080)

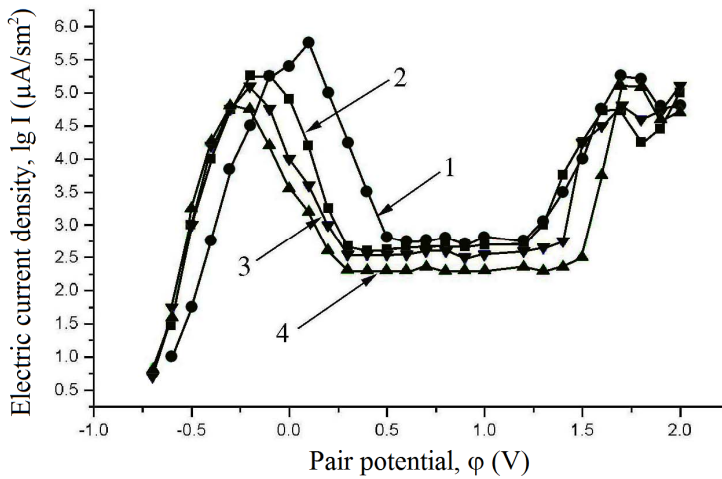


Fig. 2.6. Potentiostatic curves of the plasma eutectic coatings and the standard sample 1 – VTiNi; 2 – 12Cr18Ni9 (standard sample); 3 – CrVC; 4 – CrTiNi

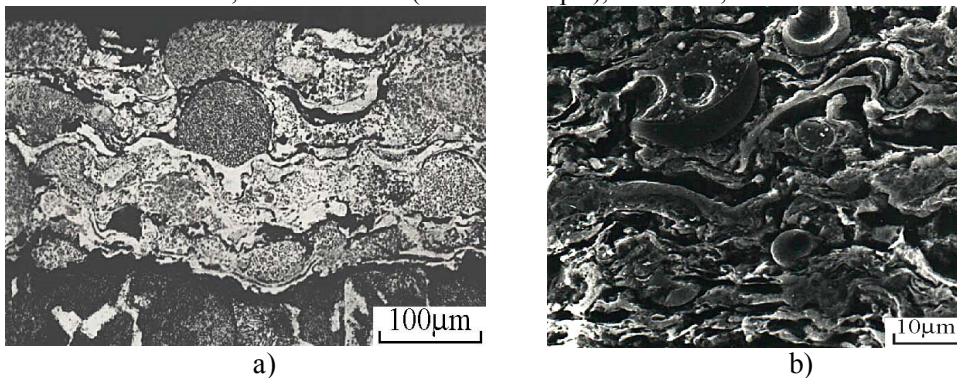


Fig. 2.7. Microstructure of the sprayed detonation eutectic coating CrVC (etched metal matrix): a) light microscope; b) SEM, etched metal matrix

Despite some minor differences in the phase composition of detonation and plasma eutectic coatings, the matrix of detonation coating is also formed by iron based solid solution ( $\alpha$ ,  $\gamma$ ) (Table 2.3). The peculiarities of the detonation spraying method affects the phase composition: different non-equilibrium compounds may appear in small amounts.

Table 2.3. Phase composition of the detonation eutectic coatings

Grade	Phase composition	Lattice parameter, nm				
		$\alpha$	$\alpha'$	$\gamma$	$\gamma'$	VC

CrTiNi (as-deposited)	$\underline{\alpha}' + \underline{\gamma} + \text{TiC} + \text{Cr}_{23}\text{C}_6 + \text{TiB}_2$	–	0.2866	0.3589	–	–
CrVC (as-deposited)	$\underline{\gamma} + \underline{\gamma}' + \underline{\alpha} + \text{VC}$	0.2866	–	0.3606	0.3684	0.4103
VTiNi (as-deposited)	$\underline{\alpha}' + \underline{\gamma}' + \underline{\gamma} + \text{VC} + \text{CrB}_2$	–	0.2876	0.3559	0.3580	0.4140

Analysis of obtained potentiostatic curves and the corrosion electric current density values depending on the applied potential to the reference electrode indicates high corrosion resistance of detonation eutectic coatings, which is comparable with the stainless steel's 12Cr18Ni9 value of corrosion resistance (Fig. 2.8).

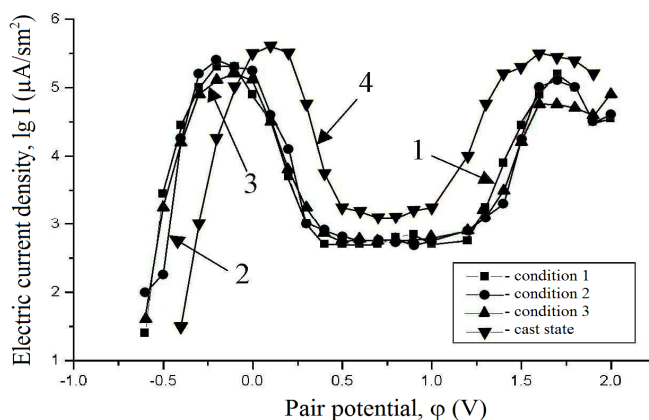


Fig. 2.8. Potentiostatic curves of the detonation eutectic coatings and the standard sample: 1 – VTiNi; 2 – 12Cr18Ni9 (standard sample); 3 – CrVC; 4 – CrTiNi

These coatings effectively form passivated films in external corrosive environment. Dependencies of corrosion effect of the eutectic coating on substrate material are not detected because corrosive environments cannot penetrate through the coating.

Analysis of the structural and phase composition of detonation coatings, their corrosion and tribotechnical properties (Fig. 2.9) indicate the corrosion and tribotechnical properties of the iron based eutectic coatings with refractory interstitial phases are mainly effected by areas of fine phases conglomeration.

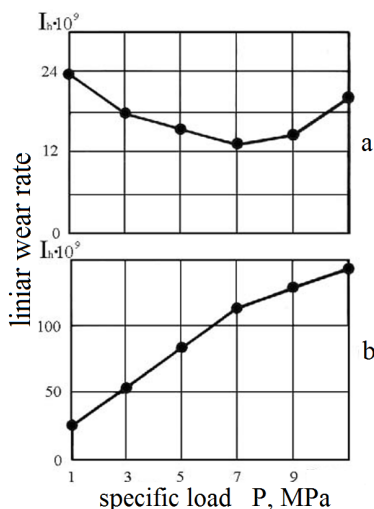


Fig. 2.9. Dependence of the linear wear rate on the specific load (slippage speed 0.25 m/sec): a) detonation coating VTiNi; b) counterbody (hardened steel 1080)

Since this is a highly non-equilibrium state, it is possible to modify the coating's properties by transferring of thermodynamic system (the coatings) to an equilibrium state. This transferring may be made in various ways: high-temperature annealing or non-all-over remelting by laser.

## 2.4. Annealing of eutectic coatings

The kinetics of changing properties of structural components of plasma coatings depending on the annealing time is shown on Fig. 2.10. For all structural components the decrease in microhardness takes place. This happens due to decomposition of supersaturated iron based solid solution.

Microhardness of the areas with a colonial structure in all three systems after annealing during  $54 \times 10^2$  sec and  $18 \times 10^3$  sec changes not significantly, than it is after annealing during  $18 \times 10^2$  sec. We assume that the initial decrease in microhardness is caused by decomposition of a metal matrix, and subsequent coagulation of interstitial phases does not lead to a significant reduction of microhardness.

The extended microhardness decrease is characteristic for the light areas with increasing the annealing time. Obviously, further coagulation of interstitial phases in the fine conglomerate phases structure leads to overageing, passing through an optimal crystal size and, consequently, reducing the strength of an iron based solid solution.

Micromodulus of light areas increases significantly after first annealing for  $18 \times 10^3$  sec, i.e. at the initial stages of decomposition, and after further soaking is

not changed. The micromodulus of elasticity increases at first stage of annealing is associated with disappear of metastable phases and decomposition of metallic solid solution. This brings the coating as a system to equilibrium state.

The change of structure and micromechanical properties of annealed eutectic coating leads to a change of tribotechnical and corrosion properties.

Fig. 2.11 shows the dependences of wear resistance of as-deposited and annealed VTiNi, CrVC, CrTiNi coatings on specific contact load at dry sliding friction. Annealing for  $18 \times 10^2$  sec is optimal for the system VTiNi and provides minimum wear of friction couple (coating and counterface). Solid oxide films are formed on the friction surface. Its composition, the coating structure characteristic for the annealing, and the properties of partially decomposed metal matrix minimize wear of the friction couple.

Magnitudes of microhardness, microelasticity, and microplasticity of main structural component of annealed coating, as well as the composition friction induced oxide films, are optimal for current friction conditions. It should be noted that the coating as a non-equilibrium thermodynamic system has a potential for further changes of its components' structure and properties being affected by other parameters of annealing, which also allows choosing the optimum structure for other frictional conditions.

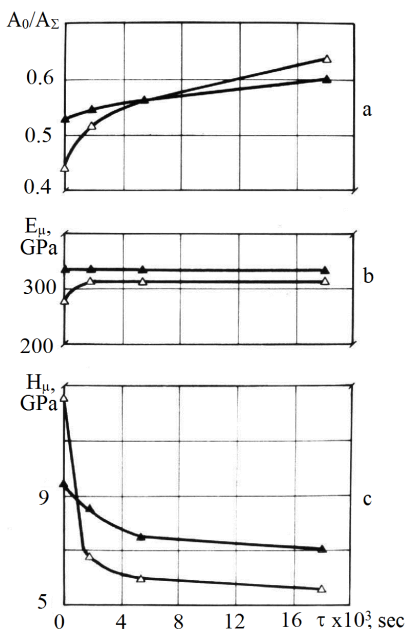


Fig. 2.10. Change of properties of light areas ( $\Delta$ ) and colonial structures ( $\blacktriangle$ ) of VTiNi plasma coating depending on annealing time ( $T = 0,75T_{melt}$ ): a – ductility,  $A_0/A_\Sigma$ ; b – modulus of elasticity,  $E_\mu$ ; c – microhardness  $H_\mu$ .

Thus, we note high wear resistance of the plasma eutectic coatings for all three systems that is provided by their structural state, ability to form protective oxide films, and degrees of strengthening in dependence on the dispersion of interstitial phases and their bonding with the metal matrix. In contrast to the cast state of eutectic with the same composition and composite strengthening mechanism (interstitial phases form bearing frame, or skeleton), for examined plasma coatings the mechanism of dispersion strengthening is realized (light areas). For dispersion strengthening the strength highly depends on the quantity, composition, degree of dispersion, and bonding of interstitial particles with matrix [53]. By controlling the size of dispersed interstitial crystals and the metal matrix state, we can vary the properties of coatings in a wide range. It is also possible to make a structure, which will have the best respond to friction. It means that the friction induced layer (which composition depends on the size and temper of strengthener and matrix, their ratio) may be controlled by heat treatment of the coating after deposition. This allows minimizing the total wear of friction couple in a wide range of parameters: material of a counterface, specific load, sliding speed, temperature and composition of the environment.

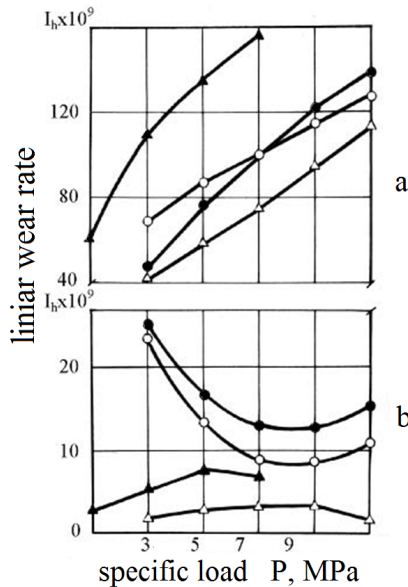


Fig. 2.11. Linear wear rate vs. specific load (sliding speed 0.25 m/sec): a) counterface (hardened steel 1080); b) plasma coating VTiNi. ▲ – as-deposited coating; Δ, ○, ● – annealed coatings for  $18 \times 10^2$ ,  $54 \times 10^2$ ,  $18 \times 10^3$  sec respectively

The areas with colonial eutectic structure did not undergo essential changes during annealing compared to the light areas since the bearing frame of the

interstitial phases has a high thermodynamic stability. Because of this its properties do not change significantly during annealing. Changes of micromechanical properties of a metal matrix for areas with colonial eutectic structure, related to its partial decomposition, do not cause significant change of properties as the metal matrix has an auxiliary role in strengthening, namely transmits and redistributes loads between different areas of the interstitial phases frame [54, 55].

It should be considered that beside the dispersion strengthening the metal matrix is solution strengthened by chromium, nickel, titanium, vanadium [56]. Changing the content of alloying elements dissolved in the matrix metal of eutectics during annealing, also changes the value of strengthening. During annealing chemical composition of solid solution and dispersed particles simultaneously change. These changes can lead both to increase and to reduction of the micromechanical properties of light areas. Thus, it is possible by annealing of the detonation eutectic coating to manage their tribotechnical characteristics changing the structure and properties of its components.

Besides changing mechanical properties, annealing also changes corrosion resistance of the coating structural components. Etching in metallographic reagent enables to observe the appearance of gray areas, which arise as a result of partial decomposition of light areas. So, annealing reduces corrosion resistance of light areas. Just as in the case of annealed plasma eutectic coatings, change of corrosion resistance of detonation coating structural components allows regulating the formation of friction induced oxide films and thereby managing their tribotechnical properties (Fig. 2.12–2.14).

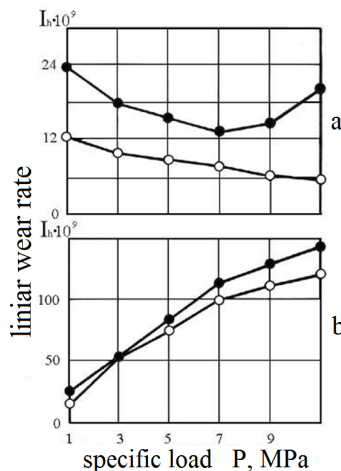


Fig. 2.12. Linear wear rate vs. specific load (sliding speed 0.25m/sec): a) detonation coating VTiNi; b) counterface (hardened steel 1080). ● – as-deposited coating; ○ – annealed coating for  $54 \times 10^2$  sec

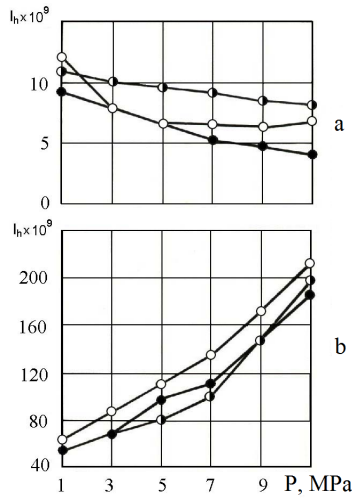


Fig. 2.13. Linear wear rate vs. specific load (sliding speed 0.25m/sec): a) detonation coating CrTiNi; b) counterface (hardened steel 1080). The coatings were annealed for:  $\circ$  –  $18 \times 10^2$ ,  $\bullet$  –  $54 \times 10^2$ ,  $\bullet$  –  $18 \times 10^3$  sec respectively

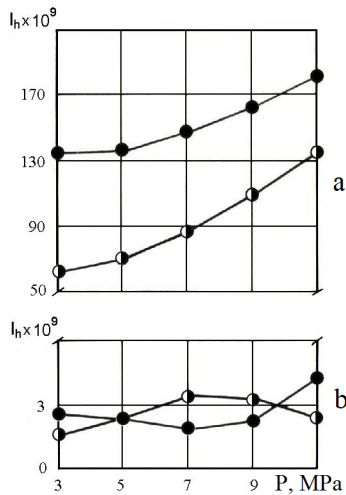


Fig. 2.14. Linear wear rate vs specific load (sliding speed 0.25m/sec): a) counterface (hardened steel 1080); b) detonation coating CrVC.  $\bullet$  – as-deposited coating;  $\bullet$  – annealed coating for  $18 \times 10^2$  sec

During wear test of annealed coating VTiNi plastic impressions have been observed (Fig. 2.15). Similar behavior is described in [58]. In [57] it is noted that alloys with high ductility in dry friction in the wide range of the specific loads have low friction coefficients.

The typical damage of friction surface for these alloys – plastic impressions. As a result of this wear process the actual contact area is increased, and surface of friction is activated that promote the formation of friction induced structures. They reduce the friction coefficient and make surface more wear resistant.

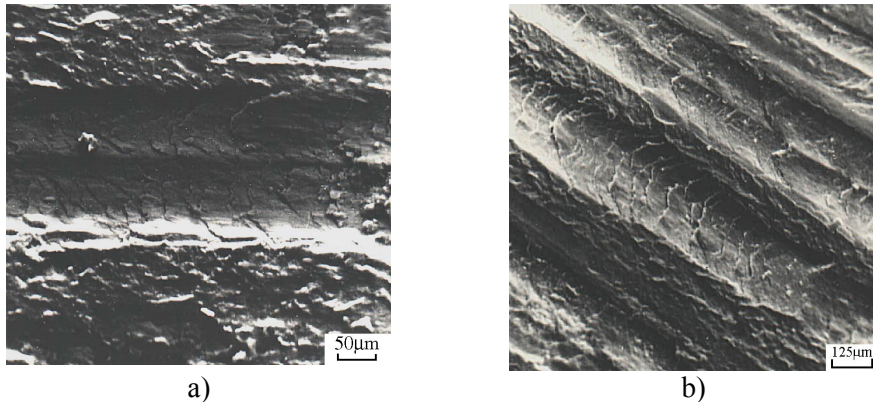


Fig. 2.15. Traces of plastic deformation on friction surface of annealed detonation coating VTiNi: a) annealing  $18 \times 10^2$  sec; b) annealing  $18 \times 10^3$  sec. SEM

It should be noted that on friction surface of annealed detonation coating there is no seizure of counterface. In the surface layers of the investigated coatings, material hardening was not detected. Therefore, the conclusion on the self-organization of friction surface through a strong plastic deformation, made in works [59, 60], is quite acceptable.

For VTiNi coating the friction coefficient reduces with increasing the specific load up to 7 MPa, followed by steady grow with further load increase (Fig. 2.16). This increase of the friction coefficient at high loads occurs due to ploughing the surface by particles of wear debris, that incorporate into the softened surfaces of friction couple. Obviously, in this case there are phenomena similar to those observed by the authors of [61] while determining the dependence of friction coefficient on sliding distance.

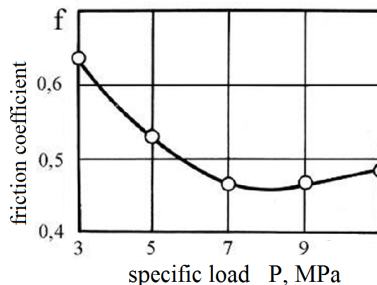


Fig. 2.16. Friction coefficient of VTiN detonation coating (annealed for  $18 \times 10^2$  sec) vs specific load

Reduction of friction coefficient with increasing of the specific load is characteristic also for CrVC and CrTiNi annealed detonation coatings, but the values of the friction coefficient are by value of 0.1–0.2 higher than for VTiNi coating. This friction regime change with increasing of specific load is agreed with [62]. Beside the formation of protective films on the friction surface some wear particles are also present (Fig. 2.15, a).

The values of friction coefficient of annealed eutectic detonation coatings are caused by the mutual action of asperities deformation under pressure of wear particles, and adhesion between flat surfaces. Relative contribution of these factors depends on conditions in a contact, which, in their turn, are determined by initial material nature and surface topography.

In the previous sections of the work it was experimentally proved, that it is possible to control the structure and properties of investigated eutectic coatings by annealing. This allows optimizing the wear rate of both coating and counterface (friction couple). The optimization effect is achieved by selection of appropriate annealing treatment of the eutectic coatings, i.e. the change of coating state is carried out without passing through a liquid phase. It was also noted that the main advantage of cast eutectic alloys compared to gas-thermal coatings of the same chemical composition is their higher macro strength. These coatings in as-cast state may be used for friction couples with higher specific loads. The physical basis of the phenomena occurring during heat treatment of plasma eutectic coatings, as well as the results of tribotechnical tests and other properties are discussed in next sections of this work

## **2.5. Eutectic coating with composite structure**

A good opportunity to control the properties of gas-thermal eutectic coatings are opened if to produce coating having areas with dissimilar properties – by alternation of regions with colonial structure and thin phases conglomerate. Since the properties of eutectic in these states are very different, changing their ratio in coatings allows providing them with desired properties. If to provide the cooling rate of the molten coating below the critical then in the coating as-cast colonial structure (formed by the mechanism of cooperative phase growth) will be restored.

In our work the possibility to improve wear resistance of eutectic coatings using combined technology: plasma or detonation coating deposition and subsequent partial melting by powerful continuous wave laser. At the same time we attempted to investigate the influence of laser emission on the state of processed eutectic coatings and to determine the optimal combination of equilibrium and non-equilibrium structures in order to provide high tribotechnical properties.

All coating formed by the gas-thermal method are porous with different densities. This brings certain features in the process of their laser processing. In [64] it is noted that during remelting of porous materials formed by cold compacting and following sintering, in the surface layer intensive energy absorption takes place, causing its partial melting and even evaporation. It is established that with decreasing of material porosity smaller zone of melt are formed. However, in [63, 64] were studied mainly physicochemical properties, structure and phase transitions, phenomena of mass transfer in porous materials exposed to laser emission. There was very little attention to tribotechnical properties of laser treated porous surfaces.

We conducted investigations to determine the effect of laser melting of the coatings formed of powders of iron based eutectic alloys with refractory interstitial phases on their tribotechnical properties.

For restoration of the colonial structures as-cast eutectic on a part of coating area, gas was used continuous CO<sub>2</sub>. It has the following beam parameters: wavelength 10,5 μm, power – 0,8 kW, focused spot diameter –  $2 \times 10^{-3}$  m, relative scanning velocity –  $3,3 \times 10^{-3}$  m/sec (beam is fixed, specimen is movable).

The action of continuous beam allows rapid heating to a liquid state and subsequent sufficiently slow cooling of the coating by adjusting the scanning velocity or power emission density. These parameters are chosen experimentally to provide remelting of the coating through the thickness. The melt zone reaches the interface between the coating and the substrate, but does not lead to a significant mixing of the coating and substrate materials. This results in the effect of adhesion increasing by metallurgical interaction at the interface, and simultaneously colonial structure in the coating was formed.

The action of continuous laser resembles slow heating alternatives, such as heating by flame torch of a gas burner or by induction heater. A continuous laser beam may be interrupted (power-off period) and moved at any given speed. It is possible to change power density, thus controlling the material heating and cooling rates. For continuous beam the uniformity of temperature field of melt pool will be higher than for pulse laser processing.

Formation of melt pool is a complex thermomechanical process that is determined by the thermophysical properties of material, laser energy parameters and thermal characteristics of the sample [65, 66]. A number of studies [68–73] confirm advantages of non-all-over (selective) laser treatment of surfaces, working in conditions of friction and wear. Thus, the treatment of internal cylindrical surfaces of sleeves to form individual longitudinal laser treated strips allowed increasing their wear resistance by an order of 10 compared to regular heat treatment.

In our work the discrete laser treatment was implemented, according to which the irradiated (molten) area was ranged from 5 to 100% of the surface area. Location of remelted zones is shown in Fig. 2.17.

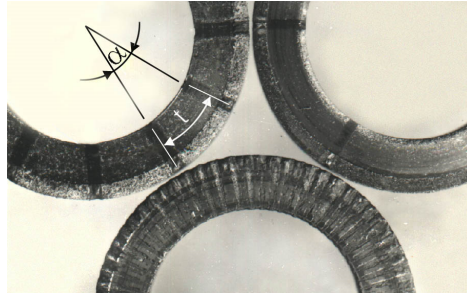


Fig. 2.17. The location and geometry of molten zones:  $t$  – the arc length between molten zones;  $\alpha$  – central angle between molten zones

Under the action of laser irradiation in the surface layer of the eutectic coating a melting zone with colonial structure is formed. This is shown on microsection of CrTiNi plasma coating (Fig. 2.18). Beside the melting zone in which the eutectic crystals of interstitial phases are oriented towards maximal heat removal, in the surrounding areas of untreated coating two zones may be distinctly seen (Fig. 2.19): transition and heat affected zone. The transition zone contains coarser eutectic crystals and is etched substantially (Fig. 2.19, b). Heat-affected zone with partially decomposed light areas, which become gray after etching, is shown in Fig. 2.18, c. Heat affected zone is similar in structure and etching degree to short time annealed plasma coating of the same composition (Fig. 2.18, a). The maximum cooling rate, which determines the minimum size of colonial eutectic crystals, is seen at the surface layer of melt pools. This agrees with well-known provisions of temperature gradient distribution [71].

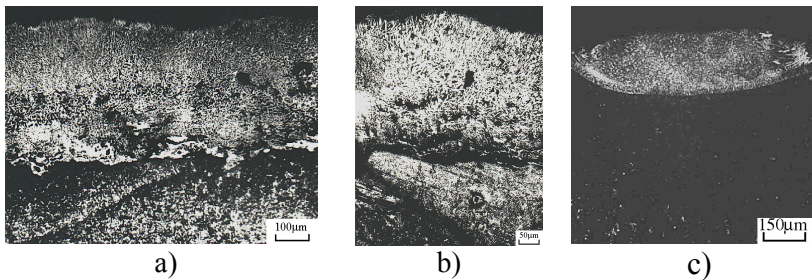


Fig. 2.18. Microstructure of laser melted gas-thermal coatings CrTiNi: a) plasma coating, the middle zone; b) plasma coating, the transition area; c) detonation coating

It should be noted that similar structures arise after the laser processing of VTiNi and CrVC plasma coatings (Fig. 2.19). The etched region with typical colonial as-cast structure state is adjacent to partially decomposed iron based solid solution. Further it changes to initial structure – fine phase's conglomerate (light area).

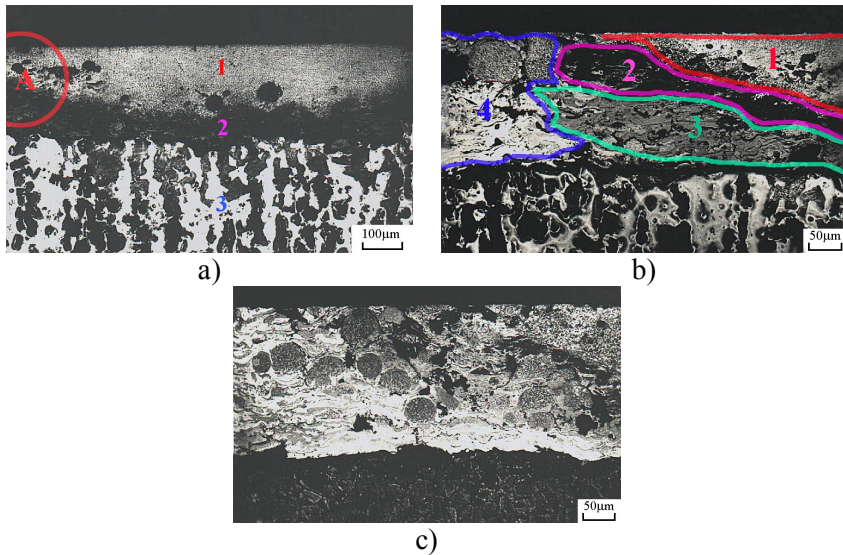


Fig. 2.19. Microstructure of remelted plasma coatings: a) VTiNi, 1 – zone of remelting, 2 – transition zone, 3 – substrate; b) VTiNi region A, 1 – zone of remelting, 2 – transition zone, 3 – heat affected zone, 4 – untreated coating; c) CrWSi coating

The transition zone and the heat affected zone are located equidistant from the melting zone that indicates high enough temperature field symmetry around the laser spot. On metallographic cross-section heat-affected zone in all cases has segmented shape that is characteristic for heat-conductive heat diffusion [72, 73].

Grains of powders with colonial structure located in the transition zone have not significantly changed structure, and thus the properties change is also insignificant.

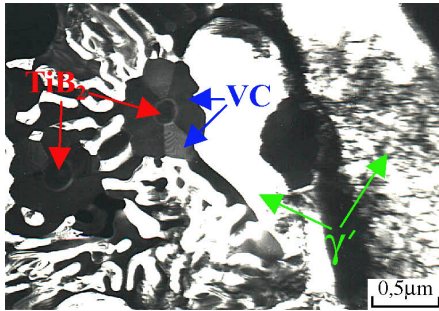
It should be noted that the microhardness of near-surface zone and areas with large colonial eutectic crystals of remelted CrTiNi coating approximately are the same and is 9.5–10 GPa (load  $P = 0.98$  N). The transformations taking place in the solid state of the light areas after laser treatment reaffirm their structural instability: the first stage of the decomposition of light areas is their transformation into gray areas, which partially collapsed.

Similar structural changes for the same eutectic plasma coatings containing light areas were observed after high-temperature annealing. The area, which was remelted, has colonial structure with eutectic crystals of varying thickness (Fig. 2.18). The fine colonial structure is characteristic for laser affected spots. On the borders of the melt zone, where liquid cooling rate steadily decreased, coarser crystals are located.

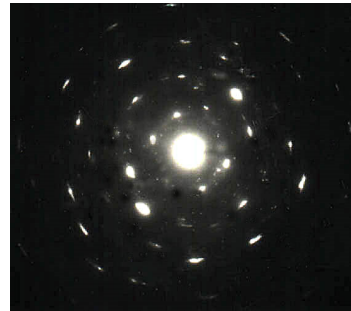
A TEM examination of thin-films cut from the local laser remelted zone of gas-thermal VTiNi coatings and the heat affected area allowed to detect the

whole spectrum of phenomena caused by various cooling conditions (Fig. 2.20). Directly in the remelting zone we can see crystals in the form of flower sockets, consisting of titanium diboride (Fig. 2.20, a), located in the center, from the faces of which, as a rule, 5–6 crystals of vanadium monocarbide grow (Fig. 2.20, a, c). In the intervals between these basic crystals, a characteristic of the cast state colonial structure is present, which forms as a result of cooperative growth of solid phase. The cooperative growth of crystals of eutectic colony begins on the faces of vanadium monocarbide crystals (Fig. 2.20, c).

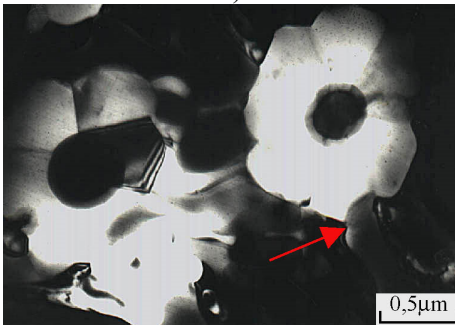
In the area located on the boundary of remelted zone and heat affected area, similar crystals having form of flower sockets are observed, but without elements of cooperative growth structure: they are surrounded by a metal matrix –  $\gamma$ -iron based solid solution (Fig. 2.19, c). Differential density of dislocations and the values of internal stresses lead to a strong unevenness of the electro-polishing of metal matrix during films preparation, so their thickness and, consequently, contrast, vary widely in different sections.



a)



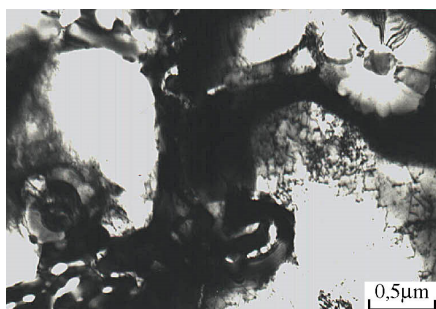
b)



c)



d)



e)

Fig. 2.20. The structure of laser melted zone of VTiNi plasma coating. TEM. a) basic crystals  $TiB_2$ ; b) VC and c) zone of cooperative eutectic growth, dark field; d) nucleation of eutectic colony from VC crystal surface, light field; e) dislocations in  $\gamma'$  solid solution

## Conclusions on section #2

1. It is established that in the investigated eutectic alloys, when the critical cooling rate is reached, a change in the crystallization mechanism occurs with the formation of a fine phase conglomeration. In eutectic alloys with this structure, there is a dispersion strengthening mechanism, and they have higher plasticity in comparison to cast eutectic alloys of the same composition.

2. A method for production of powders of iron based eutectic alloys with refractory carbides and borides by melt spraying was developed. It is shown that at the cooling rates above the critical ( $V_{cr} = (4-5.3) \times 10^5$  K/sec) in powders a fine phase conglomeration is formed in which the mechanism of dispersion strengthening is realized.

3. The laboratory coatings deposition technologies of examined eutectic alloys by methods of plasma spraying and detonation method have been developed. Laser remelting modifies the coating, changes its phase composition and structure. It was proven that in the obtained coatings, when the critical cooling rate is reached, a fine phase conglomeration may be produced. Laser treatment is an effective method of modifying the properties of these coatings. Laser remelting with controlled cooling rate returns coating material to as-cast state.

4. The properties of obtained eutectic coatings may be varied in a wide range by means of high-temperature diffusion annealing, as well as laser remelting, which allow to reproduce the optimal structural and phase states necessary for heavy duty operating conditions

5. Alloying of metal matrix of examined eutectic alloys with chromium, nickel and other elements allows to provide the necessary level of corrosion resistance while simultaneously preserving the original structure and mechanical properties.

### **3. DEVELOPMENT OF INDUSTRIAL TECHNOLOGIES OF EUTECTIC COATINGS DEPOSITION**

#### **3.1. Formation of structure and tribological properties of eutectic coatings**

One of the directions of strengthening of working surfaces of structural metallic materials is the application of coatings using laser, plasma-, gas- and other techniques. As a powdery feedstock material for the coatings, the very promising are the eutectic alloys, because they have a low melting point (1200 °C), and with an increase in cooling rate above  $10^4$  °K/sec, can significantly change their structure. The peculiarity of the eutectic transition is the formation, in the process of crystallization, of fine, much branched crystals of strengthening phases, which create a framework for reinforcement of metal matrix. This structure, in contrast to dispersion-hardening and disperse-hardened materials, makes it possible to combine in alloys various properties of the source components including high heat resistance, to change the shape and size of inclusions, the ratio of the mechanical properties of matrix and the strengthening phases, that is, significantly affects the physico-mechanical properties.

##### **3.1.1. Coatings deposited with use of concentrated energy aflows**

Since the non-equilibrium eutectic structure is formed by the method of crystallization from liquid state, it is more appropriate to use the methods for obtaining eutectic coatings, using which the deposited material passes through the liquid phase, in particular, high-frequency current (HFC), laser, plasma [74, 75].

For coatings it is possible to use powders of eutectic alloys of systems  $12\text{Cr}18\text{Ni}9\text{Ti-TiB}_2$  (TiNi alloys),  $12\text{Cr}18\text{Ni}9\text{Ti-TiB}_2\text{-CrB}_2$  (CrTiNi) and  $12\text{Cr}18\text{Ni}9\text{Ti-TiB}_2\text{-BC}$  (VTiNi). The metal matrix of alloys has chemical composition of austenitic steel  $12\text{Cr}18\text{Ni}9\text{Ti}$ , and the reinforcing compounds are diborides of titanium and chromium and vanadium monocarbide [76].

##### **3.1.1.1. Methods of cladding**

**Cladding by HFC.** The powder mixture of eutectic alloys is melted directly inside of the rotating product. In this case, proper conditions are created for the entire process of cladding (heating the product, melting the powder mixture, saturation of the reinforced layer of the metal, crystallizing the liquid phase) and providing a strong bond of eutectic coating (EC) with the base metal. The process of coating deposition to the interior surfaces of rotation bodies using heating by HFC is as follows. In the closed end of the cavity of the sleeve, the powder

mixture is filled. To the rotation body rotational motion of a certain angular velocity is given. With the help of an inductor, the part is heated, and after melting the powder mixture is cooled [77].

The structure of obtained coatings is the same as that of alloys made in electric arc furnace with a cooling rate of about 400 °C/sec (Fig. 3.1). The thickness of the titanium diboride crystals is somewhat finer and due to the intensive mixing of the components in the liquid state a regular alternation of the metal and boride phases is observed (Fig. 3.1, a).

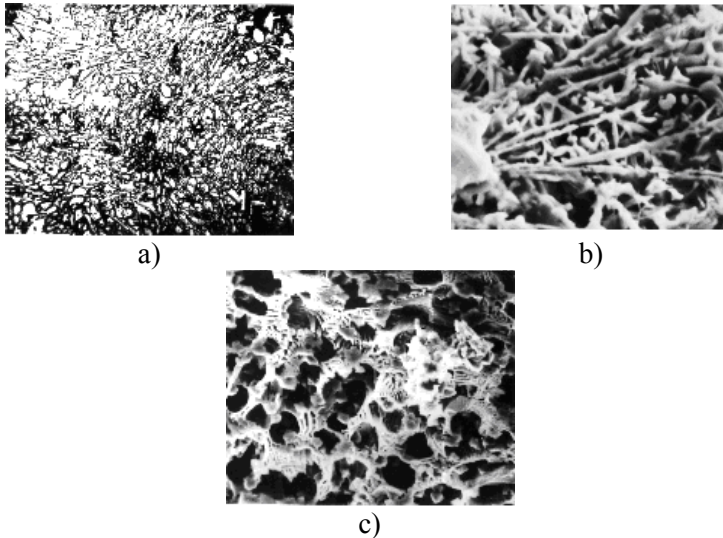


Fig. 3.1. Microstructure of a, b) TiNi and c) CrTiNi eutectic coatings: a –  $\times 312$ ; b, c –  $\times 2700$

**Plasma cladding.** The main advantage of plasma cladding is a wide range of regulation of gas dynamic of the process.

The cladding was carried out by UMP-6 plasma spraying system or a small plasma torch on a microplasma spraying system MPU-4. The essence of plasma cladding is the local melting of metal substrate by plasma torch, the interaction of melted powder with the melt pool on substrate surface and crystallization to form a deposited layer.

The results of metallographic examinations have proven that the structures of eutectic coatings, deposited by the plasma method and using HFC heating, are dissimilar (Fig. 3.1, a; 3.2). This is due to different sources of heating and the duration of heating. For plasma cladding, crystallization and the formation of coatings occurs usually under normal air cooling rates. The heating by HFC has longer process duration. In the case of centrifugal bimetalization of the sleeve with a diameter of 100 mm and a length of 150 mm it lasts for 6 minutes.

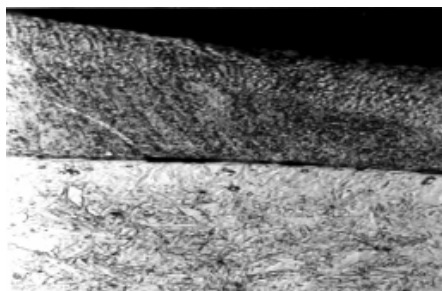


Fig. 3.2. Microstructure of plasma claded TiNi coating,  $\times 250$

The structure of coatings obtained from eutectic powder material on steels 1080 (0.8 of carbon), 12Cr18Ni9Ti by plasma cladding, consists of dendrites of austenitic matrix and strengthening phase, oriented predominantly perpendicular to the substrate surface. The size of dendrites in the transverse section is 2–6  $\mu\text{m}$ , and the minimum distance between the second order dendrites axes is 0.5–1.0  $\mu\text{m}$ , what corresponds to the cooling rate of about  $10^4$ – $10^5$   $^\circ\text{K}/\text{sec}$ . The fusion zone is a solid solution of titanium, vanadium, chromium in  $\gamma$ -Fe and has a thickness of about 5–7  $\mu\text{m}$ .

The structure of the coatings depending on the composition of the feedstock material is eutectic, eutectic, primary crystals of strengthening phase or solid  $\gamma$ -solution.

Eutectics as the main structural component of the coatings requires a thorough analysis. After melting the powder and cooling the liquid of the eutectic composition, the nuclei of the strengthening phases (interstitial phases) are formed first. They become the nuclei for the growth of the eutectic colonies intergrowing with metal matrix (Fig. 3.1, b). Each such colony is a bicrystal formation, the skeleton of which is lamellar or rod-shaped single crystals of the interstitial phase. In the intervals between these crystals a metallic matrix phase solidifies. If the pre-eutectic alloys containing the primary dendrites of a metal matrix are crystallized, then the base crystals on which the eutectic colony is formed will also be the reinforcing phases ( $\text{TiB}_2$ ,  $(\text{TiCr})\text{B}_2$ , VC). The dispersion of the eutectic structures of plasma coatings is higher than that of the coatings obtained by the HFC heating. In this case, the dispersion of the eutectic coatings of the VTiNi alloy is higher than that of TiNi and CrTiNi alloys. Consequently, the greater the degree of alloying of eutectic alloy, the more impurities are there in it, the higher is its dispersion (volume fraction of the strengthening phase: for the VTiNi – 21.2%, TiNi – 20%, CrTiNi – 13%). A characteristic feature of eutectic structures is that the increase in degree of their supercooling causes the formation of predominantly plate-like, rather than columnar structures of the colonies. Thus, the structure of eutectic colonies is less dependent on the nature

of the components (metal interstitial phase) than on the composition of alloys and the conditions of crystallization [32].

**Laser cladding.** The best properties, wear resistance in particular, are provided by laser cladding due to the formation of ultrafine structures. During the melting of the powder and the subsequent rapid cooling, a structure typical for compact material is formed. On the boundary of the substrate and the coating the interdiffusion processes provide good coating adhesion.

To obtain a high adhesion of coating with limited content of substrate components, preserving the initial properties of powder being cladded, to get high performance, the melt-to-solid contact time should be minimized. Laser may also provide high heating and cooling rates of powder feedstock material. The material overheating and evaporation are also avoided. Therefore, among the proposed coating methods (HFC, plasma and laser) laser-cladding should be preferred, since in this case powder material does not overheat, although this increases the probability of cracking increases, and residual stresses in the coating also rise.

The optimum melting temperature of the powder material is the interval between Solidus and Liquid lines. Underheating reduces the quality of fusion powder particles between themselves and to the substrate, and overheating, in turn, leads to a significant coarsening of the structure. In both cases there is a decrease in coating performance.

The advantages of cladding using high energy flow heating are that their use makes it possible to obtain high-quality coatings at lower temperatures.

Laser cladding is performed by a continuous CO<sub>2</sub> laser "LATUS-31" or laser "QUANT-16". These types of lasers have high output power, relatively high efficiency and stability of radiation parameters. The high specific power of sources ( $10^7$  W/cm<sup>2</sup>) provides the localization and short-term action of lasers on the material, reducing their heating and deformations during cladding.

Structures of coatings deposited by plasma and laser methods differ significantly (Fig. 3.2, 3.3). This is due to a different energy density (plasma energy density is about  $10^3$  W/cm<sup>2</sup>). In the case of plasma cladding, coatings solidify at conventional air cooling rates. The rapid heating and melting of the powder in the case of laser cladding ensures the crystallization in the conditions of high-speed heat transfer, directed towards a near-cold substrate.

A comparative analysis of structures of coatings produced by laser, plasma melting and HFC heating indicates a higher degree of dispersion of structures after laser treatment. The refining of proeutectic crystals of strengthening phase, as well as of eutectic, is much higher than that of plasma coatings. In the coatings deposited on 12Cr18Ni9Ti steel, high etching areas similar to martensitic needles are observed, (Fig. 3.3, a). They are the areas with finely dispersed structure. The result of metallographic analysis indicates the presence of well-defined texture – proeutectic constituents: the reinforcing or austenitic phases in the cladded

coating are oriented towards the clad surface (Fig. 3.3, a, b). During plasma cladding, this phenomenon is not observed (due to lower cooling rates). The studies using stereometric metallography method did not detect pores in a laser clad layer.

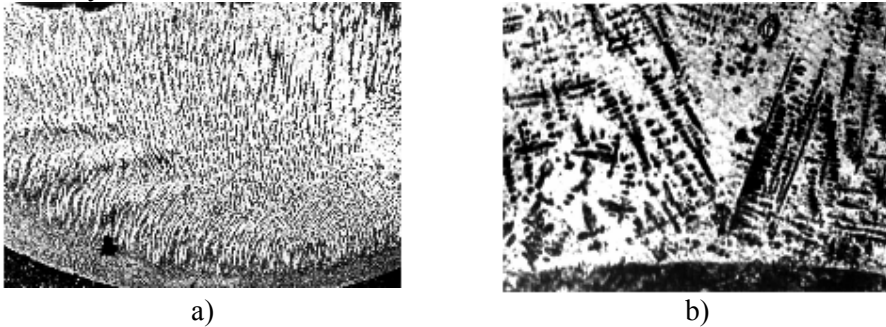


Fig. 3.3. Microstructures of laser clad coatings a) TiNi and b) VTiNi,  $\times 156$

Compared to other methods of cladding, the hardness of laser coatings is the highest, what is explained by higher degree of dispersion of structural components. However, in places with low content of strengthening phases (proeutectic composition), the hardness of plasma and laser coatings are approximately the same. This is due to the high cooling rates of the laser coatings, the formation of saturated  $\gamma$ -solution, and lesser amount of eutectic and boride phases compared to the plasma coating [78].

### ***3.1.1.2. Wear resistance of clad coatings***

Physical and chemical processes, changing the phase-structural state of metal surface layers arise and develop during the operation in conditions of friction and wear. The subsurface layer is also affected by this process. At high temperatures, due to considerable acceleration of adsorption and chemical processes on the surface, physical and mechanical properties of metals, as well as the properties of surface layers changed under the influence of operation conditions (normal loads, temperatures, etc.). Thus, the friction coefficient, wear rate are closely related to the characteristics of the material and changes of properties of contacting surfaces (hardness, structural state etc.) on one hand. On the other hand – they are related to phenomena of plastic deformation, the phenomena associated with heating and cooling and on the third hand, they are related to the change in the composition of the surface layers due to their interaction with medium, diffusion of elements in the alloy due to high temperature gradients or mass transfer phenomena. Therefore, to determine the tribotechnical properties of coatings, an integrated method of studying the characteristics of friction and wear is used. This makes it possible to thoroughly investigate the processes that arise and develop on friction surfaces in a wide range of temperatures.

The investigation of effect of strengthening phase volume fraction (for example,  $TiB_2$ ,  $CrB_2$ , VC) on the tribotechnical properties of coatings has shown that for all methods of cladding with increasing content of strengthening phases, the wear resistance increases. However, the nature of this effect is dissimilar for each method of coating. So, for coatings obtained by HFC heating, the dependence of wear on the  $TiB_2$  content remains the same as for cast alloys, but the absolute values for alloys with a larger content of eutectics differ significantly. Coatings of only the eutectic structure (with a mass fraction of  $TiB_2$  – 13%) have wear resistance twice as high compared to as-cast alloy of the same composition. The total wear of the coating and counterface made of heat resisting alloy ZhS6K is minimal for eutectic composition. The wear loss of counterface, depending on the content of titanium diboride in the coating is almost constant.

In the process of friction, large plastic deformations occur at a depth up to 50...100  $\mu m$  (Fig. 3.4, a) and the structure of the metal changes. The surface layer consists of small debris of  $TiB_2$  particles in the matrix, and the deeper layer has an initial structure (Fig. 3.4, b). At high temperatures, processes of coagulation and coalescence of the strengthening phase take place (Fig. 3.4, c).

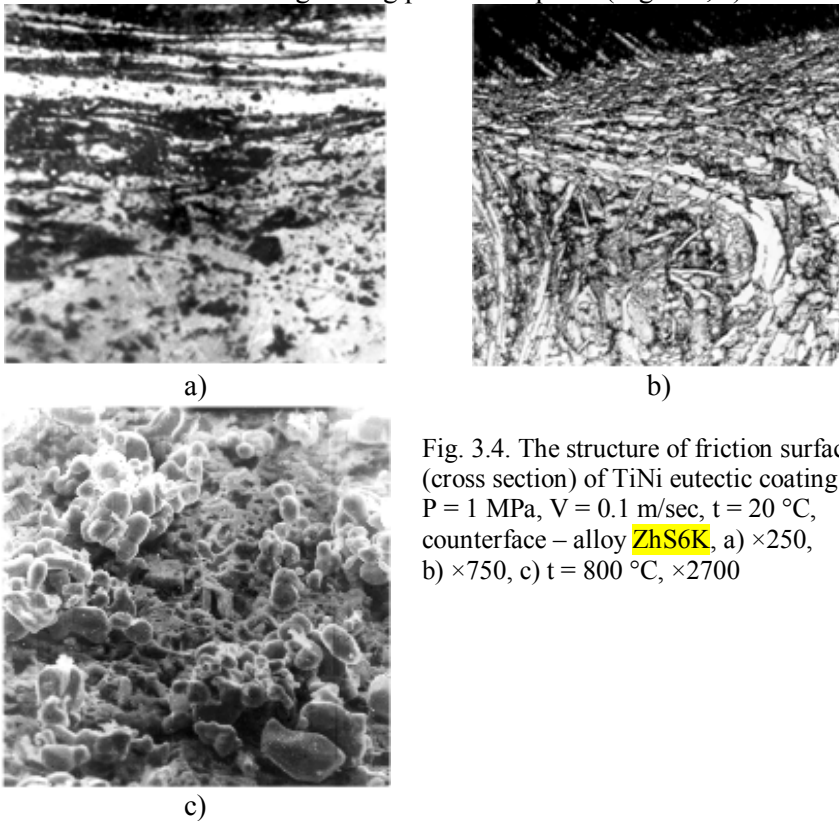


Fig. 3.4. The structure of friction surfaces (cross section) of TiNi eutectic coating:  $P = 1 \text{ MPa}$ ,  $V = 0.1 \text{ m/sec}$ ,  $t = 20 \text{ }^\circ\text{C}$ , counterface – alloy ZhS6K, a)  $\times 250$ , b)  $\times 750$ , c)  $t = 800 \text{ }^\circ\text{C}$ ,  $\times 2700$

A more thorough study of wear resistance of eutectic coating has indicated that in a wide range of friction conditions (temperature 20...800 °C, specific load – 1.0...5.0 MPa, sliding speed – 0.1...1.9 m/sec) the wear loss of eutectic coating is lower than that of a cast alloy. The superior advantage of eutectic coating is observed at a room temperature and high specific loads (about 5 MPa). Most probably in this case, as well as in a cast alloy, the mechanism of composite strengthening is implemented.

However, the thickness of TiB<sub>2</sub> strengthening crystals is finer, and, hence, the dispersion of the phases is higher, since the bulk ratio between them does not change and the efficiency of the strengthening of such crystals increases. This leads to a decrease in the level of plastic deformation in the friction zone, which increases the wear resistance of the coating compared to a cast alloy, especially at elevated temperatures, when the material degrades faster. At the same time, during the cladding, due to the temperature gradient, a better defined directional-oriented structure is formed, which is more effective under friction conditions. It should be noted that wear resistance of the hypoeutectic laser cladded coatings compared to hypoeutectic plasma coatings is lower.

The nature of the dependence correlates with a similar dependence of the change in the hardness of the laser cladded layers. This is due to the greater disequilibrium of crystallization processes of coatings, as well as the high oversaturation of solid solutions in the case of rapid cooling. The structure of coating, deposited using powders with initial eutectic structure, becomes hypoeutectic. However, this property is noticeably manifested only at small quantities of strengthening phase, when the main phase is a solid solution based on the metal component of alloy. With the increase in the content of interstitial phases, the wear resistance is more influenced by the increased amount of eutectic phase, its dispersion and texture.

Laser cladding, in comparison to plasma and HFC heating, significantly increases the wear resistance of the coatings made of hypereutectic alloys with proeutectic diboride crystals. The presence of proeutectic crystals of strengthening phase in hypereutectic alloys results in increased brittleness and tendency to cracking at significant specific loads. This leads to a higher wear loss compared to pure eutectic alloys. However, due to high crystallization rates during laser cladding and formation of supersaturated solutions, the amount of proeutectic crystals and their sizes decrease, and the coating changes its structure towards the eutectic one.

The examination of friction surfaces using raster electron microscope revealed the difference between the mechanisms of wear of coatings, deposited with laser, plasma and HFC heating. The friction surface of coating, deposited with the HFC heating looks like after an abrasive wear. Brittle particles of strengthening phases that are crushed during friction charge into the surface of the counterpart and act as abrasive seeds, whereas the friction surface of the laser cladded coatings do

not have traces of brittle destruction. High temperature wear resistance (850 °C) of a laser cladded coating is higher than that of deposited by HFC. The net wear loss of coating deposited by HFC is 35 mg/(cm<sup>2</sup>km), and wear loss of laser cladded – 12.5 mg/(cm<sup>2</sup>km).

Typical microstructures of friction surfaces of cladded coatings are shown in Fig. 3.5, in particular, the processes of microwelding (Fig. 3.5, a), fatigue failure (Fig. 3.5, b), and intense oxidation at a test temperature of 800 °C. (Fig. 3.5, c) are shown.

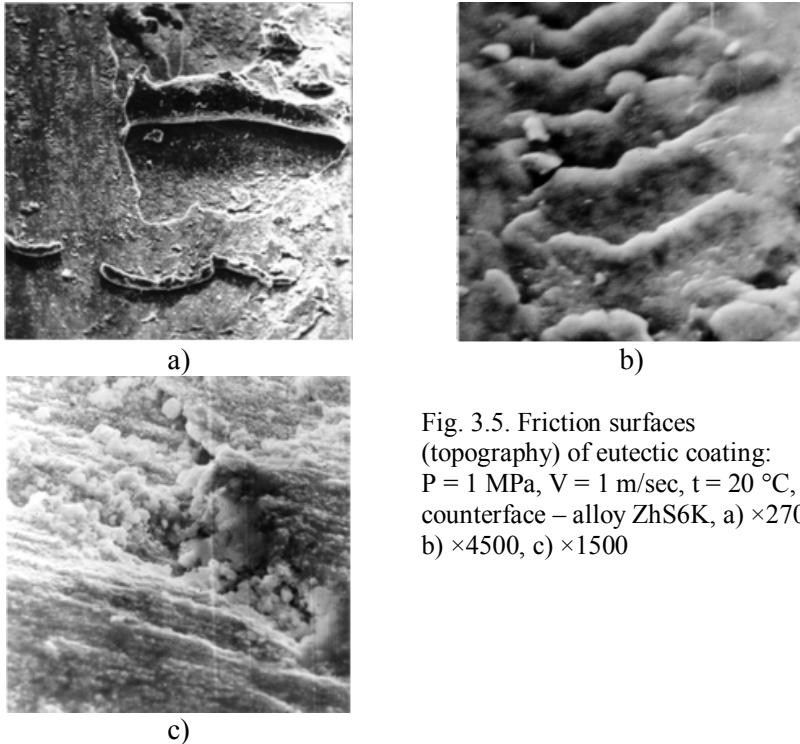


Fig. 3.5. Friction surfaces (topography) of eutectic coating: P = 1 MPa, V = 1 m/sec, t = 20 °C, counterface – alloy ZhS6K, a)  $\times 2700$ , b)  $\times 4500$ , c)  $\times 1500$

The effect of temperature on friction process is related to the change in properties of surface layers. The most important factor of heating conditions is the reduction of strength of material and increase of oxide layer thickness.

A significant plastic deformation and the effect of high temperatures lead to a significant change in structure of friction layers. It is these changes with the formation of friction induced structures that determine the wear processes, accompanied by the deformation of friction layers. At high temperatures friction is localized in thin layers and the wear loss often occurs by spallation and removal of oxide films from the contact surface.

HFC cladded coating is characterized by more intense formation of oxide films of varying thickness. This happens due to the differential oxidation of structural components. Cracks are formed on the friction surface, wear particles are crushed. At the same time, the layer of friction induced structures – oxides on the friction surface of laser coating - is thinner. Traces of brittle destruction were not found. Such a character of formation of friction induced structures on the laser coatings can be explained by a high degree of differentiation of the constituent structures with dissimilar properties and oxidation reactivity. The increase of heat resistance of laser coating is due to the decrease in its heterogeneity due to the formation of supersaturated solid solutions. Thus, with increasing wear resistance of the coatings, methods of cladding can be placed as follows: HFC cladding → plasma cladding → laser cladding. In this case, for deposition of coatings using powdery feedstock materials of hypoeutectic composition, the advantage should be given to plasma cladding [28, 79].

### 3.1.1.3. Plasma cladding

The rate of crystallization of eutectic systems in the case of plasma spraying ( $10^4$ – $10^6$  °C/sec) changes in fact the mechanism of crystallization of alloys. At the same time, finer than cast colonial structures phase conglomerates are formed: the phase composition does not change, only the mechanism of strengthening changes. For these cooling rates, formed phases and structures are usually in a metastable non-equilibrium state, which should contribute to their structural self-organization during friction.

Powders of eutectic alloys of three systems are used for coatings: TiNi, VTiNi and CrTiNi. The initial powders contain dispersed crystals of interstitial phases, and the size of these crystals depend on the cooling rate of the powder in the process of its production, that is, on diameter of particles (Table 3.1).

Table 3.1. The dependence of CrTiNi eutectic powder crystallization rate and size of eutectic crystals on powder particles diameter

Particle diameter, $\mu\text{m}$	Thickness of crystal, $\mu\text{m}$	crystallization rate $V, \text{ }^\circ\text{K/sec}$	lg, v	Note
-	3.5	20	1.3	Cast alloy
240	2.0	$5 \times 10^4$	4.7	-
150	1.2	$8 \times 10^4$	4.9	-
58	0.3	$3 \times 10^5$	5.48	-
35	-	$6 \times 10^5$	5.78	No crystals

In sprayed eutectic coatings there are weakly-etched areas, light areas, non-melted or partially melted particles and a small amount of pores (Fig. 3.6, a, b).

Porosity is an important characteristic of plasma coatings. On one hand, it is a by-product of the spraying conditions, which may be a parameter for optimizing the spray process, and on other hand, it directly affects the effectiveness of protective properties of coatings (corrosion resistance, heat resistance, etc.), their thermal and electrical conductivity, mechanical and other characteristics. The porosity of these coatings is relatively small (about 10%). In addition to it, there are gray layers in coatings that are marked by etching color.

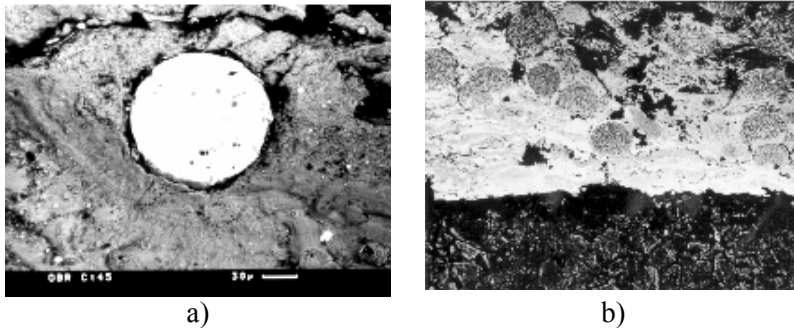


Fig. 3.6. Microstructure of VTiNi plasma coating: a) surface general view (steel 1045); b) cross section, substrate – steel 1080 ( $\times 500$ )

The main volumes of coatings are light, weakly etched (70–80%) areas. The formation of light areas by spraying is definitely due to the features of eutectic iron based alloys. They apparently arise due to rapid crystallization of liquid droplets on a cold substrate. Such layers have high chemical resistance; they almost do not interact with the etchant used to determine the structure of the alloy before spraying. Exploring the structure of light areas is difficult due to high dispersion of phase components. Since the eutectic systems under study are prone to the formation of ultrafine structures at the indicated cooling rates, light areas may even appear in amorphous state. [80].

A characteristic feature of sprayed coatings is higher (compared to the cladded) microhardness. A precondition for this may be the implementation of the dispersion hardening mechanism in plasma sprayed coatings, in contrast to the predominantly composite mechanism of cladded eutectic coatings. Light areas in particular have high microhardness. Their microhardness at a load of 0.98 N is 12.7 GPa, and untreated particles and areas with eutectic structure have hardness of – 8.7 GPa. The microhardness of coating gradually drops down from coating surface towards the substrate.

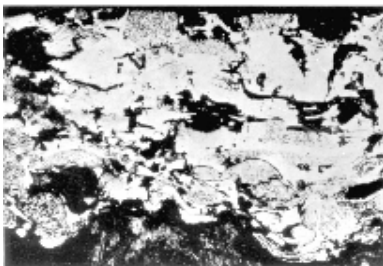
The results of studies indicate a low adhesion of plasma sprayed coatings to the substrate (16–20 MPa). Such level of adhesion means, apparently, a large gradient of properties (from a fairly hard coating to a soft substrate), and hence,

large stresses in the interface, as well as the nature of bonding of sprayed coating with substrate.

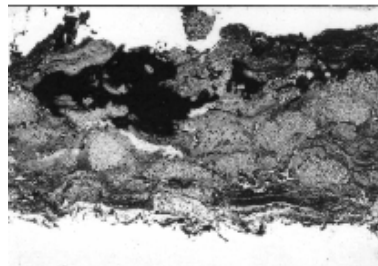
#### ***3.1.1.4. Wear resistance of plasma coatings***

The wear resistance of eutectic alloys in cast state is worse than in form of coatings. High results were obtained by covering parts of equipment for food processing industries by plasma eutectic coatings. The obtained data confirm high wear resistance of the coatings. Increased dispersion of interstitial strengthening phase and its uniform distribution in the iron-based coatings create preconditions for inverse consecutive structural transformations during the transition to a new state when coating is affected by high plastic deformation and local heating in friction zone. In addition to this, the non-equilibrium state of eutectic plasma coatings, obviously, contributes to the structural self-organization during friction. The wear intensity and friction factor vs. specific load for VTiNi and CrTiNi eutectic coatings shows that in both systems of coatings, friction factor is reduced with increasing load. The nature of the wear of VTiNi and CrTiNi coatings is similar.

On cross-sectional microphotographs of samples after wear test it is clearly seen that the areas with eutectic structure (in VTiNi coating) appear on the friction surface (Fig. 3.7, a). They determine the extent of wear loss and the nature of wear intensity dependence on specific load, which corresponds to previously obtained data for as-cast material. Sections of light areas placed between eutectic sections, due to their low plasticity and lack of cohesion, wear away. Deteriorated debris of solid light areas, being spalled off into the friction zone, acts as abrasive powder (Fig. 3.7, d). In this case, the wear of the contiguous couple is intensified. The brittle fracture on the friction surface is clearly seen for CrTiNi plasma coating (Fig. 3.7, c). At the specific loads of 8 MPa, the denting of the coating is clearly seen (Fig. 3.7, b).



a)



b)

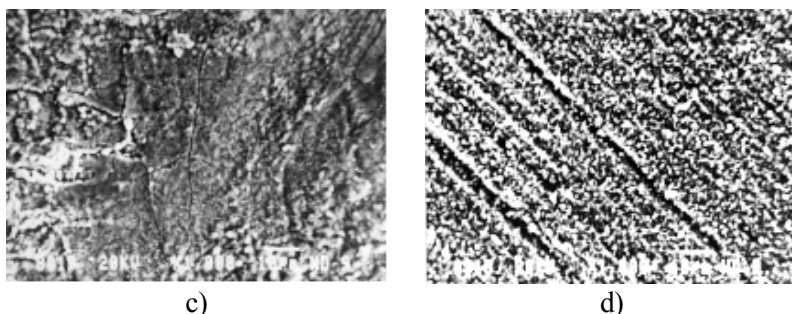


Fig. 3.7. Microstructure a, b) of plasma VTiNi-powder coating,  $\times 200$ , and c, d) wear scar,  $\times 500$

Dissimilar oxidizing ability of coatings structural components during friction can be indirectly determined by the degree of their etching during preparation of metallographic microsections. Thus, white constituents, which occupy a considerable area of plasma coatings, almost do not interact with a reagent that clearly detects the alloy structure in as cast state. Probably, the increase in the temperature of the friction surface at high slip rates leads to the decomposition of metastable light areas and, consequently, to increase of oxidizing ability.

Based on X-ray structural analysis it was established that iron oxides  $\text{Fe}_3\text{O}_4$  and  $\text{Fe}_2\text{O}_3$  are formed on the friction surfaces of VTiNi and CrTiNi coatings tested at the temperature of  $20^\circ\text{C}$ . In case of high temperature test (about  $850^\circ\text{C}$ ), when plastic deformation is localized in thin surface layers and the wear is mainly due to the removal of oxide films, the wear resistance of plasma coating will be lower than the wear resistance of eutectic alloy in the cast state. This occurs due to the instability of their phase composition, the complete decomposition of solid metastable structures, and the removal of oxide films from friction surface, which are intensively formed in the coating through its developed surface.

Based on X-ray spectral analysis data it was found a high oxygen content in coating's surface layer (the mass fraction is almost 34%). At the same time, the friction surface is depleted by nickel. After a high temperature test, a more even distribution of elements in the coating is observed.

The diffractograms of the friction surface of the CrTiNi coating reveal reflexes of  $\text{Fe}_3\text{O}_4$ ,  $\text{Fe}_2\text{O}_3$ ,  $\text{Cr}_2\text{O}_3$ ,  $\text{TiO}_2$ ,  $\text{B}_2\text{O}_3$  oxides; this is consistent with the data of the thermodynamic analysis of the interaction of eutectic coating material (TiNi, VTiNi and CrTiNi) with air at a temperature of  $600\text{--}850^\circ\text{C}$ , performed using computer program "ASTRA". According to the thermodynamic analysis, in the coating of CrTiNi system, compared to the coating of VTiNi, a larger number of oxides  $\text{B}_2\text{O}_3$ ,  $\text{Cr}_2\text{O}_3$  is formed. Probably, this factor, as well as high heat resistance, explains higher wear resistance of CrTiNi coatings at elevated temperatures than it is at lower temperatures [81].

Thus, the tribotechnical characteristics of deposited plasma eutectic coatings, depending on the load and temperature, are determined by the level of their non-equilibrium state, porosity and adhesion-cohesive durability. A normal friction mode of plasma coatings may be observed in a broad range of loads and temperatures. If the load  $P > 5$  MPa, there is intensification of wear due to the brittle fracture of coating, which is accompanied by the excretion of its elements having abrasive properties.

At high temperatures ( $T > 600$  °C), low wear resistance is due to the decrease in the hardness of the coating as a result of decomposition of supersaturated solid solutions, and the coating is worn out by removing soft oxide films from the friction zone that are intensively formed on a porous friction surface.

So, plasma coatings cannot realize their potentially high tribotechnical properties. There is only a limited range of external factors, in which the coating is workable, satisfactorily interact and form reliable friction induced structures [82].

### ***3.1.1.5. Treatment of plasma coatings by laser remelting and thermocycling***

**Remelting of plasma coatings by laser.** There is a number of technological methods aimed to increase both surface and bulk strength of sprayed coatings. Such methods include surface melting, thermal and thermochemical processing, solder infiltration, and others.

Taking into account the results of laser clad eutectic coatings testing, the effect of melting and thermocycling with a laser beam on the structure and properties of plasma coatings was studied. In this case, an irradiation mode is selected so that the melting depth is equal to or exceeds the thickness of the coating. The microstructure of plasma coatings on steels 1080 and 12Cr18Ni9Ti melted by laser is shown on Fig. 3.8.

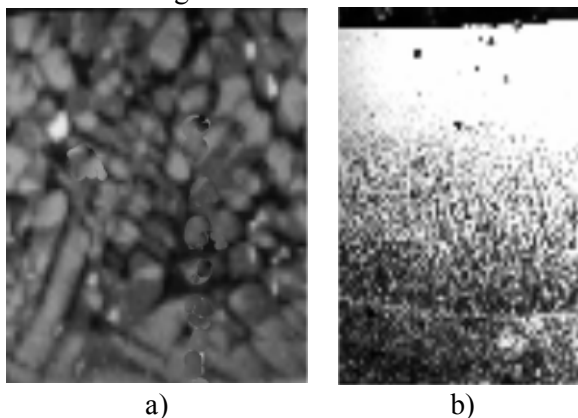


Fig. 3.8. Microstructure of laser melted VTiNi plasma coating: a) substrate – steel 12Cr18Ni9Ti,  $\times 300$ ; b) substrate – carbon steel 1080 (double remelting), 500

Coating has a columnar-dendritic structure. Compared to the original microstructure, the metal under the action of concentrated energy of radiation was turned into a liquid state. Under the influence of a large temperature gradient and, as a result, a high rate of crystallization, the main axes of dendrites grew parallel to the direction of heat removal. Near the surface itself, the direction of heat removal is less apparent and directed parallel to laser beam scanning direction. Thus, the orientation of dendrites in the melted zone may be determined by the direction of heat removal [83, 84].

The technological mode is chosen taking into account the most favorable influence on the processes of friction and wear of finely differentiated structure (radiation power, laser scanning speed), which ensures the formation of this microstructure. For this purpose, the melted coating was repeatedly treated using faster scanning speeds (more than 1 m/min) of continuous laser. The surface layer treated under this mode has no dendritic structure, is hardly etched and has an increased hardness – 1.1...1.2 GPa (Fig. 3.8, b). SEM examinations have indicated that this layer has a microcrystalline structure.

A characteristic feature of remelted coatings is the reduction of their microhardness compared to the original microhardness of as deposited coatings. The hardness from the surface of coating to substrate changes more smoothly than it is in untreated plasma sprayed coating. The highest microhardness has a melted plasma coating on 1080 tool steel substrate compared to the coatings on steels 1045 and 12Cr18Ni9Ti. The reason for this is carbon, the content of which is 0.8% for steel 1080, 0.45% for steel 1045 and only 0.12% for alloy steel.

The facts of carbon diffusion into the solid phase at a distance of 150–200  $\mu\text{m}$  at laser pulse duration of 4 ms are determined. This is caused by high deformation rates occurring in the heat affected area under pulsed laser influence. At the same time, the laser irradiation of the austenitic steel does not cause significant changes to its structure. The microhardness of the heating zone does not differ from the hardness of the original steel structure and is 2.7 GPa. The melted coatings become almost non-porous (porosity 0.5...1.0%), the adhesion strength rises to 400...450 MPa.

**Thermocycling of plasma coatings by laser.** Thermocyclic treatment (TCT) of coating (heating by a laser beam in the range of temperatures 1000...600  $^{\circ}\text{C}$ ) was done by laser system "LATUS-31". The temperature of upper limit of the cycle is chosen based on phase equilibrium diagrams ( $0.75 T_{\text{melt}}$ ). This temperature does not allow any morphological changes in equilibrium eutectic interstitial crystals, but can significantly affect decomposition of a metal matrix, coagulation of dispersed crystals of interstitial phases contained in light areas. It also will au, and also the diffusion process in the "coating-steel" interface. The number of thermocycles is chosen with aim to obtain the levels of structural state which are close to equilibrium. Thus, the selected temperature of TCT and

number of treatments allow affecting the diffusion processes in coating-substrate interface, the structural state and the thermodynamic equilibrium of light areas.

In eutectic coatings (VTiNi and CrTiNi), starting with three thermocycles, decomposition of light areas begins. In CrTiNi coating after three times of TCT, the number of gray areas (reacted with etchant) increases as a result of partial decomposition of white areas. As a result of increase in number of thermocycles to five there is a more complete decomposition of light areas with accompanied by separation of dispersed particles of interstitial phases. The microhardness of the coating after this treatment is slightly lower than that of an untreated coating, but higher than hardness of laser remelted coating.

### ***3.1.1.6. Wear resistance of laser treated plasma coatings***

**Laser remelting.** Based on tribotechnical tests, a superior wear resistance of remelted coatings compared to the original untreated coatings (more than twice at room temperature and in 5 times at high temperature) was revealed. Namely, if reduced wear loss of sprayed VTiNi coating at a temperature of 20 °C is 51.1 mg/cm<sup>2</sup>, and at a temperature of 850 °C – 47.5 mg/cm<sup>2</sup>, the reduced wear loss of remelted coating is 27.9 and 12.14 mg/cm<sup>2</sup> respectively. A wear of counterface during friction over the sprayed coating is less than it is during friction over melted coating. This can be explained by more intense formation of oxide films on the plasma coatings that act as solid lubricant.

The sprayed coating during friction deteriorates mainly due to the wear of individual particles, due to the presence of pores, high brittleness, and low relaxation ability. Melting of sprayed coatings increases their efficiency in extreme conditions, preventing them from being dented, crushed and delaminated.

Two times remelted coatings have the highest wear resistance, due their structure, which provide a positive gradient of properties in the coating (Fig. 3.8, b). At the same time, the surface layer with fine-grained structure promotes self-organization of friction induced structures, and the lower layers of columnar structures of strengthening phases effectively dampen external normal and shear loads. At a high temperature, the columnar structure of refractory interstitial phases promotes high strength, and the surface layer promotes the formation of dense (optimal thickness) oxide films. The obtained results are in agreement with the data of analytical study of the stress-strain state of composite coating loaded with friction forces [85].

The examination of friction surfaces of remelted coatings indicate that at room temperature friction induced structures do form, but wear off as a result of fatigue failure. At elevated temperatures (850 °C), the processes of friction and wear are dependent on the formation of oxide films (Fig. 3.9, a). The diffraction patterns of friction surfaces of VTiNi coating tested at a temperature of 850 °C

revealed traces of  $\text{Fe}_3\text{O}_4$ ,  $\text{Fe}_2\text{O}_3$ ,  $\text{Cr}_2\text{O}_3$ ,  $\text{TiO}_2$ ,  $\text{V}_2\text{O}_5$ ,  $\text{B}_2\text{O}_5$  oxides, which is consistent with the data of the thermodynamic analysis.

During high-temperature coating tests in a certain range of external loads ( $T = 850\text{ }^\circ\text{C}$ ,  $P = 5\text{ MPa}$ ,  $V = 1.5\text{ m/sec}$ ), contact melting of friction surfaces occurs. The wear track includes flows of solidified metal and crystals of re-solidified eutectic structures (Fig. 3.9, b). At the same time there is a sharp decrease in the coefficient of friction down to values of boundary or even semi-liquid lubrication (0.05 – 0.10).

Thus, the melting of plasma coatings effectively increases their adhesion and wear resistance. However, this is not the most optimal method for improving the properties of gas-thermal coatings. To control the wear resistance of plasma coatings, a part of their surface is melted by laser. Melting is carried out either completely (al-over) or partially (non-all-over), but so that the total area of remelted coating is 5–100% of the entire surface. Partial remelting of coating combines advantages of initial sprayed coatings – high microhardness of structural components (light areas) with molten portions, which significantly increase the wear resistance of the coatings under severe dynamic loads. The wear intensity of coating with various fraction of melted area is not the same – it is lower compared to an untreated coating. The wear of a all-over remelted coating is 1.5–2 times less than that of an untreated coating. The most wear resistant is the coating where only about 15% of the surface is transferred to the cast state.

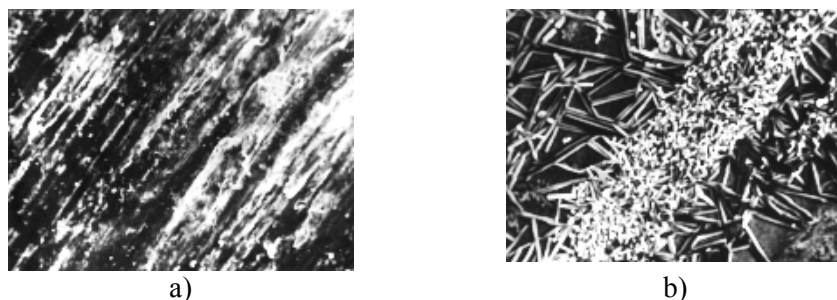


Fig. 3.9. Microstructure of wear tracks of remelted VTiNi eutectic plasma coating at temperatures: a)  $850\text{ }^\circ\text{C}$ ,  $\times 43$ ; b)  $850\text{ }^\circ\text{C}$ ,  $\times 750$

The friction surface on the boundary of remelted and untreated areas of VTiNi plasma coating is shown in Fig. 3.10. On the friction surface of the original part of the coating there are traces of a brittle destruction in the form spallation, while the remelted part is smooth, without visible signs of destruction. This is confirmed by profiles of the friction surface (Fig. 3.10, b), taken along the scanning line (Fig. 3.10, a). The study of specimen's roughness after wear test

was carried out using electron microscope JSM-840 in scanning mode along the chosen line «Lainskan».

The studies conducted have confirmed that plasma sprayed coatings with a non-equilibrium ultrafine structure should have higher tribotechnical properties. However, low adhesion and cohesive properties do not allow realizing the friction mechanism with self-organization of plasma coatings [86].

Even a slight melting (10%) of part of the coating contributes to a significant increase in its wear resistance. The restoration of the eutectic equilibrium structure of as-cast state, in case of melting, increases the adhesion properties, but at the same time, certain advantages of the sprayed coating are lost: high microhardness, non-equilibrium structure (metastable phases, supersaturated solid solutions of the phases in the metal matrix). Therefore, this method of plasma coating treatment deserves attention, which would help to increase the adhesion-cohesive properties while preserving their structural state. It is known that in the case of instability of the structure under load conditions (i.e., the ability to rebuild) the deformation energy is consumed by favorable relaxation processes and the wear resistance of the material increases.

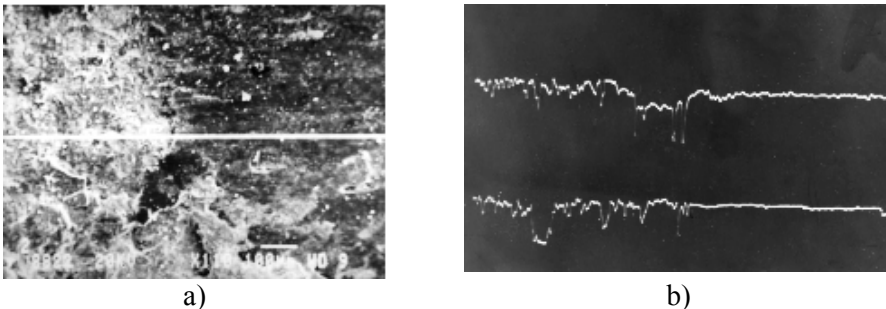


Fig. 3.10. Microstructure (a) and profile (b) of wear track of VTiNi coating with partially remelted surface (vertical magnification  $\times 10000$ ; horizontal magnification  $\times 100$ )

**Thermocycling of plasma coatings.** The wear tests of plasma coatings in untreated state and after TCT show their varying resistance. Thermocyclic treatment enables to change the structural state and the thermodynamic equilibrium of light areas, while increasing the number of sections of plasticized eutectic structure. Such structure can absorb a significant portion of energy and, to a greater extent, relief stresses during friction. In addition, the increase of the modulus of elasticity of light areas in the process of their decomposition, simultaneously with the growth of microplasticity increases the stress of the beginning of plastic flow of coating material and, accordingly, increases its wear resistance. Reducing brittleness and increasing the plasticity of the coating after TCT increases its ability to form friction induced structures, indicating its favorable rheological properties.

All-over oxide films are formed on friction surfaces of coatings subjected to TCT, whereas on the surfaces without TCT these films have the appearance of individual separated areas. A prerequisite for the formation of individual friction induced areas may be the reduction of corrosion resistance of light areas in the process of their decomposition. Wear resistance of CrTiNi coating after TCT increases more significantly than wear resistance of VtiNi coating. The friction coefficient also decreases, which, as shown by the studies of the stress-deformed state, helps to increase the stresses required for the beginning of plastic deformation in the coating material. This, along with other previously noted factors, increases the wear resistance of coatings after TCT.

Tribotechnical tests at high temperatures have shown that wear resistance of untreated plasma coatings and coatings after TCT is approximately the same. This is due to the complete decomposition of solid metastable structures and the intense oxidation of coatings due to their porosity.

Consequently, the melting and plasma coatings by laser increase their tribotechnical properties in a wide range of temperatures. For elements of friction units operating in low temperatures sprayed plasma coatings with additional TCT, and for operation at high temperatures – remelted plasma coatings may be recommend.

### ***3.1.1.7. Bilayer coatings***

A characteristic feature for high temperatures, the condition for which mentioned coatings are purposed – mode of heat transfer, – are diffusion processes on coating and substrate boundary. The intensity of these processes largely impacts the wear resistance of the coating.

Since the intensification of the diffusion processes during TCT contributes to increasing of the adhesion strength of the coating, and in the case of its prolonged exposure leads to degradation of the initial structure, the study of the properties of bilayer coating with a barrier layer produced by laser alloying has been carried out. In addition to limiting the mutual diffusion of elements between coating and substrate, the barrier layer should reduce the gradient of properties and increase adhesion [87, 88].

The technology of barrier layer formation consists of surface preparation, application of coating layer, melting and thermocycling with a laser. Laser alloying was done to steels 1080 and 12Cr18Ni9Ti using paste containing amorphous boron, or a mixture of amorphous boron with boron carbide. A laser treatment and thermocycling at high temperatures 1000–600 °C (including temperature of phase transformations) has been performed using laser "LATUS-31" with a power of 1.2 kW.

The conducted studies have shown that alloyed layers on steels have a structure of the eutectic type based on the system Fe-B-C and mostly consist of two zones: the bottom, which was crystallized in the form of a columnar structure

of borides, and the upper, fine-grained, which is not identified by ordinary etchants.

The analysis of kinetics of doped layers formation shows that the thickness of the boride layer on the alloyed steels is 2–3 times less than that for carbon steel. Thus, the structure of this coating on steel 12Cr18Ni9Ti consists of borides FeB, Fe<sub>2</sub>B, Cr<sub>2</sub>B, and the transition zone. Transition zone consists of solid solution of boron in austenite and chromium carbide Cr<sub>23</sub>C<sub>6</sub>. The microhardness examinations indicate that the microhardness of alloyed layers of steels 1080 and 12Cr18Ni9Ti is 11 and 6.5 GPa, respectively.

The analyses of TCT impact on the structure, phase and chemical composition of the melted layer revealed that with increasing multiplicity of thermocycles the thickness of the alloyed layer increases and the content of chemical elements also changes. Thus, with an increase in the number of thermal cycles, there is a redistribution of alloying elements, which indicates the possibility of purposeful control of chemical composition through the coating (from surface to substrate direction) with the help of TCT.

Thermocyclic treatment slightly increases the microhardness of alloyed layer in steel 1080 – up 14 GPa, and 9 GPa on the steel 12Cr18Ni9Ti. This is due to the change in the phase composition and dispersion of alloyed layers. Namely, as a result of additional thermal cycling, the phase Fe<sub>23</sub>(C, B)<sub>6</sub> disappears and Fe<sub>2</sub>B boride appears.

Since for laser alloying followed by TCT there is a competition between two processes – the accumulation of stresses (mainly thermal and stresses associated with phase work hardening) and their relaxation – cracking is possible in the coatings (Fig. 3.11, a). For the laser alloying of 12Cr18Ni9Ti steel, no cracks were observed (Fig. 3.11, b). Steel 1080 is more prone to crack formation. At the same time, the probability of their formation is higher in case of alloying using mixture B + B<sub>4</sub>C, which is due to the composition of the strengthening phases, greater thickness and microhardness of the layer.

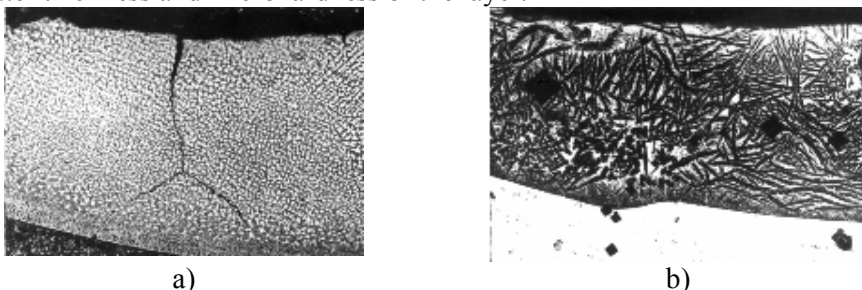


Fig. 3.11. Microstructure of alloyed layer produced using the following paste: amorphous boron+B<sub>4</sub>C: a) steel 1080, ×200; b) steel 12Cr18Ni9Ti, ×200

The structure of a bilayer coating, consisting of a plasma CrTiNi coating, sprayed on steel 12Cr18Ni9Ti with a pre-applied by laser alloying boride layer, is shown in Fig. 3.12. It has been experimentally established that the adhesion

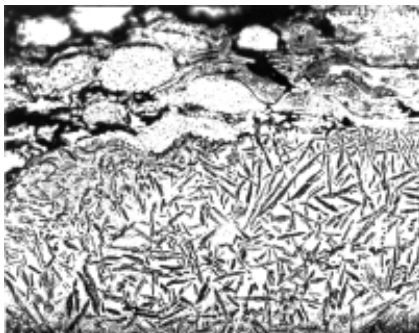


Fig. 3.12. Microstructure of bilayer coating on steel 12Cr18Ni9Ti (alloyed boride layer and plasma CrTiNi coating),  $\times 156$

of the plasma coating with alloyed layer is 22...30 MPa, which is superior then adhesion to untreated steel substrate – 16...22 MPa.

The X-ray spectral examination of samples with a bilayer coating subjected to a 50 times TCT did not reveal mutual diffusion of elements of eutectic coating and barrier layer. There was only diffusion of boron from barrier layer into both plasma coating and substrate, and diffusion of iron into barrier layer. The arresting of interdiffusion of elements out/into the coating contributed to the preservation of its high properties

### ***3.1.1.8. Tribological properties of bilayer coatings***

Tribotechnical tests have revealed that wear resistance of bilayer coatings throughout the temperature range is higher than that of monolayer ones. This is primarily due to an increase in adhesion properties, a decrease in the hardness gradient of the coating and an increase in its thermal stability due to the barrier boride layer. At room temperature on the friction surface, friction induced structures and a small number of areas of brittle fracture seen. The friction coefficient is more stable and lower in magnitude than friction coefficient of monolayer coating. The microstructure of individual areas along the depth of bilayer VTiNi coating after the wear test at 850 °C are shown on Fig. 3.13. It indicates the thermal stability of the coating, the absence of oxidation and the interaction between its individual layers.

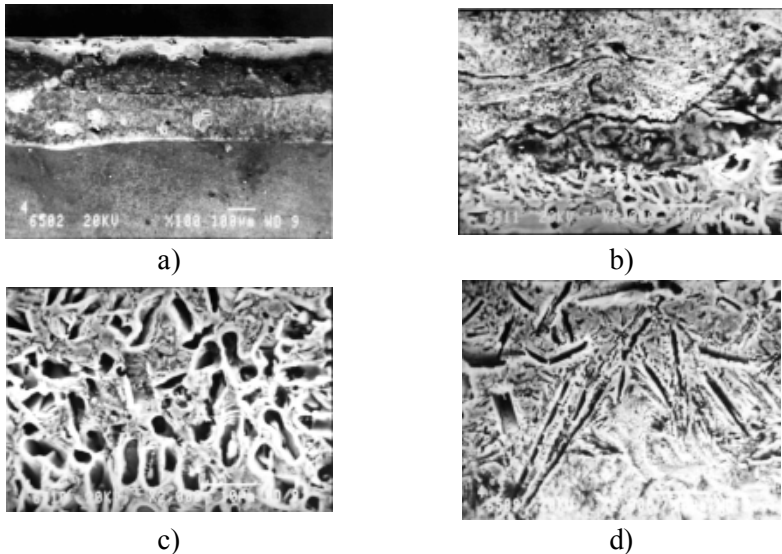


Fig. 3.13. Microstructure of bilayer coating after tribotest at temperature 850°C:  
 a) general view, 50; b) transition zone between VTiNi plasma coating + boride coating,  $\times 2000$ ; c) microstructure of alloyed boride layer,  $\times 2000$ ; d) transition zone between boride layer and substrate (steel 12Cr18Ni9Ti),  $\times 2000$

High wear resistance of bilayer coating at elevated temperatures is due to not only the barrier properties of the alloyed boride layer, but also due to the intensity of their oxidation, the composition of oxide films and, first of all, the formation of  $B_2O_3$ . I temperature is above 600 °C, it turns to liquid and provides uniform heating of plasma coating and acts as liquid lubricant. The friction coefficient and wear loss at this time are reduced; this is confirmed by studies of heat resistance, X-ray diffraction and metallographic analysis. So, on a friction surface there is a bright glass-like layer. The possibility of formation of  $B_2O_3$  under this temperature during friction is also confirmed by thermodynamic calculations.

The wear resistance of bilayer CrTiNi coating is higher than that of VTiNi coating. This correlates with their heat resistance.

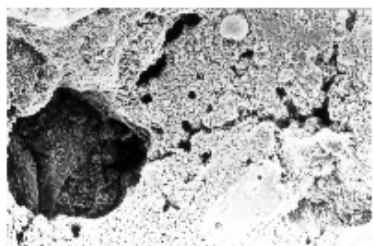
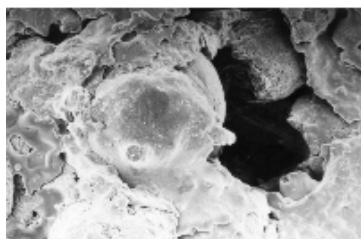
Consequently, the laser treatment of plasma eutectic coatings by remelting and thermocycling, as well as the application of barrier boron layers, substantially increases their tribotechnical properties in a wide range of temperatures. At the same time, for friction couples operating in low temperatures, plasma spray coatings with additional TCT and double remelted coatings, may be proposed. A good choice for high temperature friction couples, are the remelted plasma and bilayer coatings.

### ***3.1.1.9. Cavitation resistance of eutectic coatings***

Cavitation substantially affects the wear of parts of almost all machines having fluid as working body. Cavitation wear of structural materials has a mechanical nature. However, one cannot ignore the corrosion processes assisting cavitation. This indicates the complexity of the mechanism of cavitation-erosion wear of metals.

Cavitation resistance was tested using magnetostrictional method. The deterioration of the coatings was determined by the weight loss of the sample. The kinetic curves of the cavitation resistance of plasma eutectic coatings have the form of "stairs" in the general trend of increasing weight loss with increasing test time. Probably they reflect the layering of the coating structure. The intensity of the wear at the initial stages of cavitation is due to the high roughness of the surface of the plasma coatings (which corresponds to the parameter  $Ra = 0.2-0.3 \mu\text{m}$ ), the presence of surface porosity and a large number of brittle structural components. These features of the coating structure significantly affect their physical and mechanical properties: reduced plasticity and strength. The cyclicity of loading and the multiple action of the fluid voids during the fatigue processes in the material cause spallation of microvolumes of coating surface layer.

The fatigue destruction of material begins with the accumulation of submicroscopic defects. This leads to the emergence of microcracks. Their growth to critical dimensions, in which the energy is accumulated by the defect, which is greater than the energy of the forces of particle engagement at its apex, causes elementary destruction. Substratum layers thus undergo significant influence, which results in their compacting and lead to microcracks. The orientation of microcracks indicates their emergence at the boundaries of the particles and numerous surface defects in the coating. This is confirmed by microfractograms of the wear surface (Fig. 3.14). The arising microcrack is a mechanism for the dissipation of cavitation energy, and the separation of wear particles is the result of brittle destruction. Other dissipation phenomena are possible in a plasma coating due to their non-equilibrium state. However, the favorable rheological properties of eutectic coatings cannot be realized because of their low adhesion and cohesion (bond strength of the substrate is 16–20 MPa).



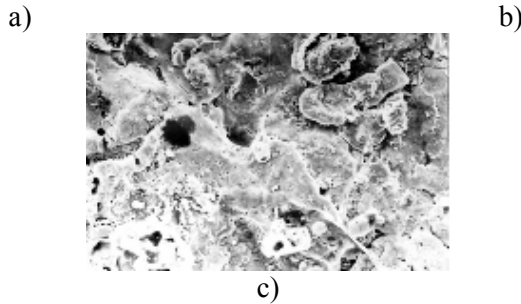


Fig. 3.14. Microfractures of coating surface after cavitation test during 10 hours,  $\times 600$ :  
 a) 12Cr18Ni9Ti-TiB<sub>2</sub> (plasma sprayed); b) 12Cr18Ni9Ti-TiB<sub>2</sub>-CrB<sub>2</sub> (laser treated);  
 c) 12Cr18Ni9Ti-TiB<sub>2</sub>-CrB<sub>2</sub> (electro-spark alloying)

Metallographic studies have revealed that light areas appear on the surface of the coating after cavitation wear, which also indirectly confirms their higher wear resistance in comparison to the heterogeneous eutectic structure. Having almost the same plasticity, light areas are characterized by a greater microhardness and lower values of the elastic modulus than eutectic components of coating. The thickness of crystals in the eutectic areas of deposited coatings is 1.2–2.0  $\mu\text{m}$ . However, the eutectic coating is inferior for steel 12Cr18Ni9Ti in wear resistance. As a result of cavitation, the microhardness of 12Cr18Ni9Ti steel surface layer increases up to 6000 MPa due to the transformation of metastable austenite into strain induced martensite. As the dispersion of the structure increases and plasticity rises, the interconnection of the wear processes with the local plasticity parameter  $A0/A$  and the elastic modulus  $E$  is revealed. However, it is impossible to uniquely estimate the effect of dispersion on plasma coatings, since the significant contribution to the wear resistance is made by porosity and adhesion and cohesion.

The cavitation wear of the coating is a result of spallation of microparticles from the surface. The main structural components of the electro-spark coating applied by an electrode made of CrTiNi alloy – are solid solutions of alloying elements in iron. Electrospark coating is a light area of fine crystalline structure (thickness of crystals up to 1  $\mu\text{m}$ ) and is characterized by strong adhesion with substrate. It has almost theoretical density. The cavitation resistance of electro-spark coating is intermediate between plasma coating and steel 12Cr18Ni9Ti. The electro-spark coating is harder and more plastic than the plasma coating.

Remelting of plasma coatings has a significant effect on the structure, physical and tribotechnical properties. The microstructure of HFC and laser remelted coatings has a dendritic structure. Compared to a visible microstructure of metal, due to the action of concentrated energy flow, it turns to a liquid state. Being affected by strong temperature gradient and, consequently, a huge rate of crystallization, the main axis of dendrites grow parallel to the direction of heat

removal. Remelted coatings have almost theoretical density (no pores). The cavitation resistance of plasma coatings melted by laser is higher than of HFC treated coatings. This is explained by optimal physical and mechanical properties of the coatings after laser treatment and high degree of differentiation of the components of eutectics. The processes of micronucleation and fatigue are localized in its small interplate volumes.

There is a certain correlation between the microscopic area of cavitation influence ( $10 \mu\text{m}^2$ ) and the size of the grains (dendrites) and the interplate distance of eutectic components. Refining the structure of the same eutectic coatings obtained by different methods, according to the fractograms (Fig. 3.14), reduces the wear loss. (Fig. 3.14, a). This is explained by a fact that microcracks which originate mainly interface of neighboring sprayed particles. In these areas a mesh of small cracks is formed, material's density decreases and worm particles are removed by fluid. In case of cavitation of laser remelted coatings, cracks also originate at the boundaries of the grains, but their size is slightly smaller than that in plasma coatings without processing (Fig. 3.14, b). At the same time, the higher cavitation resistance of VTiNi system is due, probably, to greater carbon content in strain induced martensite. Eutectic electro-spark coatings are characterized by the finest parameters of the structure (Fig. 3.14, c) and very high cavitation resistance. The dimensions of coating structural components for this method are about  $1 \mu\text{m}$ . The ratio of the size of the structural components of the coating and the area of hydraulic impact (1:10) allows the best use of this material. In this case, the resistance of the coating to the hydraulic shock is determined by the averaged properties of the phase components of the ultrafine structure, rather than the separate structural components [89].

The problem of optimal design of tribosystems and the use of efficient lubricants is on time. But the problems of material science are extremely relevant and often crucial in achieving the required reliability and durability of machine parts. Analyses of modern trends in the development of advanced researches have allowed highlighting three actual trends.

1. Figuring out of possible mechanisms of wear process – is to prevent surface destruction through the separation of the wear particles.

2. Study the possibility of forecasting wear resistance based on mechanical properties of material.

3. Investigation of structural aspects of surface destruction during wear. The study of evolution of the structure of near-surface volumes, which leads to the separation of wear particles, allows us to better understand the phenomenon of friction.

These research areas form the basis for the development of new alloys and methods for producing optimal surface structures using concentrated energy flows (laser, plasma, electron beam, ion flow – ion implantation, explosion energy). These technologies are promising because, by changing the structure

and, consequently, properties of surface layers, they leave deeper material unchanged. Consequently, structure modification will provide increasing properties of metallic materials.

### **3.2. Technological deposition processes and industrial testing of eutectic coatings**

Complex researches of eutectic alloys and coatings made it possible to figure out main rules, or processes of eutectic coatings deposition. They may be effectively used for both parts strengthening and overhaul repairs. Application of concentrated energy flows (laser, plasma, high frequency currents) allows altering their properties in a very wide range of magnitude.

The technological process consists of the following main stages: preparation of powder materials, surface preparation, coating deposition, surface finishing.

**a. Preparation of powder materials.** Powder of eutectic alloys of the specified chemical compositions is produced by spraying in a stream of inert gas (argon), as well as nitrogen. The Powders should not contain moisture; therefore they are pre-dried at temperatures of 120–150 °C for 1...3 hours. By this we remove the moisture absorbed from air, which leads to increased “fluidity” of powders, one of the main technological indicators, as well as to improve the deposited or sprayed layer. The necessary fractions of powders are obtained by calibration. It is most appropriate to do this using a sieve with a grid of 10–125 µm.

When preparing the coating material for cladding to external cylindrical surfaces, a mixing of powder with a binder – 8–10% of liquid glass aqueous solution is carried out on the working surfaces before coating application.

The main source alloys, for which the technological processes of coatings deposition are designed, are VTiNi and CrTiNi with additional alloying elements, as well as powder materials based on them.

The alloy grade, powder size, type and amount of alloying elements are chosen based on the required performance properties of the coating and the method of application. The powder of the VTiNi alloy, which additionally contains aluminum and copper, with a hardness of 35...50 HRC, is the best on our opinion. The coatings were deposited by plasma spraying and HFC cladding of following products: shafts of pumps, guide surfaces of drills, mill cutters, and spindles of drilling machines and other details of metalworking machines. When working with these materials shock loads are allowed.

For strengthening and recovery by plasma-, HFC- and laser-aided deposition technologies, we applied them to the surfaces of protective sleeves, rollers and roller bearings of thermal units, knives for hot cutting of metal, sleeves, shafts, rods, spindles, shires and valves of steam-and-water armature, parts of pumps and high-speed fans and other elements, working in aggressive environments and

high temperatures we recommend to use CrTiNi alloy, which provides high wear, heat and corrosion resistance of the coatings. A very effective solution is preapplication of diffusion barrier coating by alloying the substrate with Al and Si.

**b. Surface preparation.** Cleaning of fatty contaminants is carried out by washing in a washing emulsion MS-3 with a composition, % (wt.): water 18–38; kerosene 60–80. The emulsion temperature is 60–75 °C. Washing time is 2–3 minutes. After washing the parts are rinsed with cold water and dried under a stream of warm air. Before applying the coating, in particular by ion-plasma spraying, preparing the metal surface in vacuum is an effective method [90].

To ensure reliable adhesion of the coating, it is necessary to remove corrosion deposits, possible scale, etc. from the surface being strengthened. This may be done by machining on turning or grinding machines. In the process of grit blasting, it is necessary to prevent the introduction of moisture and oil to the prepared surface. To do this, before the air is fed into the blasting unit, it is cleaned by passing through an oil-solving cleaner.

Permissible shelf time for completely prepared parts of the coating is not more than 3–4 hours before coating application.

**c. Coating deposition.** The final stage of production of protective coatings is cladding or spraying.

*Cladding with HFC heating.* One of the most productive methods of deposition of eutectic coatings is cladding by HFC heating, in particular, centrifugal bimetalization. The powder mixture melts directly into the rotating product.

In this case, good conditions are created for combination of product heating process, melting of powder mixture and melt crystallization. This technological process provides high adhesion of eutectic coating.

The essence of coating process on the inner surfaces of rotation bodies using heating by HFC is as follows. In closed cavity of sleeve the powder mixture is supplied. The part being recovered is rotated with defined angular velocity, while formation of deposited layer runs under the action of centrifugal forces. Then with the help of an inductor, heating of the part is performed, and after the powder mixture is melted, heating is stopped and the coating is cooled on a still air.

Specific conditions for heat supply, kinetics of heating, cooling and crystallization, the action of gravity allow obtaining wear-resistant layers with high mechanical properties, and in combination with induction heating, to achieve significant technical and economic advantages over other methods of cladding.

The bimetalization plant consists of an induction unit (heating source) and a modernized grinding machine (ZA250 model) that allows rotation and reciprocating motion of component relative to the fixed inductor (Fig. 3.15). The

installation provides the optimum ratio of heating cylinders of given size. Technical performance of installation allows making cladding of cylinders (sliding bearings) in diameter from 50 to 200 mm and of length up to 300 mm. The deposited coatings have smooth surface (Fig. 3.16), which allows strengthening and recovery of parts with a minimum amount of further machining, improving the economic efficiency of this technology.

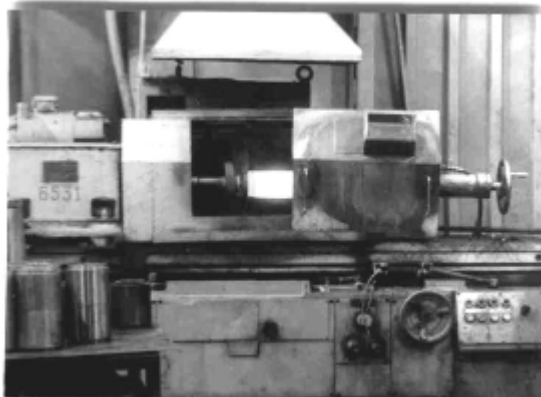


Fig. 3.15. Installation for centrifugal metallization with induction heating

The kit of the induction unit includes: machine frequency converter, high-frequency lowering transformer, block of capacitors and control unit. Some of the recovered parts are presented on Fig. 3.16.



Fig. 3.16. The parts that are subjected to centrifugal cladding by eutectic coating to their internal surface

Among the non-standard units of the installation are: inductor, flange for fastening the workpiece, screen. Technical performance of installations for centrifugal induction cladding is shown in Tab. 3.2.

A blank filled with the necessary amount of powder should be fixed in the machine (Fig. 3.17) using the centering flanges mounted at its ends (Fig. 3.18). In order to prevent welding the flanges and for better sealing, they were coated with

alcohol-acetone paint. The composition and technology of paint deposition was selected experimentally on the basis of paint intended for foundry molds.

The heating of the sleeve with the charge was being carried out for a certain time, the duration of which was set using a time relay. During the whole period of heating, the heater's modes remained unchanged. 6 minutes after the start of heating, when the temperature of the workpiece reached 1200–1300 °C, the heater was switched off automatically using the time relay.

Table 3.2. Specification of bimetallization installation

No	Name	Value
1	Required power, KW	100
2	Rated frequency, Hz	8000
3	Supply voltage with frequency of 50 Hz, V	220/380
4	Cooling water flow rate, m <sup>3</sup>	5,9
5	Pressure in cooling system, MPa	0.3
6	Detail rotational speed, rpm	10–1600
7	Working speed of moving the carriage with a part, m/min	1.5–5

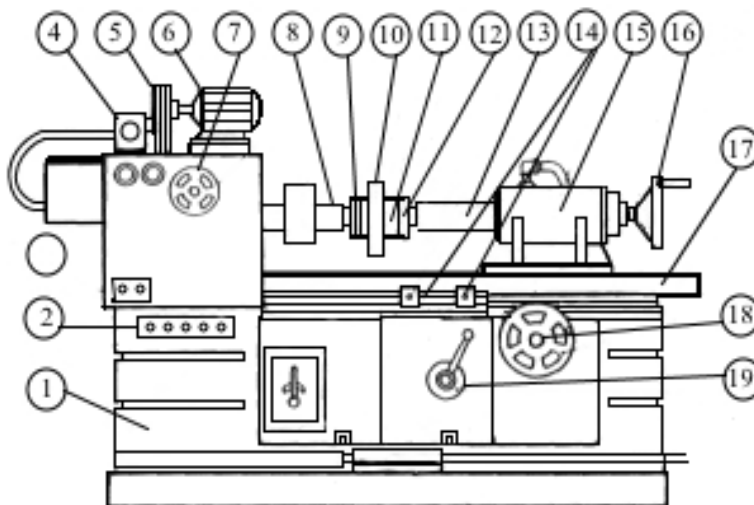


Fig. 3.17. Lathe of ZA250 model, re-equipped for centrifugal bimetallization with induction heating: 1 – frame; 2 – control panel; 3 – buttons for switching on and off the heating; 4 – tachometer; 5 – the pulley belt drive; 6 – electric motor; 7 – flywheel of variator; 8 – spindle of machine tool; 9,12 – sealing caps; 11 – heated sleeve; 10 – circular inductor; 13 – quill of tailstock; 14 – end stops for switching the reciprocating movement; 15 – tailstock; 16 – mechanism of pressing the sleeve; 17 – table of the machine tool; 18 – handwheel of table manual movement; 19 – handle for turning on the reciprocating motion of the table

Since the melting temperature of the mixture is lower than the melting point of the sleeve material (steel 1010, 1020), it melts and evenly distributes on the inner surface, which is achieved by rotating the sleeve. After the heating was stopped, the sleeve continued to rotate until the end of the crystallization process until the temperatures of outer surface reduces down to 600–700 °C. Then it was removed from the machine and air cooled. Since the termination of heating and before removal from machine, the sleeve 1 was cooled by a stream of compressed air. In order to reduce the temperature stresses that contribute to the occurrence of internal cracks, it is possible to slowly cool the parts in dry sand or furnace. After application, the coatings were machined to the required dimensions.

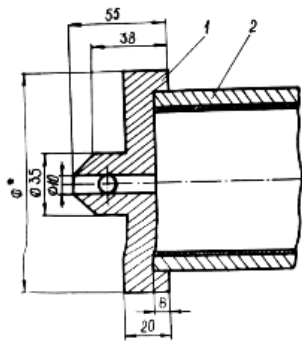


Fig. 3.18. Sealing flange for fixing a steel blank: 1 – flange; 2 – blank

*Plasma cladding.* To strengthen or recover parts such as knives for hot cutting of metal (subjected to shock loading), the most acceptable are the powders of 12Cr18Ni9Ti+(TiB<sub>2</sub>; VC) system, additionally alloyed with copper.

In order to strengthen the roller supports, which operate in conditions of wear in aggressive medium and high temperatures, the recommended powder material is 12Cr18Ni9Ti+(TiB<sub>2</sub>; CrB<sub>2</sub>) additionally alloyed with Al and Si. The cladding was carried out using plasma spraying system UMP-6, and microplasma system MPU-4 (Fig. 3.19) with the delivery of the powder feedstock directly into a plasma flow (Fig. 3.20). The cladding was carried out at a current of  $J = 110...170$  A, voltage  $U = 30...35$  V.

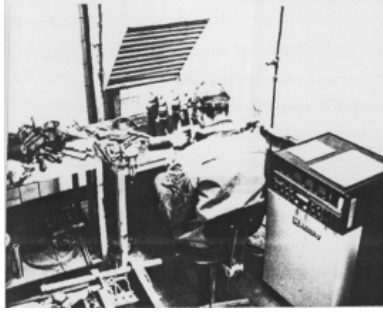


Fig. 3.19. Microplasma cladding section (installation of MPU-4)

The number of revolutions of the part depends on the diameter of the surface to be covered and is, for example, for diameters 20...60 mm —75...30 rpm, respectively. The most suitable is powder with granulometric composition of 40...120 micrometers. The powder consumption is about 45 g/min. The thickness of deposited layer in one pass is 0.5...1.5 mm. The required hardness of the surfaced coating is in the range of 30...62 HRC is ensured by the amount of strengthening phase and the corresponding alloying of the metal matrix of eutectic alloys.

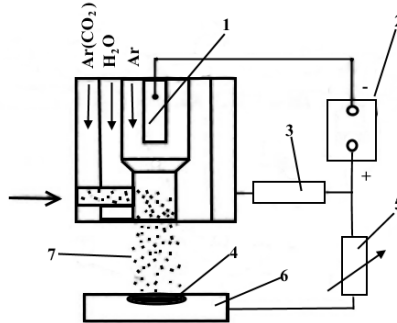


Fig. 3.20. Layout of plasma cladding using metallic powders: 1 – tungsten electrode; 2 – power supply; 3 – impedance resistance; 4 – coating; 5 – ballast resistance; 6 – the product; 7 – powder

The elements of the steam and water fast closing units of heat and power generators (valve sockets, latch spindles, etc.) were subjected to the plasma cladding (Fig. 3.21). It has been established that the manufacturing properties of cladding eutectic powder is not inferior to powder PG-10H-01. The deposited layer has no entities, splashes, structural inhomogeneities. The hardness of the coatings was 850–930 HV.

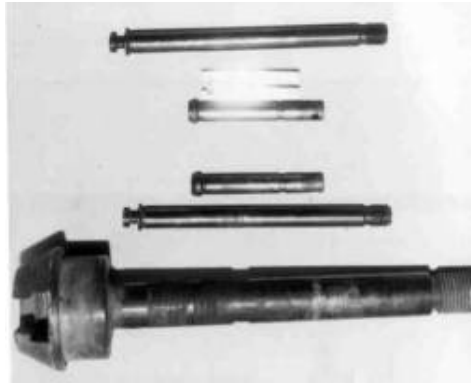


Fig. 3.21. Appearance of details of steam-water fittings subjected to plasma cladding

*Gas flame cladding.* On the widest scale, the technology of strengthening and repairing of worn parts by gas-flame cladding is tested for parts of centrifugal pumps (shaft, sleeve, impeller), elements of forage grinders, pipe fittings.

Thermal spraying allows production of high quality eutectic coatings with minimal losses of cladding material during cladding and machining. With this type of deposition, there is no need for the use of expensive inflatable burners and it is possible to apply large fractions of cladding powders, the cost of which is much lower than that of smaller ones. The part being cladded is fixed in the installation centers, rotated at a frequency of 60 rpm, heated in reducing flame (750...900 °C). The powdered alloy is fed to the heated surface of the part.

After cladding, it is advised to slowly cool the parts in a container filled with asbestos crumb

*Laser cladding.* Eutectic powders were deposited to the bars of the calipers made of steel 1045 and steel 40Cr. The cladding was carried out at the installation "LATUS-31" (Fig. 3.23) at a power  $P = 1$  kW, rate of cladding  $Q = 5...20$  mm/sec, degree of focusing  $F = 15...30$ , the mass flow rate of the powder  $G_n = 0.2...0.8$  kg/sec, the distance to the part  $L = 5...35$  mm, the angle of powder flow  $\alpha = 10...70^\circ$ . An important parameter that significantly influences the process of coating deposition to the surface of rollers is the direction of powder supplying relative to the movement of the part. When cladding, the powder supply was made in the direction of the sample movement (Fig. 3.23) using nitrogen, helium, argon. Optimum granulation of powder is within the range of 30...120 micrometers. Larger particles result in uneven flow due to jamming in the feeder channel. Particles of smaller sizes shrink.



Fig. 3.22. General view of laser installation "LATU-31"

Microstructure of eutectic coating obtained by laser cladding has different microstructure compared to plasma cladded coating. This is due to the peculiarities of technological process of laser cladding, consisting of possibility of adjusting the time of liquid phase existence and providing high cooling rates of cladded material.

*Electro-spark deposition.* The electro-spark deposition was used to strengthen foundry molds, dies, cutting and measuring instruments, cutters, etc. The process of electro-spark deposition is carried out using "ETI-23" and "Elitron-20" systems. For this purpose cast electrodes made of eutectic alloys (diameter of 2–5 mm and length up to 100 mm) were used. The best results are obtained with the use of alloy VTiNi additionally alloyed by Al and Cu. Electro-spark deposition was conducted with a short circuit current  $I = 4$  A, voltage  $V = 28$  V, capacity of the discharge circuit  $C = 300$   $\mu$ f, the processing rate 1.5...2  $\text{cm}^2/\text{min}$ . The thickness of deposited coating is 0.1...0.14 mm, the microhardness is 10–20 GPa.

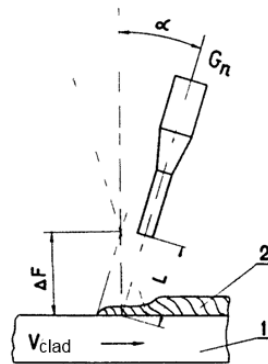


Fig. 3.23. Layout of laser cladding with the supply of powder in the direction of sample motion: 1 – sample; 2 – roller being cladded

Eutectic coatings are characterized by a greater thickness than the coatings produced of T15K6 alloy, but have higher roughness. Increasing the processing time and coating deposition speed to over 3 cm/min leads to the destruction of the coating, deteriorating its surface finish. When applying coatings on steel 12Cr18Ni9Ti there is a seizing of the electrodes, the process becomes less stable than when treating steel 1045. This reduces the thickness of the coating and increases the roughness of the surface.

In addition to the processes of eutectic coatings cladding, in which, in the largest possible extent, the advantages of eutectic structure with a composite strengthening (especially at elevated temperatures) are in some cases completely acceptable for plasma coatings. However, it is worth remembering that they are characterized by much lower adhesion to the substrate. To improve the properties of the spray coatings associated with increasing the bond strength with substrate and increasing compacting of spray material, it is necessary to do remelting or thermocycling laser treatment.

*Machining.* The required final size and roughness of the surfaces are formed after machining, usually grinding. For softer coatings it is possible to blade with cutters with elbor or hexanite plates on a lathe. Grinding is carried out on circular grinding, flat-grinding and grinding machines with wheels made of green silicon carbide or white electrocorundum. Grinding wheel speed – 5 cm/sec, longitudinal feed 0.3 m/min, transverse feed  $3 \times 10^{-6}$  m/sec. It should be noted that in case of PG-10H-01 powder coating treatment, the grinding efficiency is lowered by 8 times.

To improve the quality of the treated surface by reducing the roughness and increasing the stability of grinding wheels, we have developed a composition for impregnation of abrasive wheels, which includes chemicals, surfactants and solvent.

### **3.3. Performance and economic output of developed materials and coatings**

Developed eutectic alloys and iron-based coatings, compared to commonly used nickel-based alloys, are characterized by a complex of useful properties, in particular: good manufacturing properties, heat resistance, corrosion resistance, tribotechnical characteristics, availability (Tab. 3.3).

Coatings based on eutectic powder alloys on an iron-based substrate have 1.5...1.9 times better grinding ability compared to analogues coatings on nickel substrate. Wear resistance of covered parts increases in order of 3–5 times. Plasma cladding and cladding using HFC were used for pumps GK6, 2X9, ZK6, shafts working in a corrosive environment in dry friction (steel 12Cr18Ni9Ti); knives for hot cutting of metal, working at elevated temperatures (5CrNiV steel); rollers and roller supports of thermal furnaces, working in friction and wear

mode at high temperatures (5CrNiV steel). High efficiency of these coatings allows increasing the service life of parts, possibility of their multiple recoveries, saving of expensive steels, reducing the current repairs.

The proposed technology of electro-spark deposition by electrodes made of eutectic alloys allows increasing the durability of casting molds by 70% compared to alloy TI5K6 and 85% in comparison with traditional manufacturing technology.

Cladding of eutectic alloys by HFC may increase the service life of conventional parts, (made of cast iron) by order of 4–6.

Strengthening of parts of fast closing valve (type 15Ch8R) by deposition of eutectic coating allowed increasing their workability by 3 times compared with serial parts.

Application of cladding technology allowed to increase the stability of parts of centrifugal pumps (shaft, bushing, impeller) in order of 2...3. The most effective were coatings using CrTiNi-alloy.

As a result of industrial tests, the possibility to use eutectic coatings for increasing the durability of cutting elements (knives KPI-2.4 and IKM-5) feed choppers in order of 1.7...2 compared to serial processes of quenching using HFC heating (steel 65Mn).

Technologies of strengthening and recovery of worn parts may be widely used at power plants. Comparative tests have proved that the durability of steam-water fast closing units (rods, gate valves, regulators etc) cladded with powder eutectic alloys has increased more than by 3 times in comparison with serial ones. The increase of service life of friction units (5–4 times), reduction of labor intensity (2–3 times) was achieved. We also have developed eco-friendly eutectic powder materials which provide savings of nickel and chromium up to 650 kg per 1 metric ton of powder alloy.

Table 3.3. Characteristics of already used and new developed alloys

Designation and alloying system	Strengthening phase, % vol.	Max. Operating temperature, °C	Hardness HRC	Heat resistance, (800°C, 6 hours) mg/cm <sup>2</sup>	Relative wear resistance	
					20 °C	800 °C
Already used alloys						
12Cr18Ni9Ti (Fe-Cr-Ni)	-	600	130-180 HB	2,8	1	1
PG-SR3 (Ni-Cr-B-Si)	-	700	50-55	2,6	7	12
PG-10N-01 (Ni-Cr-B-Si-C-Fe)	-	700	56-62	2,7	8	18

PG-10K-01 (Co-Ni-Cr-W-B-Si-C)	-	800	45-50	3,2	7	20
WSNGN-80 (Ni-Cr-B-Si-C-Mn)	W C35-80	600	58-62	3,2	10	14
New developed alloys						
VTiNi-26 (Fe-Ni-Cr-V-B-C-Ti)	(TiB <sub>2</sub> +VC)23	600	48-52	65	21	
TiNi (Fe-Ni-Cr-B-Ti)	TiB <sub>2</sub>	700	45-50	1,5	12	15
CrTiNi-23 (Fe-Ni-Cr-V-B-C-Al)	(TiB <sub>2</sub> + CrB <sub>2</sub> )20	750	45-50	0,75	9	14
CrTiNi+Al (Fe-Ni-Cr-B-Ti-Al)	(TiB <sub>2</sub> + CrB <sub>2</sub> )20	800	48-52	0,5	12	29
CrTiNi+Si (Fe-Ni-Cr-B-Ti-Si)	(TiB <sub>2</sub> + CrB <sub>2</sub> )20	800	48-52	0,7	11	40
VTiNi+Cu (Fe-Ni-Cr-V-B-C-Ti-Cu)	(TiB <sub>2</sub> + VB <sub>2</sub> )23	600	42-48	70	35	-
VTiNi+MoS <sub>2</sub> (Fe-Ni-Cr-V-B-C-Ti-MoS <sub>2</sub> )	(TiB <sub>2</sub> + VB <sub>2</sub> )23	500	42-48	84	35	-

### Conclusions on section #3

1. Based on conducted studies, new iron eutectic alloys reinforced by refractory phases having the structure of fine phase conglomeration or colonial structure have been developed.

2. Laser, gas thermal, HFC methods of cladding eutectic coatings are the effective methods to provide high wear resistance of various machine parts.

3. Industrial technologies for deposition of eutectic coatings by gas-thermal, laser, and HFC methods have been developed. They provide combination of two (with dissimilar degree of equilibrium) structures, and respectively, two strengthening mechanisms.

4. Based on wear tests it has been shown that the developed eutectic coatings have high tribological properties. A selective (non-all-over) remelting and thermocycling laser treatment changes properties of coating and increases their wear resistance in order of 2 magnitudes and even more.

5. Laser thermocycling treatment improves the adhesion of plasma coatings and reduces their hardness. Reheating of coating being in non-equilibrium state turns them back to equilibrium. Controlling the reheating temperature and time is an effective method to control tribological properties of clad coatings.

## **4. POWDER EUTECTIC MATERIALS OF FE-MN-C-B SYSTEM FOR COATINGS OF INCREASED ABRASIVE WEAR**

In this section, selected problems of manufacturing coatings with high wear resistance obtained based on eutectic materials of the quaternary Fe-Mn-C-B system are discussed. With regard to the structural state and physico-mechanical properties of eutectic powder alloys and coatings correspond to the composite dispersion-strengthened materials. The formation of a hardened layer with the structure of eutectic on the metal surface is the creation of a new material with certain mechanical properties. The analysis of different material properties and of alloy addition enabled to work out new eutectic powder alloys based on iron of the Fe-Mn-C-B system. In particular, it enabled to determine eutectic ranges and element contents.

One of the basic possibilities for obtaining surface layers with present properties is to apply coatings of powder based on eutectic alloys of, among other systems, the quaternary Fe-Mn-C-B system to specific material. Such materials offer the possibility of selecting multi-component eutectic alloys by alloying with elements such as silicon, nickel, chromium. These components are most frequently used to obtain products with required wear resistance properties of their surfaces. It means that the research on selection of such materials relates to searching for answers concerning the possibility of producing eutectic alloys as a family of multiphase dispersion-strengthened composite alloys with a structural gradient.

### **4.1. Materials and methods**

The issue discussed in this chapter relates to new materials, particularly resistant to the abrasive wear, and it has been the subject of permanent research for many years. This subject matter is of current interest due to the development and requirements for properties of various friction pairs used under increasingly new conditions. Such steel elements of some machines represent a group of items for which the research is conducted with regard, but not limited, to production of new composites with specified properties of their surface layers. The main issue for their development is the analysis of phase equilibrium systems. This also applies to the manufacture of new powder materials as eutectic alloys.

The equilibrium systems can be used as a basis for determination of phase composition, existence area and possible phase transitions in the production of eutectic alloys. The analysis of physico-chemical properties of alloying elements, considering possible phase transitions in the system, allows the possibilities of

introducing elements into a specific alloy to be evaluated and the nature of their impact to be determined.

The production of solid solutions, chemical compounds, mixture of specified elements with proper predetermined structure and alloy content makes it possible to predict the properties of produced alloys based on properties of input components. In other words, there is a specific relationship between the equilibrium system and the properties of alloys. In practice, a lot of useful alloyed materials consist of more than two components, although the literature has mainly described and studied two-component systems and not many three-component ones, and there are almost no studies on systems consisting of a higher number of components [91–93]. Taking into consideration the positive impact of borides and carbides (in particular, iron and manganese ones) on physico-mechanical properties, operating characteristics of materials and surface layers as well as specific features of producing eutectic layers, the equilibrium systems with eutectic transition using specified elements (components) were analysed. The analysis shows that eutectic systems are obtained in Fe-C, Fe-B, Fe-Mn-C, Fe-Cr-C and Fe-Ni-C systems (Tab. 4.1) [94, 95].

For production of materials with specified properties of resistance to the abrasive wear, Fe<sub>3</sub>C carbides as well as Fe<sub>2</sub>B, FeB and Cr<sub>2</sub>B borides were selected. The selection of carbides and borides as dispersion (strengthening) phases within the structure of alloy is dictated by their high hardness, wear resistance, corrosion resistance and thermal stability. Furthermore, the addition of manganese allows the ductility of Fe<sub>3</sub>C iron carbide and produced eutectic alloy to be increased. Mn forms a solid solution with iron, extends the temperature-concentration area of the existence of Fe<sub>3</sub>C-Mn<sub>3</sub>C carbides and, at the same time, increases the dispersibility of their distribution [96].

In all equilibrium systems, the formation of eutectic areas is caused by the effects of elements such as Fe, Mn, C, B, Si, Ni and Cr. The discussed research is focused on increasing the yield point of surface layers while ensuring their high hardness. This can be achieved owing to formation of various eutectic layers by introducing (alloying) elements to increase the hardness and ductility. In view of the foregoing and by analysing the properties of phase components, most efficient turns out to be the Fe-B-C system followed by the Fe-Mn-C one [97]. Therefore, it is appropriate to produce powder materials and eutectic layers of the Fe-Mn-C-B system.

In the Fe-Mn-C system, there is a very durable (Fe, Mn)<sub>7</sub>(B, C)<sub>3</sub> phase with rhombic structure. Ternary intersection of the Fe-Mn-C system [3] shows that the eutectic existence area is restricted by the carbon content only and, what is more, over a wide range of concentrations (0.2–0.8 wt%), while manganese content is not limited according to iron because of their unlimited solubility in a solid form.

Table 4.1. Characteristics of eutectic alloys formed based on iron and selected elements

System	Alloying elements	Content of elements in eutectic alloy wt%	Phase composition of alloy	Melting point, K	
				Eutectic mixture	Alloying element
Fe-B-C	Fe	95.6	$\alpha$ -Fe + Fe <sub>2</sub> B + Fe <sub>3</sub> C	1373	1811
	B	2.9			2350
	C	1.5			4413
Fe-Mn-C	Fe	97.4–86.6	$\alpha$ -Fe+(Fe, Mn) <sub>3</sub> C	1473	1811
	Mn	2.2–13			1518
	C	0.4			4413
Fe-Ni-B	Fe	70.2	$\gamma$ -Fe + (Fe, Ni) <sub>2</sub> B + (Fe, Ni) <sub>3</sub> B		1811
	Ni	25.0			1728
	B	4.8			2350
Fe-Cr-C	Fe	88.4	$\gamma$ -Fe + F <sub>3</sub> C + Cr <sub>7</sub> C <sub>3</sub>	–	1811
	Cr	8			2122
	C	3.6			4413
Fe-Ni-C	Fe	48	$\gamma$ -(Fe, Ni) <sub>2</sub> B + Fe <sub>3</sub> C		1811
	Ni	50			1728
	C	2			4413

In general, it can be concluded that types of elements and their specific contents in ternary systems are known. The Fe-B-C eutectic alloys contain,

respectively, in wt%, 1.5% C and 2.9% B, and the Fe-Mn-C alloys contain 0.4% C and 2.2–13% Mn. As a result, the subject of development of the Fe-Mn-C-B system to identify the possibilities of producing a eutectic mixture, determine the area of its existence as well as its phase composition and content of elements is still of current interest.

Based on the X-ray structural and microstructural examinations and thermal analysis of the Fe-Mn-C-B alloys, the content of elements in the eutectic areas of Fe-Mn-C and Fe-B-C systems was determined (Tab. 4.2) [97].

Table 4.2. Contents (wt%) of elements in eutectic areas of Fe-Mn-C and Fe-B-C systems

<b>Element</b>	<b>Fe-Mn-C</b>	<b>Fe-B-C</b>
<b>Fe</b>	73.3–92.5	85.1–92.5
<b>Mn</b>	3.1–23.8	1.6–7.6
<b>C</b>	0.6–6.4	2.6–7.0
<b>B</b>	0.6–2.5	0.2–3.5

Taking into consideration the specificity and technological details of producing eutectic alloys and surface layers as well as the obtained properties, in particular reduction in a tendency to cracking, it is advisable to adopt the same carbon and boron contents as in the Fe-Mn-C eutectic mixture. The elements of the Fe-Mn-C system offer the possibility of alloying with components such as Ni, Cr, Ni-Cr and others. This allows manufacturing powder materials with diverse properties, i.e. provides the possibility of influencing the properties of surface layers produced.

Therefore, it is justified to choose iron, manganese, carbon and boron as the basic elements for manufacturing the base eutectic powder material.

Iron – the main material, included in metallic products – forms solid solutions, chemical compounds and is a carbide former. Carbon and boron in combination with iron form eutectic systems as well as iron carbides and borides with high hardness and strength. In addition, the above-mentioned elements are characterised by high diffusive permeability in the process of saturation of iron-based alloys. In combination with iron, they form chemical compounds and interstitial solid solutions. For the eutectic alloys being developed, the elements were selected based on their known interactions in iron-based alloys [91–93, 98].

Manganese is characterised by high similarity to iron, and it can exchange with it very easily in carbides, at the same time increasing their ductility and dispersion while maintaining rather high strength and thermocyclic stability. Thus, manganese is a very good carbide former. Manganese carbides  $Mn_3C$  and iron carbides  $Fe_3C$  dissolve in each other, with virtually no limitations. Manganese in combination with iron forms a solid solution. Manganese atoms may substitute iron atoms in  $Fe_3C$  carbides. When manganese content is

increased in steel, its quantity also increases in carbides, while maintaining a constant ratio of 4:1. In low-carbon steels, carbon content in carbides is much higher than that in high-carbon ones. This difference can be explained by the absolute amount of carbide particles in steel and the related difference in depletion of  $\alpha$ -solid solution of iron with manganese. The depletion grows with the increase in amount of carbide particles, and thus carbon content in steel. This is because the basic factor that determines manganese content in carbide is not its amount in steel, but the ratio of equivalent amount of manganese in solid solution to the amount of carbon particles being formed. The weight content of manganese in carbides for steels containing approx. 1% C varies from 0 to 2%, while increasing manganese content in steel from 0 to 50%, respectively (ratio of 4:1). The equivalent content of manganese carbide can only be achieved as a result of rather long steel holding of steel at high temperatures (approx. 1000 K). Manganese extends the area of the existence of  $\gamma$  iron. In particular, manganese increases carbon solubility in  $\gamma$  solid solution at high temperatures. With increasing manganese content, the carbide transition point shifts towards the area of low-carbon contents. Manganese favours shifting of the  $\gamma$ - $\alpha$  transition towards low temperatures. At the same time, the rate of ongoing diffusion processes decreases, which reduces the rate of the transformation of austenite to martensite. It can be noticed that increasing manganese content in steel makes the degree of pearlite dispersion increase. However, manganese shows no visible impact on the steel hardness after quenching, tempering stability, cutability and heat resistance, which results from the absence of manganese carbides in steels.

During the formation of boride phases in surface layers, e.g.  $\text{Fe}_2\text{B}$  phase, boron atoms are transformed into  $\text{Sp}^2$  electron configurations, which try to turn into even more energetic equivalent  $\text{Sp}^3$  configurations. Therefore, iron tends to give some of its electrons to boron atoms and turn into a more equivalent state with formation of stable  $\text{d}^5$  configurations. In the state of isolated atoms, boron and iron show the following configuration of valence electrons:  $2\text{s}^22\text{p}^1$  and  $3\text{d}^64\text{s}^2$  [92]. As a result of the electron exchange and formation of energetically stable  $\text{Sp}^3$  and  $\text{d}^5$  configurations, strong covalent compounds are formed between iron and boron atoms. It means that the boride phase, which shows high degree of localisation of the atomic valence electrons, is characterised by relatively high hardness, wear resistance and corrosion resistance.

With the increase in principal quantum number of valence  $\text{Sp}$  electrons, the stability of  $\text{Sp}^3$  boron electron configuration is reduced, and thus the reliability of their occurrence is reduced too. The iron compounds containing silicon that form in the surface layer show considerably lower microhardness than iron borides.

Borides are characterised by significant resistance to abrasive wear compared to high-melting carbides and oxides. Wear resistance of boride-based surface layers decreases due to their high brittleness. In surface layers containing a slight amount of borides, wear resistance is also reduced due to the existence of a large

amount of core (matrix) material. It follows that the eutectic layers containing metal borides may be characterised by high ductility, hardness, durability and significant resistance to abrasive wear.

Boron is added to practically all heat-resistant nickel-based alloys for casting in the amount of 0.01–0.10% to strengthen the grain boundaries. It shows poor solubility in nickel. First of all, it dissolves according to the grain boundaries, at contents exceeding 0.015%. Along the grain boundaries, it is precipitated as borides, thus forming the eutectic mixture. Its reinforcing effect is realised mainly by inhibiting diffusion processes at the grain boundaries. This reduces the strength of the alloys, which is connected with formation of  $TiB_2$ ,  $CrB_2$  (Mo, W,  $Cr$ ) $_3B_2$  borides that practically contain no basic element – nickel.

The heat treatment being conducted has virtually no effect on the hardness of carbides and borides.

By changing the amounts of iron and ferromanganese, the eutectic degree of surface layers can be controlled. Adding B, Ni, Cr, Fe, Si, Cu, FeSi, FeB and other compounds to the base mixture makes it possible to develop a group of mixtures for forming surface layers with various properties. It allows selecting the range of mixture components to enhance the ability to saturate the surface layer while maintaining a relatively high hardness, wear resistance and ductility of produced layers. Taking into account the discussed effects, the base system of elements, i.e. Fe-Mn-C-B, as well as the area of the existence of eutectic and details of its formation were selected and defined. Based on the above-mentioned base system, the possibility of forming materials with defined phase composition as well as properly controlled physical, chemical and mechanical properties and operating characteristics was adopted.

The developed eutectic materials were made as a powder based on iron of the Fe-Mn-C-B system for build-up welding or spraying with partial melting of the surface layer. In these processes, this may cause their insufficient deoxidation, which, in turn, may adversely affect the formation of strengthened surface layer. To prevent the potential occurrence of the above-mentioned negative effects, boron and silicon were adopted as the elements to counteract oxidation. The enhancement of diffusion properties of eutectic alloys, in particular carbon, can be achieved by addition of silicon. Silicon forms limited solid solutions with iron and manganese. In recent years, much emphasis is placed on the development of self-deoxidising iron-based alloys containing boron and silicon. These materials replace expensive toxic deoxidisers, improve working conditions, simplify technologies and increase the efficiency of surface treatment by various methods. Thus, boron and silicon can be considered together with manganese as the perspective elements for production of low-cost surface layers compared to alloys in the form of nickel-based powder [95, 96].

Silicon favours the formation of boron from  $B_2O_3$  and production of increased amount of  $Fe_2B$  iron boride within the structure of eutectic layers. The applied silicon

content in eutectic layers [99] varies between 1.2 and 9.75 wt%. Due to the impact of silicon as deoxidiser and enriching the solution with iron atoms during the partial melting of treated material, its local content in the eutectic layer varied between 0.1 and 5%. The applied silicon concentration along the layer's depth varies between 1 and 2%. At FeSi content of 13% in the mixture (0.1–5 wt% per layer), the surface layer of Fe-Mn-C-B system with increased Fe<sub>2</sub>B content is formed. At a lower silicon content in the mixture, layers with sub-eutectic structure are produced. The use of silicon in the base system is due to the fact that it is a good deoxidiser, and together with manganese and boron it enhances self-oxidation of powder materials. Self-oxidation is necessary, particularly, while forming the surface layers by build-up welding, spraying or spraying with partial melting of the surface layer, when there is no possibility of introducing additional self-oxidising elements, like, for example, the use of B<sub>2</sub>O<sub>3</sub> in build-up welding with high-frequency currents. Therefore, it is necessary to use silicon for alloying the base powder Fe-Mn-C-B system.

Iron in combination with silicon forms solid solutions (maximum silicon content is approx. 1.5%), which are characterised by good resistance to various acids and high temperatures. Steels usually contain very low amounts of silicon (0.0–1.3%). The impact of silicon on properties is slight if ignoring its effect as a deoxidiser, which is similar to that of manganese. At contents of 0.5–0.6% and above, silicon is considered as an alloying element, which increases hardness and ultimate strength of alloys at high temperatures and corrosion resistance at low temperatures and reduces ductility. When reducing silicon content within the areas of  $\gamma$ -solutions in alloys containing more than 3 wt% Si, there are no phase transitions up to the melting point.

In selection of elements, it is taken into consideration that silicon is the second most important component after carbon in cast irons. By reducing silicon content, the graphitisation coefficient of cast iron can be controlled. Already at Si content of 4% and more, practically all cast irons used in thin-walled casts are replaced with cast irons with grey cast iron structure. The castable cast irons usually contain 1.25–4.2% Si, while the workable ones contain 0.2–2% Si, which is taken into consideration when selecting the amounts of silicon and boron in eutectic alloys.

Silicon quickly reduces the amount of carbon in eutectic mixture. At Si content of 16%, hypereutectic are even alloys containing 0.6–1.0% C. Alloys containing 14–16% Si are characterised by high-corrosion resistance, and hence they are commonly used in the chemical industry.

Silicon is an element, which significantly reduces the diffusion coefficient of carbon in the  $\alpha$ - and  $\gamma$ -crystal lattice. In steel, carbides contain a small amount of silicon as its atoms are quickly moved from carbides to solid solution. Silicon is not a typical carbide former. In alloys with high silicon content (20–23% Si), SiC carbide is formed. Therefore, the limit of alloying eutectic alloys with silicon is

assumed to be approx. 3–4% because the ductility of eutectic alloys decreases at its greater contents.

For examinations of the Fe-Mn-C-B phase equilibrium system, the preparation of samples from carbonyl iron (99.99%), manganese (99.5%), amorphous boron (99.3%) and synthetic graphite (99.94 %) powders by alloying in an electric furnace in a purified argon atmosphere was adopted. The annealing of samples was carried out in vacuum quartz containers at 1273 K for 350 h. To determine samples with a eutectic structure, thermal and metallographic tests (Neophot-2 MIM-8, DAT, AT) were carried out and the concentration of elements ('Kamebax,' Superprobe-733) in alloys in the as-annealed (1273 K, 350 h) and standardised condition was analysed. Based on obtained data, a quasi-ternary Fe-Mn-C-B-Si system was developed (Fig. 4.1). The component contents in individual intersections were changed every 10 molar parts. The area of iron concentration was 0.67–0.79 at% [96, 98].

For evaluation of the structure and phase composition of elements, the X-ray analysis of phase composition of the alloys produced and the micro-X-ray structural analysis of the content of elements was carried out.

The obtained effects of structural analyses of the alloys, in particular their phase composition and content of elements, are presented as a description of phase areas, I and II, and areas of the existence of Fe-Mn-C and Fe-B-C eutectics, A and B, in four quasi-ternary intersections (Fig. 4.1, a–d) [99].

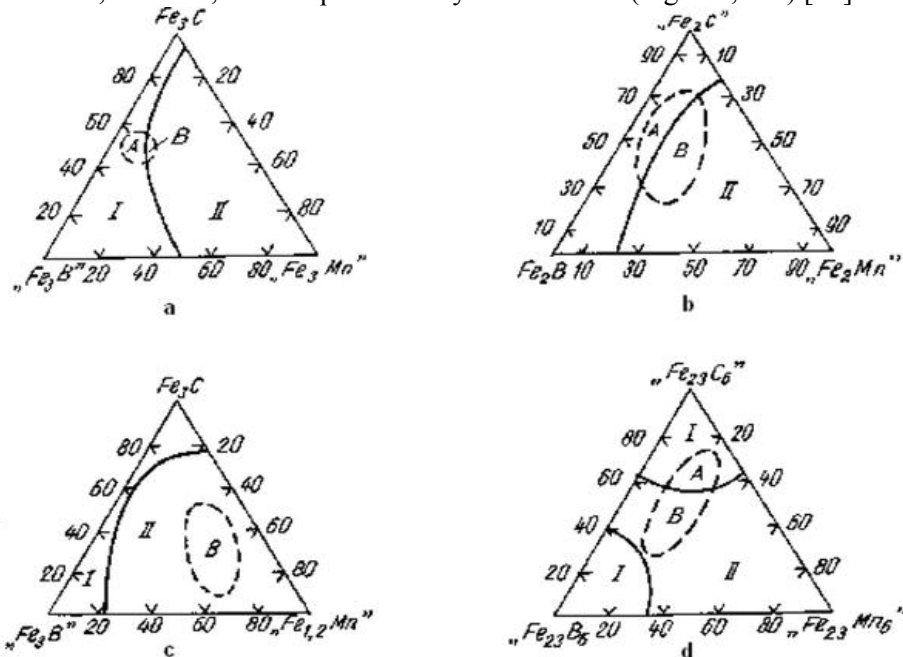


Fig. 4.1. Phase areas (I, II, A, B) in quasi-ternary intersections: a)  $\text{Fe}_3\text{C}$ - $\text{Fe}_3\text{B}$ - $\text{Fe}_3\text{Mn}$ , b)  $\text{Fe}_2\text{C}$ - $\text{Fe}_2\text{B}$ - $\text{Fe}_2\text{Mn}$ , c)  $\text{Fe}_3\text{C}$ - $\text{Fe}_3\text{B}$ - $\text{Fe}_{1.2}\text{Mn}$ , d)  $\text{Fe}_{23}\text{C}_6$ - $\text{Fe}_{23}\text{B}_6$ - $\text{Fe}_{23}\text{Mn}_6$ .

## 4.2. Examination and analysis of Fe<sub>3</sub>C–Fe<sub>3</sub>B–‘Fe<sub>3</sub>Mn’ quasi-ternary intersection

In order to determine the phase areas and content of elements, the micro-X-ray and microstructural examinations of the Fe<sub>3</sub>C–Fe<sub>3</sub>B–‘Fe<sub>3</sub>Mn’ quasi-ternary intersection were carried out. Based on the examinations performed, two phase areas were identified (Fig. 4.1, a; Tab. 4.3). Area I consists of Fe<sub>3</sub>(B, C),  $\alpha$ -(Fe, Mn),  $\gamma$ -(Fe, Mn), and area II consists of  $\alpha$ -(Fe, Mn),  $\gamma$ -(Fe, Mn), (Fe, Mn)<sub>23</sub>(C, B)<sub>6</sub>, (Fe, Mn)<sub>2</sub>B.

Table 4.3. Phase composition of Fe-Mn-C-B samples with iron content of 0.75 at%

#	Component contents; molar part 10			Phase composition	Alloy type	Phase area (Figure 4.1, a)
	Fe <sub>3</sub> C	“Fe <sub>3</sub> B”	“Fe <sub>3</sub> Mn”			
3	5	4	1	Fe <sub>3</sub> (B, C) + $\alpha$ -(Fe, Mn) + trace amount of $\gamma$ -(Fe, Mn)	Hyper-eutectic alloy	I
1	1	8	1	Fe <sub>3</sub> (B, C) + trace amount of $\alpha$ -(Fe, Mn)	Solid solution	
2	3	6	1			
6	2	6	2			
4	7	2	1	Fe <sub>3</sub> (B, C) + $\alpha$ -(Fe, Mn)		
10	1	6	3			
11	3	4	3			
12	8	1	1	$\alpha$ -(Fe, Mn)+(Fe, Mn) <sub>2</sub> B+(Fe, Mn) <sub>23</sub> (C, B) <sub>6</sub>	II	
13	6	2	2			
14	4	4	2	$\alpha$ -(Fe, Mn) + traces of transient phase +(Fe, Mn) <sub>23</sub> (C, B) <sub>6</sub> + $\gamma$ -(Fe, Mn) +		
15	2	3	5			

#	Component contents; molar part 10			Phase composition	Alloy type	Phase area (Figure 4.1, a)
	Fe <sub>3</sub> C	“Fe <sub>3</sub> B”	“Fe <sub>3</sub> Mn”			
18	2	2	6	trace amount of $\alpha$ -(Fe, Mn)		
17	4	1	5	(Fe, Mn) <sub>23</sub> (C, B) <sub>6</sub> + $\gamma$ -(Fe, Mn) + $\alpha$ -(Fe, Mn)	Solid solution	II
18	1	2	7			
19	3	2	5	(Fe, Mn) <sub>23</sub> (C, B) <sub>6</sub> + $\gamma$ -(Fe, Mn)		

As a result of micro-X-ray examinations, the following content of elements in hypereutectic alloys was determined (in at%): 67.8–75.0 Fe, 1.2–4.5 Mn, 8.5–14.3 B, 11.0–13.9 C [6, 10].

The quasi-ternary intersection of the equilibrium system was examined for 19 samples, annealed at 1273 K. In the analysed intersection, the (Fe, Mn)<sub>23</sub>(C, B) and (Fe, Mn)<sub>3</sub>(B, C) phases with Fe<sub>23</sub>C<sub>6</sub> and Fe<sub>3</sub>C structures, respectively, were established. For example, sample nos. 6 and 10 contain a phase with cementite structure the lattice of which has the following parameters: a = 0.5341, b = 0.6650, c = 4.459 nm. Parameters of the cementite structure phase lattice correspond to those of Fe<sub>3</sub>C. Samples 1–4 and 11 contain the Fe<sub>3</sub>C phase only with increased lattice parameters, which corresponds to those of Fe<sub>3</sub>(B,C) borocarbide. Some of the samples include the (Fe, Mn)<sub>23</sub>(B, C)<sub>6</sub> phase, Fe<sub>2</sub>B-(Fe, Mn)<sub>2</sub>B-based solid solution. The peculiarity of sample nos. 1–8, 10, 11, 15, 17, 18, 19 (Tab. 4.3) is that they include the  $\alpha$ -(Fe, Mn) solid solution. The obtained phase composition of hypereutectic alloy samples is presented in Tab. 4.3.

As it can be seen in Tab. 4.3, for phase area I (Fig. 4.1, a), the hypereutectic alloy is formed in sample no. 3 only, whereas all other samples represent solid solutions.

As it was determined from experimental metallographic and X-ray structural examinations of the alloys, sample no. 3 Fe<sub>75</sub>Mn<sub>3.6</sub>B<sub>10</sub>C<sub>12.5</sub> is a hypereutectic alloy composed of Fe<sub>3</sub>(B, C) +  $\alpha$ -(Fe, Mn) eutectic between which Fe<sub>0.4</sub>Mn<sub>3.6</sub>C iron-manganese carbides are arranged. The second grade dendrites are arranged in the crystallographic direction [101] (Fig. 4.2, a). The annealing of Fe<sub>75</sub>Mn<sub>3.6</sub>B<sub>10</sub>C<sub>12.5</sub> alloy at 1273 K for 350 h results in the formation of pearlitic grooves (Fig. 4.2, b). In carbon-enriched alloys, the Fe<sub>0.4</sub>Mn<sub>3.6</sub>C iron-manganese carbide lamellas of 15–35  $\mu$ m in length are formed (Fig. 4.2, c). A strip of the

second eutectic phase – pearlite – is formed on the lamella surface and grows along the surface. It has the appearance of a flat dendrite. The results of the examinations confirm that in the crystallisation process, the leading phase in the phase carbon-solid solution eutectics is always carbide crystals. The structure of other examined samples –  $\alpha$ - and  $\gamma$ -(Fe, Mn)-based solid solutions with  $\text{Fe}_3(\text{C}, \text{B})$ ,  $(\text{Fe}, \text{Mn})_2\text{B}$  borocarbide or  $(\text{Fe}, \text{Mn})_{23}(\text{C}, \text{B})_6$  carbide inclusions. The Fe-B-C eutectic exists in area A, while the Fe-Mn-C eutectic is observed in area B (Fig. 1, a).

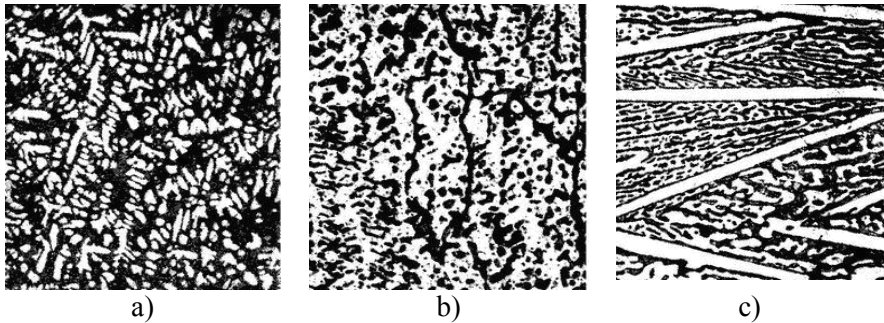


Fig. 4.2. Microstructure ( $\times 200$ ) of the examined samples (markings according to Tab. 4.3), hyper-eutectic alloy [a, b] sample no. 3] and solid solution [c] sample no. 5]; a) after normalising; b, c) after annealing (at 1273 K, 350 h)

### 4.3. Examination and analysis of ‘ $\text{Fe}_2\text{C}$ ’– $\text{Fe}_2\text{B}$ –‘ $\text{Fe}_2\text{Mn}$ ’ quasi-ternary intersection

To determine the phase areas and the content of elements, the examinations of ‘ $\text{Fe}_2\text{C}$ ’– $\text{Fe}_2\text{B}$ –‘ $\text{Fe}_2\text{Mn}$ ’ intersection samples (Fig. 4.1b) containing the  $\text{Fe}_3(\text{B}, \text{C})$ ,  $\text{Fe}_2\text{B}$ ,  $\gamma$ -(Fe, Mn) and  $(\text{Fe}, \text{Mn})_{23}(\text{C}, \text{B})_6$  phases were carried out. Phase composition of the samples with iron content of 0.667 at% is presented in Tab. 4.4.

Table 4.4. Phase composition of Fe-Mn-C-B samples with iron content of 0.667 at% (‘ $\text{Fe}_2\text{C}$ ’- $\text{Fe}_2\text{B}$ -‘ $\text{Fe}_2\text{Mn}$ ’ intersection (Fig. 4.1, b))

#	Component contents; molar part 10			Phase composition	Alloy type	Phase area
	‘ $\text{Fe}_2\text{C}$ ’	$\text{Fe}_2\text{B}$	‘ $\text{Fe}_2\text{Mn}$ ’			
1	1	8	1	$\text{Fe}_3(\text{C}, \text{B})$	Solid	I
2	3	6	1	..	..	

#	Component contents; molar part 10			Phase composition	Alloy type	Phase area
	'Fe <sub>2</sub> C'	Fe <sub>2</sub> B	'Fe <sub>2</sub> Mn'			
3	5	4	1	„	Hyper- eutectic alloy	
4	7	2	2	„	-"-	I
5	7	2	2	Fe <sub>3</sub> (C, B)	Solid solution	II
9	1	1	1	(Fe, Mn) <sub>23</sub> (B, C) <sub>6</sub> + Fe <sub>2</sub> B + Fe <sub>3</sub> (B, C)		
6	3	5	2	(Fe, Mn) <sub>23</sub> (B, C) <sub>6</sub> + Fe <sub>2</sub> B + Fe <sub>3</sub> (B, C)	Hyper- eutectic alloy	
7	5	3	2	(Fe, Mn) <sub>23</sub> (B, C) <sub>6</sub> +γ-(Fe, Mn)		
10	5	2	3	(Fe, Mn) <sub>23</sub> (C, B) <sub>6</sub> +γ-(Fe, Mn)	Solid solution	
11	1	5	4	„	„	
12	3	3	4	„	„	
13	5	1	4	„	„	
15	2	2	6	„	„	
14	1	3	6	γ-(Fe, Mn)+(Fe, Mn) <sub>23</sub> (C, B) <sub>6</sub>	Solid solution	
16	3	1	6	„	„	
17	1	1	6	„	„	

#	Component contents; molar part 10			Phase composition	Alloy type	Phase area
	'Fe <sub>2</sub> C'	Fe <sub>2</sub> B	'Fe <sub>2</sub> Mn'			
8	7	1	2	$\gamma$ -(Fe, Mn)	Solid solution	

Based on the micro-X-ray and microstructural examinations performed in the 'Fe<sub>2</sub>C'–Fe<sub>2</sub>B–'Fe<sub>2</sub>Mn' quasi-ternary intersection, two phase areas were identified (Fig. 4.1, b; Tab. 4.4). Area I consists of Fe<sub>3</sub>(C, B) and area II consists mainly of (Fe, Mn)<sub>23</sub>(C, B)<sub>6</sub> +  $\gamma$ -(Fe, Mn). Hypereutectic alloys are in area II (Fig. 4.1, b). The Fe-B-C eutectic exists in area A, while the Fe-Mn-C eutectic is observed in area B (Fig. 4.1, b). Content of elements in hypereutectic alloys (at%): 66.7 Fe, 3.3–6.7 Mn, 10.0–23.3 C, 6.7–16.6 B. In hypereutectic alloys (sample Nos 3–4), the primary Fe(B, C) crystals and (Fe, Mn)<sub>23</sub>(C, B) iron-manganese carbide dendrites are formed, Fig. 4.3a and b. No borocarbide inclusions were identified. In boron-enriched alloys, the primary austenite crystals are formed. In  $\gamma$ -(Fe, Mn)-(Fe, Mn)<sub>23</sub>(C, B)<sub>6</sub> eutectic alloys, the micro-areas of  $\gamma$ -(Fe, Mn) solid solution and austenite dendrites were revealed. In alloys containing an increased amount of manganese, the primary dendrites (Fe, Mn)<sub>23</sub>(C, B)<sub>6</sub> are formed (Fig. 4.3, c). Content of elements in eutectic alloys (at%): 66.6 Fe, 1.7–11.0 Mn, 7.7–25.0 C, 4.0–8.4 B [94, 99].

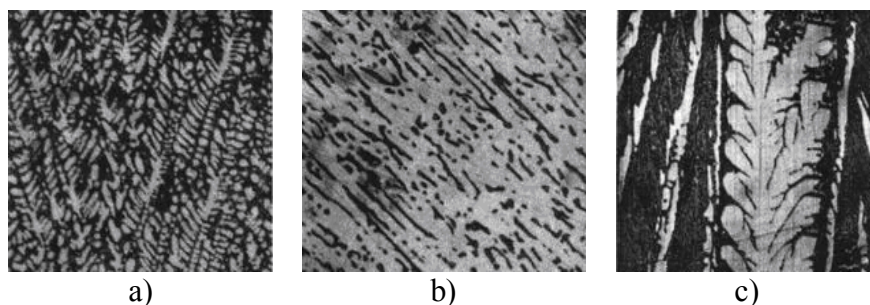


Fig. 4.3. Microstructure ( $\times 200$ ) of the examined 'Fe<sub>2</sub>C'–Fe<sub>2</sub>B–'Fe<sub>2</sub>Mn' quasi-ternary intersection alloys (markings according to Table 4): a, b) sample no. 3, c) sample no 10; a, c) after normalisation; b) after annealing at 1273 K, 350 h

#### 4.4. Examination and analysis of Fe<sub>3</sub>C-Fe<sub>3</sub>B-‘Fe<sub>1.2</sub>Mn’ quasi-ternary intersection

In the examined quasi-ternary intersection, most of the Fe<sub>3</sub>C-Fe<sub>3</sub>B-‘Fe<sub>1.2</sub>Mn’ samples (Fig. 4.1, c) comprise the (Fe, Mn)<sub>23</sub>(C, B)<sub>6</sub> phase, which is in equilibrium with the Fe<sub>3</sub>(B, C) and γ-(Fe, Mn) or γ-(Fe, M) phase. According to the results of phase analysis, the (Fe, Mn)<sub>23</sub>(C, B)<sub>6</sub> + γ-(Fe, Mn) + Fe<sub>3</sub>(C, B) phase area is visible very well [97, 98]. The samples contain no α-Fe-based phase. Phase composition of the samples is presented in Tab. 4.5. The most complex structure (number of phases) is visible in sample nos. 4, 24.

Based on the micro-X-ray and microstructural examinations performed in the Fe<sub>3</sub>C-Fe<sub>3</sub>B-‘Fe<sub>1.2</sub>Mn’ quasi-ternary intersection, two phase areas were identified (Fig. 4.1, c; Tab. 4.5). Area I consists of (Fe, Mn)<sub>23</sub>(C, B)<sub>6</sub>, Fe<sub>3</sub>(C, B) and γ-(Fe, Mn) and area II consists of (Fe, Mn)<sub>23</sub>(C, B)<sub>6</sub>, γ-(Fe, Mn) and Fe<sub>3</sub>(B, C). Sub-eutectic alloys are in area II (Fig. 4.1, c). In the intersection determined, there is only the Fe-Mn-C eutectic in area B (Fig. 4.1, c).

Table. 4.5. Phase composition of Fe-Mn-C-B samples, Fe<sub>3</sub>C+Fe<sub>3</sub>B+‘Fe<sub>1.2</sub>Mn’ intersection (Fig. 4.1, c)

#	Component contents; molar part 10			Phase composition	Alloy type	Phase area
	Fe <sub>3</sub> C	Fe <sub>3</sub> B	Fe <sub>1.2</sub> Mn			
6	1	7	2	(Fe, Mn) <sub>23</sub> (C, B) <sub>6</sub> + small amount of Fe <sub>3</sub> (B, C)	Solid solution	I
1	1	8	1	Fe <sub>3</sub> (C, B) + γ-(Fe, Mn)	-"-	
2	2	7	1	Fe <sub>3</sub> (B, C)	-"-	I
5	8	1	1	-"-	-"-	
13	2	2	3	(Fe, Mn) <sub>23</sub> (B, C) <sub>6</sub> + γ-(Fe, Mn)	Sub-eutectic	II
20	4	1	5	-"-	Solid solution	
21	1	3	6	-"-	-"-	

#	Component contents; molar part 10			Phase composition	Alloy type	Phase area
	Fe <sub>3</sub> C	Fe <sub>3</sub> B	Fe <sub>1,2</sub> Mn			
3	4	5	1	--	--	
7	3	5	2	--	--	
12	3	4	3	--	--	
14	6	1	3	--	--	
16	3	3	4	--	--	
17	5	1	4	--	--	
22	2	2	6	(Fe, Mn) <sub>23</sub> (B, C) <sub>6</sub> + trace amount of $\gamma$ -(Fe, Mn)	--	II
26	1	1	8	--	--	
25	2	1	7	(Fe, Mn) <sub>23</sub> (B, C) <sub>6</sub> + small amount of $\gamma$ -(Fe, Mn)	--	

In manganese-enriched sub-eutectic alloys, the primary dendrites  $\gamma$ -(Fe, Mn) are formed and the (Fe, Mn)<sub>23</sub>(C, B)<sub>6</sub>+ $\gamma$ -(Fe, Mn) eutectic is arranged between them (Fig. 4.4, a). The annealing of alloys results in homogenisation and coagulation of  $\gamma$ -(Fe, Mn) crystals (Fig. 4.4, b). Content of elements in sub-eutectic alloys (at%): 65.3–71.1 Fe, 8.7–21.5 Mn, 2.8–15.4 C, 2.9–10.4 B.

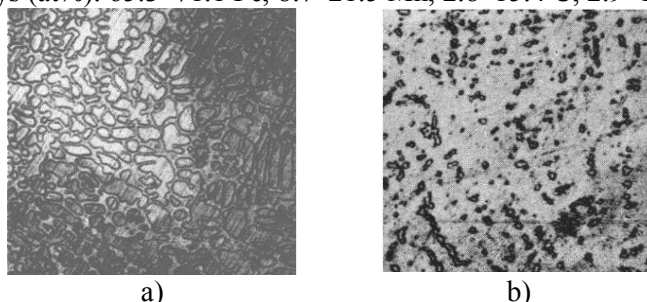


Fig. 4. 4. Microstructure ( $\times 200$ ) of the examined Fe<sub>3</sub>C-Fe<sub>3</sub>B-‘Fe<sub>1,2</sub>Mn’ quasi-ternary intersection alloys (markings according to Tab. 4.5): a) sample no. 13, sub-eutectic alloy after normalising; b) solid solution, sample no. 20, after annealing at 1273 K, 350 h

#### 4.5. Examination and analysis of 'Fe<sub>23</sub>C<sub>6</sub>'-'Fe<sub>23</sub>B<sub>6</sub>'-'Fe<sub>23</sub>Mn<sub>6</sub>' quasi-ternary intersection

To determine the phase areas and the content of elements, the examinations of 'Fe<sub>23</sub>C<sub>6</sub>'-'Fe<sub>23</sub>B<sub>6</sub>'-'Fe<sub>23</sub>Mn<sub>6</sub>' intersection (Fig 4.1, d) containing the phase with carbide structure (Fe, Mn)<sub>23</sub>(C,B)<sub>6</sub> in Fe-B-C i Fe-Mn-C ternary systems, which restrict the examined intersection, were carried out. The highest number of phases in equilibrium is found in phase area II – (sample no. 7) (Fe, Mn)<sub>23</sub>(B, C)<sub>6</sub> + α-(Fe, Mn) + Fe<sub>3</sub>(B, C) and in phase area I – (sample no. 10) Fe<sub>3</sub>(B, C) + traces of α-(Fe, Mn) + γ-(Fe, Mn). Samples 4, 5, 7, 10 and 19 (Tab. 4.6) comprise the ternary phase Fe<sub>3</sub>(B, C) [7]. Some of the samples comprise the quaternary phase (Fe, Mn)<sub>23</sub>(C, B)<sub>6</sub>. At the intersection of Fe-Mn-C-B system, at Fe content of 0.79 atomic parts, the phase equilibrium of (Fe, Mn)<sub>23</sub>(C, B)<sub>6</sub> + Fe<sub>3</sub>(C, B) + γ-(Fe, Mn) + γ-(Fe, Mn) was identified too. In particular, the γ-(Fe, Mn) phase was observed in samples 2, 5, 7, 9, 10 and 11 (Tab. 4.6).

Table 4.6. Phase composition of Fe-Mn-C-B samples; intersection at iron content of 0.79 at%

#	Component contents molar part 10			Phase composition	Alloy type	Phase area
	'Fe <sub>23</sub> C <sub>6</sub> '	'Fe <sub>23</sub> B <sub>6</sub> '	'Fe <sub>23</sub> Mn <sub>6</sub> '			
7	3	5	2	(Fe, Mn) <sub>23</sub> (B, C) <sub>6</sub> + α-(Fe, Mn) + Fe <sub>3</sub> (B, C)	Sub-eutectic	II
9	5	3	2	(Fe, Mn) <sub>23</sub> (B, C) <sub>6</sub> + trace amount of α-Fe	--	
11	1	6	3	γ-(Fe, Mn) + Fe <sub>3</sub> (B, C) + (Fe, Mn) <sub>23</sub> (B, C) <sub>6</sub> + α-(Fe, Mn)	--	
3	5	4	1	(Fe, Mn) <sub>23</sub> (B, C) <sub>6</sub>	--	
12	2	4	3	(Fe, Mn) <sub>23</sub> (B, C) <sub>6</sub> + γ-(Fe, Mn)	Solid solution	
13	5	2	3	--	--	
32	2	2	6	γ-(Fe, Mn) + (Fe, Mn) <sub>23</sub> (B, C) <sub>6</sub>	--	

#	Component contents molar part 10			Phase composition	Alloy type	Phase area
	'Fe <sub>23</sub> C <sub>6</sub> '	'Fe <sub>23</sub> B <sub>6</sub> '	'Fe <sub>23</sub> Mn <sub>6</sub> '			
23	3	1	6	-"-	-"-	
2	3	4	3	$\alpha$ -Fe + Fe <sub>23</sub> (B, C)	-"-	I
4	7	2	1	Fe <sub>3</sub> (B, C)	-"-	
5	8	1	1	Fe <sub>3</sub> (B, C) + trace amount of $\alpha$ -Fe	-"-	
10	7	1	2	Fe <sub>3</sub> (B, C) + trace amount of $\alpha$ - (Fe, Mn) + $\gamma$ -(Fe, Mn)	Sub- eutectic	
19	3	2	5	$\gamma$ -(Fe, Mn) + $\alpha$ -(Fe, Mn) + Fe <sub>3</sub> (B, C)	-"-	

Based on the micro-X-ray and microstructural examinations performed in the 'Fe<sub>23</sub>C'-Fe<sub>23</sub>B'-Fe<sub>23</sub>Mn' quasi-ternary intersection, two phase areas were identified (Fig. 4.1, d; Tab. 4.6). Area I consists of Fe<sub>3</sub>(C,B),  $\alpha$ -(Fe, Mn),  $\gamma$ -(Fe, Mn) and  $\alpha$ -Fe and area II consists of (Fe, Mn)<sub>23</sub>(C, B)<sub>6</sub>,  $\alpha$ -(Fe, Mn),  $\gamma$ -(Fe, Mn) and Fe<sub>3</sub>(B, C). Sub-eutectic alloys are in areas I and II (Fig. 4.1, d). The Fe-B-C eutectic exists in area A, while the Fe-Mn-C eutectic is observed in area B (Fig. 4.1, d).

Content of elements in sub-eutectic alloys (at%): 79.3 Fe, 2.7–6.2 Mn, 5.4–15.5 C, 1.1–10.8% B. In sub-eutectic alloys, austenite dendrites are formed at elevated carbon contents, while at lower carbon contents, pearlite dendrites are formed (Fig. 4.5, a). Austenite dendrites are evenly distributed throughout the alloy volume. The annealing of subeutectic alloys results in coagulation of  $\gamma$ -(Fe, Mn) crystals (Fig. 4.5, b).

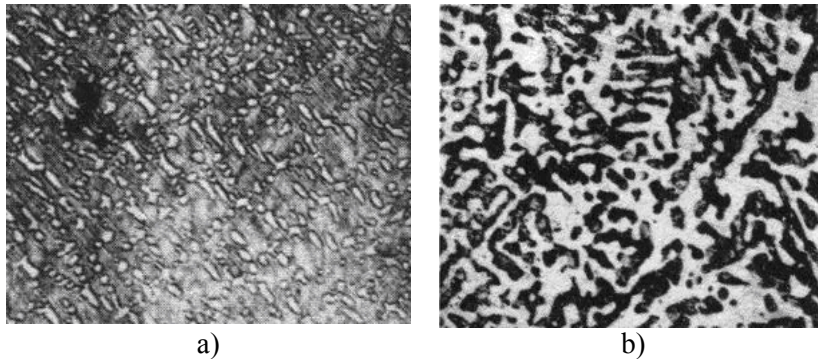


Fig. 4.5. Microstructure ( $\times 200$ ) of sub-eutectic alloy, sample no. 7 (markings according to Tab. 4.6); a) after normalising; b) after annealing at 1273 K, 350 h

By comparing the nature of the effects of components, it can be concluded that the  $(\text{Fe, Mn})_{23}(\text{C, B})_6$  phase was found at all intersections. As a pure phase, it exists at Fe content of 0.79 at% (molar parts $^{\circ}10$ ):  $5\text{Fe}_{23}\text{C}_6\text{Fe}_{23}\text{Mn}_64\text{Fe}_{23}\text{B}_6-4\text{Fe}_3\text{CFe}_{12}\text{Mn}5\text{Fe}_3\text{B}$ , intersection  $\text{Fe}_3\text{C}-\text{Fe}_3\text{B}-\text{Fe}_{1.2}\text{Mn}$ .

The areas were identified where quaternary borocarbide is included as the basic phase:  $(3-4)\text{Fe}_3\text{B}(4-5)\text{Fe}_3\text{Mn}(2-3)\text{Fe}_3\text{C}-\text{Fe}_3\text{B}8\text{Fe}_3\text{Mn}2\text{Fe}_3\text{C}$  at Fe content of 0.75 atomic parts and  $(1-5)\text{Fe}_2\text{B}4\text{Fe}_2\text{Mn}(1-5)\text{Fe}_2\text{C}-(2-3)\text{Fe}_2\text{B}(2-6)\text{Fe}_2\text{Mn}(2-5)\text{Fe}_2\text{C}$  at Fe content of 0.667 atomic parts. A relationship was observed according to which with the reduction in iron content, the area of the existence of  $(\text{Fe, Mn})_{23}(\text{C, B})_6$  phase moves towards the area of higher manganese and boron contents and lower carbon content (Fig. 4.1, a and b).

Based on theoretical assumptions and experimental verification, the areas of the existence of Fe-Mn-C-B eutectic, as a new family of dispersion-strengthened eutectic alloys with a structural gradient, were identified. The areas of the existence (Fig. 4.1; Tab. 4.7) of hyper- and sub-eutectic alloys were identified too.

Eutectic alloys are dispersion-reinforced composites with a structural gradient in which the soft matrix lamellar phase (alloying pearlite or austenite) is strengthened with hard and resistant  $\text{Fe}_{0.4}\text{Mn}_{3.6}\text{C}$  phase. The structure and properties of the alloys can be controlled by changing the contents of their components [102–116]. The alloying can be carried out with the majority of selected metallic elements in the periodic table over their wide concentrations. Carbon content in alloys, according to the Fe-Mn-C equilibrium diagram, can be changed in a broad range – 0.6–6.4 wt%.

**Table 4.7.** Content of elements in eutectic areas of  $\text{Fe}_2\text{C}-\text{Fe}_2\text{B}-\text{Fe}_2\text{Mn}$ ,  $\text{Fe}_3\text{C}-\text{Fe}_3\text{B}-\text{Fe}_3\text{Mn}$ ,  $\text{Fe}_3\text{C}-\text{Fe}_3\text{B}-\text{Fe}_{1.2}\text{Mn}$ ,  $\text{Fe}_{23}\text{C}_6-\text{Fe}_{23}\text{B}_6-\text{Fe}_{23}\text{Mn}_6$  intersections of the Fe-Mn-B-C system. \* numerator: wt%, denominator: at%.

Quasi-ternary intersection		Content of elements*			
		Fe	Mn	C	B
System	Fe-Mn-C-B	73.3–92.5	1.6–23.8	0.6–7.0	0.2–3.5
		65.3–79.3	1.2–21.5	2.8–25.0	1.1–18.4
Eutectic	Fe-Mn-C	73.3–92.5	3.1–23.8	0.6–6.4	0.6–2.5
		65.3–79.3	2.7–21.5	2.8–23.4	2.9–18.4
Eutectic	Fe-B-C	85.1–92.5	1.6–7.6	2.6–7.0	0.2–3.5
		66.6–79.3	1.2–6.2	10.5–25.0	1.1–17.7
Intersection	Fe <sub>2</sub> C-Fe <sub>2</sub> B- “Fe <sub>2</sub> Mn”	81.2–89.2	2.2–13.1	2.0–7.0	0.9–4.5
		66.6	1.7–11.0	7.7–25.0	4.0–8.4
Eutectic	Fe-Mn-C	81.2–86.3	6.0–13.1	2.0–6.4	0.9–4.6
		66.6	4.7–11.0	7.7–23	4.0–18.4
Eutectic	Fe-B-C	85.1–89.2	2.2–7.6	3.0–7.0	0.9–4.4
		66.6	1.7–6.0	11.0–25.0	4.0–17.7
Intersection	Fe <sub>3</sub> C- Fe <sub>3</sub> B- “Fe <sub>3</sub> Mn”	87.1–92.5	1.6–5.7	2.8–3.7	1.9–3.5
		67.8–75.0	1.2–4.5	11.0–13.9	8.5–14.3
Eutectic	Fe-Mn-C	90.1–91.2	3.3–4.8	2.8–3.5	1.9–2.4
		75.0	2.8–4.0	11.0–13.7	8.5–10.0
Eutectic	Fe-B-C	87.1–92.5	1.6–5.7	2.8–3.7	2.0–3.5
		67.8–75.0	1.2–4.5	11.0–13.9	8.5–14.3
Intersection	Fe <sub>3</sub> C-	73.3–84.9	10.2–23.8	0.6–0.4	0.6–2.3

Quasi-ternary intersection		Content of elements*			
		Fe	Mn	C	B
Eutectic	Fe-Mn-C	65.3–71.1	8.7–21.5	2.8–15.4	2.9–10.4
Intersection	“Fe <sub>23</sub> C <sub>6</sub> ”- “Fe <sub>23</sub> B <sub>6</sub> ”- “Fe <sub>23</sub> Mn <sub>6</sub> ”	89.7–92.5	3.1–6.9	1.4–3.9	0.2–2.5
		79.3	2.7–6.2	5.4–15.5	1.1–10.8
Eutectic	Fe-Mn-C	89.7–92.5	3.1–6.9	1.4–2.9	0.7–2.5
		79.3	2.7–6.2	5.4–10.9	3.6–10.8
Eutectic	Fe-B-C	89.7–92.5	3.1–6.7	2.8–3.9	0.2–1.5
		79.3	2.7–6.1	10.7–15.5	1.1–6.8

For the development of chemical composition of eutectic alloys, the examinations of the Fe-Mn-C-B phase equilibrium system were used to determine the eutectic areas (Tab. 4.3–4.6; Fig. 4.1–4.5). The composition of elements for the production of eutectic alloys of the Fe-Mn-C-B system is as follows (wt%):

Fe 86.6–97.4

Mn 2.2–13.0

C 0.4–1.5

B 2.9

The following content of elements in eutectic areas was identified by X-ray phase analysis after four quasi-ternary intersections (Fig. 4.1; Tab. 4.7).

#### Conclusions on section #4

The following conclusions can be put forward based on the works performed:

1. The analysis of the examined systems makes it possible to conclude that

Fe 73.3–92.5

Mn 1.6–23.8

C 0.6–7.0

Fe 85.1–92.5

B 0.2–3.5

C 2.6–7.0

2. There is a possibility of alloying the Fe-Mn-C-B system with virtually any elements in the periodic table over a wide range of their concentrations.
3. By selection of chosen alloying elements, such as Si, Ni, Cr, it is possible to produce alloys with diverse physico-mechanical properties as a result of selection of various alloying components.
4. Based on the examinations of the Fe-Mn-C-B system according to four quasi-ternary intersections and micro-X-ray examinations, the following content of elements in eutectic areas was identified (Fig. 4.1; Tab. 4.7):
  - Fe-B-C eutectic, at manganese content of 1.6–7.6%: 85.1–92.5 Fe; 0.2–3.5 B; 2.6–7.0 C;
  - Fe-Mn-C eutectic, at boron content of 0.6–2.5%: 73.3–92.5 Fe; 3.1–23.8 Mn; 0.6–6.4 C.

In particular, the examinations of the Fe-Mn-C-B system after four quasi-ternary intersections: 'Fe<sub>2</sub>C'-Fe<sub>2</sub>B-'Fe<sub>2</sub>Mn', Fe<sub>3</sub>C-Fe<sub>3</sub>B-'Fe<sub>3</sub>Mn', Fe<sub>3</sub>C-Fe<sub>3</sub>B-'Fe<sub>1,2</sub>Mn', 'Fe<sub>23</sub>C'-Fe<sub>23</sub>B-'Fe<sub>23</sub>Mn' and the X-ray analysis of the samples annealed at 1270 K for 350 h would make it possible to conclude as follows:

- Based on the X-ray and metallographic examinations, it has been determined that there are two phase areas at all quasi-ternary intersections, which correspond to ternary Fe-Mn-C and Fe-B-C systems (Fig. 4.1): area I, Fe-B-C system: Fe<sub>3</sub>(C, B) + γ-(Fe, Mn) + α-(Fe, Mn); area II, Fe-Mn-C system: (Fe, Mn)<sub>23</sub>(C, B)<sub>6</sub> + γ-(Fe, Mn) + α-(Fe, Mn).
- The alloys of the Fe<sub>3</sub>C-Fe<sub>3</sub>B-'Fe<sub>1,2</sub>Mn' intersection at 0.667 at. parts of Fe contain no α-(Fe, Mn)-based phase. This phase was detected in alloys at intersections with increased iron content (0.75 atomic parts) only. It is the γ-(Fe, Mn) phase, which does not exist after quenching of samples from 1270 K.
- In eutectic alloys within the area of the highest iron content (0.79; 0.75 atomic parts), the (Fe, Mn)<sub>23</sub>(C, B)<sub>6</sub> + α-(Fe, Mn) + γ-(Fe, Mn), Fe<sub>3</sub>(C, B) + α-(Fe, Mn) + γ-(Fe, Mn) phases are in equilibrium. With the reduction in iron content [0.667 atomic parts (Fe<sub>3</sub>C-Fe<sub>3</sub>B-'Fe<sub>1,2</sub>Mn' intersection)], the transition from γ- into α-Fe does not occur and the (Fe, Mn)<sub>23</sub>(C, B)<sub>6</sub> + γ-(Fe, Mn), Fe<sub>3</sub>(C, B) + γ-(Fe, Mn) phases are in equilibrium.
- The eutectic areas in 'Fe<sub>2</sub>C'-Fe<sub>2</sub>B-'Fe<sub>2</sub>Mn', Fe<sub>3</sub>C-Fe<sub>3</sub>B-'Fe<sub>3</sub>Mn' and 'Fe<sub>23</sub>C'-Fe<sub>23</sub>B-'Fe<sub>23</sub>Mn' quasi-ternary intersections were found in two phase areas, at the Fe<sub>3</sub>C-Fe<sub>3</sub>B-'Fe<sub>1,2</sub>Mn' intersection – in area II (Fe-Mn-C eutectic). Generally, the Fe-B-C eutectic is formed in the area of increased carbon and boron contents, while the Fe-Mn-C eutectic is observed in the area of increased Mn content.

## REFERENCES

- [1]. Шурин А.К., *Квазибинарные и квазитройные эвтектические сплавы с тугоплавкими фазами внедрения*, Диссертация на соискание ученой степени доктора технических наук, К.: Институт металлофизики АН УССР, 1980.
- [2]. Барабаш О.М., Шурин А.К., *Фазовые равновесия в сплавах Mo-N-Ti, Mo-N-Zr и Mo-N-Hf*, Известия АН СССР. Металлы, 1978, № 4, с. 243–246.
- [3]. Барабаш О.М., Шурин А.К., *Фазовые равновесия в сплавах на основе ниобия с нитридами титана, циркония и гафния*, Металлофизика, К.: Наукова думка, 1978, вып. 71, с. 83–87.
- [4]. Шурин А.К., Дмитриева Г.П., *Современное состояние и перспективы развития исследований квазибинарных и квазитройных сплавов железа, никеля и кобальта с карбидами*, Диаграммы состояния карбид- и нитридсодержащих систем, К.: ИПМ АН УССР, 1981. с. 28–38.
- [5]. Дмитриева Г.П., Черепова Т.С., Шурин А.К., *Диаграммы плавкости тройных кобальт-карбидных систем*, Диаграммы состояния в материаловедении, К.: ИПМ АН Украины, 1991, с. 71–77.
- [6]. Шурин А.К., Дмитриева Г.П., Разумова Н.А., *Фазовые равновесия в тройных никель-карбидных сплавах*, Известия АН СССР. Металлы, 1988, № 6, с. 67–73.
- [7]. Дмитриева Г.П., Шурин А.К., *Диаграмма состояний квазитройной системы Fe-VC-NbC*, Порошковая металлургия, 1980, № 10, с. 48–51.
- [8]. Дмитриева Г.П., Разумова Н.А., Шурин А.К., Хандрос Э.Л., *Фазовые равновесия в сплавах систем Ni-TiC-MeC (Me: Zr, Hf, Nb, Ta)*, Известия АН СССР, Металлы, 1986, № 1, с. 206–211.
- [9]. Дмитриева Г.П., Черепова Т.С., Шурин А.К., *Сечение Co-TiC<sub>0,86</sub>-NbC<sub>0,9</sub> диаграммы состояния системы Co-Ti-Nb-C*, Порошковая металлургия, 1992, № 4, с. 78–82.
- [10]. Шурин А.К., Дмитриев Г.П., Черепова Т.С., *Фазовые равновесия в сплавах Co-Me'C-Me''C. Системы с трехфазным эвтектическим равновесием*, Порошковая металлургия, 1996, № 11/12, с. 44–51.
- [11]. Шурин А.К., *Фазовые равновесия в трехкомпонентных сплавах, содержащих элемент внедрения, и стабильность композиционных материалов*, Порошковая металлургия, 1973, № 1, с. 52–56.

- [12]. Шурин А.К., Дмитриев Г.П., *Фазовые равновесия в сплавах переходных металлов с тугоплавкими карбидами*, Металлофизика. К.: Наукова думка, 1974, № 53, с. 91–97.
- [13]. Шурин А.К., Панарин В.Е., *Некоторые общие закономерности тройных диаграмм состояний металлов с бором*, Металлофизика, К.: Наукова думка, 1976, № 66, с. 85–91.
- [14]. Барабаш О.М., Шурин А.К., *Термодинамическая оценка растворимости фаз внедрения в тугоплавких металлах*, Металлофизика, К.: Наукова думка, 1974, № 53, с. 101–103.
- [15]. Барабаш О.М., Шурин А.К., *Влияние легирования на растворимость элементов внедрения в ОЦК твердых растворах*, Известия АН СССР, Металлы, 1978, № 5, с. 195–203.
- [16]. Барабаш О.М., Шурин А.К., *Растворимость нитридов Ti, Zr и Hf в ванадии*, Известия АН СССР, Металлы, 1974, № 4, с. 194–197.
- [17]. Шурин А.К., Локтионо В.А., Дмитриев Г.П., *Растворимость кислорода в сплавах Nb-Zr*, Известия АН СССР, Металлы, 1970, № 1, с. 231–233.
- [18]. Шурин А.К., Барабаш О.М., Панарин В.Е., Легкая Т.Н., *Строение эвтектических псевдодвойных сплавов переходных металлов с фазами внедрения*, Известия АН СССР, Металлы, 1974, № 6, с. 183–187.
- [19]. Шурин А.К., Барабаш О.М., Дмитриев Г.П., Легкая Т.Н., др., *Образование ободков в эвтектических квазибинарных сплавах переходных металлов с фазами внедрения*, Металлофизика, К.: Наукова думка, 1975, № 59, с. 83–91.
- [20]. Шурин А.К., *Исследование фазовых равновесий и структуры сплавов с фазами внедрения для задач разработки материалов с композиционным упрочнением*, Фазовые равновесия в металлических сплавах, М.: Наука, 1981, с. 209–217.
- [21]. Шурин А.К., Дмитриев Г.П., Панарин В.Е., *Твердость квазибинарных эвтектических сплавов с фазами внедрения*, Металлофизика, К.: Наукова думка, 1979, № 76, с. 81–85.
- [22]. Барабаш О.М., Козырский Г.Я., Сульженко В.К., Шурин А.К., *Структура и прочность сплавов Nb-ZrN*, Известия АН СССР, Металлы, 1976, № 3, с. 200–225.
- [23]. Дмитриева Г.П., Шурин А.К., Васильев Д.А., *Строение и механические свойства сплавов железа с карбидом ванадия*, Металловедение и термическая обработка металлов, 1978, № 4, с. 64–66.

- [24]. Шурин А.К., *Жаропрочные эвтектические сплавы*, Жаропрочность и жаростойкость металлических материалов, М.: Наука, 1976, с. 64–70.
- [25]. Шурин А.К., *Диаграммы состав-свойство квазибинарных и квазитройных эвтектических систем с фазами внедрения*, Диаграммы состояния в материаловедении, К.: ИПМ АН УССР, 1980, с. 59–67.
- [26]. Тихонович В.И., Шурин А.К., Локтионов В.А., Панарин В.Е., *Исследование строения и износостойкости сплавов железа с диборидом титана*, Литые износостойкие материалы, К.: Институт проблем литья АН УССР, 1972, с. 70–75.
- [27]. Локтионов В.А., Панарин В.Е., Тихонович В.И., Шурин А.К., *Исследование строения и износостойкости сплавов на основе стали X18H9T с диборидом титана*, Проблемы трения и изнашивания, К.: Техника, 1974, № 5, с. 82–85.
- [28]. Шурин А.К., Панарин В.Е., Киндрачук М.В., *Износостойкость нержавеющей эвтектических сплавов с фазами внедрения*, Проблемы трения и изнашивания, К.: Техника, 1981, с. 65–73.
- [29]. Шурин А.К., Панарин В.Е., *Диаграммы состояния железа с фазами внедрения как основа разработки износостойких эвтектических сталей*, Металловедение и термическая обработка металлов, 1984, № 2, с. 55–57.
- [30]. Шурин А.К., *Получение и обработка эвтектических сталей и сплавов с повышенными эксплуатационными характеристиками*, Новые процессы термической обработки сталей и сплавов, К.: Общество «Знание» УССР, 1975, с. 18–19.
- [31]. Панарин В.Е., Шурин А.К., *Эвтектические стали для износостойких порошковых покрытий*, Исследование и разработка теоретических проблем в области порошковой металлургии и защитных покрытий. Материалы Всесоюзной конференции, Минск, 1984, Ч. 3, Принципы оптимизации структуры и свойств порошковых материалов и защитных покрытий, Минск: БелНИИНТИ, 1984, с. 170–175.
- [32]. Шурин А.К., Панарин В.Е., Киндрачук М.В., Голего Н.Н., *Износостойкие наплавки эвтектическими сплавами на основе железа*, Защитные покрытия, К.: Наукова думка, 1983, вып. 17, с. 40–43.
- [33]. Шурин А.К., Панарин В.Е., *Повышение абразивной стойкости стали 120Г13*, Металловедение и термическая обработка металлов, 1985, № 6, с. 57–59.

- [34]. Шурин А.К., Панарин В.Е., Назаренко П.В., Макаркин А.Н., *Износостойкость эвтектических сталей при трении в среде газообразного водорода*, Работоспособность конструкционных металлических материалов в среде водорода, Препринт, № 33, Львов: Физико-механический институт АН УССР, 1980.
- [35]. Назаренко П.В., Макаркин А.Н., Шурин А.К., Панарин В.Е., *Исследование износостойкости композиционных сплавов на основе железа при трении в среде газообразного водорода*, Трение и износ, 1982, т. 3, № 3, с. 495–500.
- [36]. Таран Ю.Н., Мирошниченко И.С., *О трех типах эвтектических структур*, Рост и дефекты металлических кристаллов, К.: Наукова думка, 1972.
- [37]. Крагельский И.В., *Трение и износ*, М.: Машиностроение, 1968.
- [38]. Костецкий Б.И., *Трение, смазка и износ в машинах*, К.: Техника, 1970.
- [39]. Бершадский Л.И., *Структурная термодинамика трибосистем*, Киев, Знание, УССР, 1990.
- [40]. Костецкий Б.И., Натансон М.Э., Бершадский Л.И., *Механо-химические процессы при граничном трении*, М.: Наука, 1972.
- [41]. Марцевой Е.П., Гринченко Н.Н., Пащенко В.Н., *Газовоздушный плазменный факел – рабочая среда для напыления*, Теплотехнические вопросы применения низкотемпературной плазмы в металлургии, Магнитогорск, 1989, с. 28–32.
- [42]. Хасуй А., *Техника напыления*, Пер. с япон., М.: Машиностроение, 1975.
- [43]. Хороших В.М., *Катодный узел электродугового источника плазмы*, Вопросы атомной науки и техники, Сер.: Вакуум, чистые материалы, сверхпроводники, 1999, Вып. 2 (10), с. 6–9.
- [44]. Кудинов В.В., Пекшев П.Ю., Белашенко В.Е., *Нанесение покрытий плазмой*, О.П. Солоненко и др., М.: Наука, 1990.
- [45]. Бартенев С.С., Федько Ю.П., Григоров А.И., *Детонационные покрытия в машиностроении*, Л.: Машиностроение, Ленинградское отделение, 1982.
- [46]. Kaban I., Hoyer W., Il'inskii A., Slusarenko S., Slukhovskii O., *Short-range order in liquid silver-tin alloys*, J. Non-Cryst. Solids, 2003, No. 9, p. 1–9.

- [47]. Эванс Р., и Гринвуд Д., *Жидкие металлы*: Пер. с англ., М.: Металлургия, 1980.
- [48]. Мирошниченко И.С., *Кристаллизация сплавов эвтектического типа при больших скоростях охлаждения*, Кристаллизация и фазовые переходы, Минск.: Изд. АН БССР, 1962, с. 133–145.
- [49]. Мирошниченко И.С. *Закалка из жидкого состояния*, М.: Металлургия, 1982.
- [50]. Stauffer R.N., *Amorphous Metals Noncrystalline Metals Offer Unique Properties*, *Manuf. Eng.*, 1981, V. 87, No. 1, p. 63–71.
- [51]. Ishimaru Y., *Fundamentals and Applications of Powder Metallurgy*, Tokyo: Gijutsu Shoin Co., Ltd., 1993.
- [52]. Разработка технологии получения порошков эвтектических сплавов с повышенной износостойкостью: Отчет о НИР (окончательный)/ НИИ НПО «Тулачермет». Шифр: -14А.30-16-80/П-4-а-ПП. Г. Тула, 1981.
- [53]. Новиков И.И., *Теория термической обработки металлов*, М.: Металлургия, 1986.
- [54]. Марукович Е.И., Карпенко В.М., Карпенко М.И., *Композиционное упрочнение и легирование литых износостойких деталей и инструментов из железоуглеродистых сплавов*, Упрочняющие технологии и покрытия, 2005, № 12, с. 17–23.
- [55]. Mark R., *Introduction to Materials Science and Engineering. Rev.*, De Duire, EMSE 201, 1998. Vol. 3, No. 3. p. 111–117.
- [56]. Конева Н.А., *Физика прочности металлов и сплавов*, Соросовский образовательный журнал, Физика, 1997, №7, с. 95–102.
- [57]. Takao K., Kohji K., *The Adhesive Transfer of the Slip-tongue and the Wege*, ASLI Trans., 1981, Vol. 24, No. 2, p. 164–174.
- [58]. Носкова Н.И., Павлов В.А., Брегман Т.П. и др., *Разрушение при трении и дислокационная структура твердых растворов системы золото-платина*, Физика металлов и металловедение, 1983, Т. 55, Вып. 3, с. 583–591.
- [59]. Гарбер И.И., *Кинетика развития дислокационной структуры меди в процессе трения*, Трение и износ, 1982, Т. 35, №5, с. 880–888.
- [60]. Крагельский И.В., Алексеев Н.М., Рыбакова Л.М., Назаров А.М., *Влияние степени упрочнения материалов в процессах трения на их стойкость против задира*, Машиноведение, 1977, № 6, с. 88–94.

- [61]. Сорокин Г.М., *Трибология сталей и сплавов*, М.: Недра, 2000.
- [62]. Suh N.P., Sin H.C., *On the Genesis of Friction and its Effect on Wear, Solid Contact and Lubrication*. Presented at the Winter Annual Meeting of ASME, Chicago, Nov. 1980, Vol. 16–21, p. 167–183.
- [63]. Виноградов В.Г., Подольский Ю.А., *Механизм противоизносного и антифрикционного действия смазочных сред при тяжелых режимах граничного трения*, Тр. Всесоюзной конф. «Симпозиум о природе трения твердых тел», Минск.: Наука и техника, 1969, с. 30–32.
- [64]. Костановский А.В., *Переплавление поверхностного слоя керамики из AlN под действием лазерного излучения*, Теплофизика высоких температур, 1994, Т. 32, № 5, с. 742–748.
- [65]. Коваленко В.С. и др., *Технология лазерной обработки*, Казань, 1999.
- [66]. Новиков В.М., Змиевской Г.Н., *Лазерная и оптическая техника и технология*, Учебное пособие, Курск, 1997.
- [67]. Шмырева Т.П., Береза Е.Ю., *Быстроохлажденные эвтектические сплавы*, К.: Техника, 1990.
- [68]. Лахтин Ю.М., *Металловедение и термическая обработка металлов*, М.: Металлургия, 1993.
- [69]. Коваленко В.С., Головкин Л.Ф., Чернетко В.С., *Упрочнение и легирование деталей машин лучем лазера*, Киев.: Техника, 1990.
- [70]. Новиков В.В. и др., *Модификация и упрочнение трущихся поверхностей лазерной обработкой*, Иваново, 2000.
- [71]. Рыжкин А.А., *Поверхностное лазерное упрочнение режущего инструмента*, Ростов-н/Д, 1999.
- [72]. Трегубов Н.Г., Соколов Б.К., Варбанов Г.П., и др., *Лазерные технологии на машиностроительном заводе*, Уфа, 1993.
- [73]. Вильский Г.Б., *Технология и оборудование обработки металлов концентрированными потоками энергии*, Ленинград, 1991.
- [74]. Кіндрачук М.В., Черненко В.С., Дудка О.І., *Променеві методи обробки: навчальний посібник*, К.: Кондор, 2004.
- [75]. Кіндрачук М.В., Панарин В.Е., Микуляк О.В., *Использование высококонцентрированных источников энергии для повышения триботехнических свойств эвтектических покрытий*, Кн.: Защитные покрытия на металлах, К.: Наукова думка, 1993, Вып. 27, с. 50–54.

- [76]. Киндрачук М.В., Корнеев В.Г., Мелентев О.П., Панарин В.Е., *Порошковый материал для износостойких покрытий*, А.с. № 1050179 СССР, № 3411077/27 Заявл, 05.03.1982; Опубл, в БИ 1983.
- [77]. Киндрачук М.В., Голубец М.В., Пашечко М.И., *Технологические основы нанесения и свойства эвтектических покрытий, получаемых из порошковых смесей методом центробежной биметаллизации*, Физико-химическая механика материалов, 1984, № 3, с. 96–98.
- [78]. Киндрачук М.В., Куницький Ю.А., Дудка О.І., Сухенко Ю.Г., Коржик М.В., *Структуроутворення та формування триботехнічних властивостей евтектичних покриттів*, К.: Вища шк, 1997.
- [79]. Киндрачук М.В., Лабунець В.Ф., Пашечко М.І., Корбут Є.В., *Трибологія: підручник*, Київ, видавництво Національного авіаційного університету “НАУ-друк”, 2009.
- [80]. Киндрачук М.В., Панарин В.Е., Микуляк О.В., Бондарь А.И., *Газотермические покрытия из эвтектических сплавов на основе железа с ультрадисперсной структурой*, Защитные покрытия, К.: Наукова думка, 1988, Вып. 22, с. 26–30.
- [81]. Киндрачук М.В., Панасюк О.Я., *Формування евтектичних покриттів різного функціонального призначення*, Проблеми металознавства та обробки легованих сталей: Матеріали наук.-техн. Семінару, К.: ІПЛ НАНУ, 1994, с. 9–10.
- [82]. Киндрачук М.В. Вплив структури евтектичних плазмових покриттів на їхні триботехнічні властивості в широкому діапазоні температур, Фізико-хімічна механіка матеріалів, 1994, № 4, с. 66–71.
- [83]. Киндрачук М.В., *Влияние лазерной обработки и термоциклирования на триботехнические характеристики эвтектических плазменных покрытий на основе никеля*, Защитные покрытия на металлах, К.: Наукова думка, Вып. 28, 1994, с. 34–39.
- [84]. Киндрачук М.В., Панарин В.Є., Москаленко Ю.Н., *Вплив термоциклічної обробки на структуру і властивості плазмових покриттів із евтектичних сплавів на основі заліза*, Металознавство та обробка металів, К.: 1995, № 1, с. 38–45.
- [85]. Киндрачук М.В., Душек Ю.Я., Лучка М.В., *Аналитическое исследование напряжен-но-деформированного состояния композиционного материала, нагруженного силами трения*, Порошковая металлургия, 1994, № 9–10, с. 56–61.

- [86]. Панарін В.С., Кіндрачук М.В., Джамаль І.М., *Використання метастабільних станів у формуванні властивостей зносостійких евтектичних сплавів на основі заліза*, *Металознавства та обробка металів*, 2006, № 3, с. 19–25.
- [87]. Кіндрачук М.В., *Применение лазерного легирования и термоциклирования для получения износостойких боридных покрытий*, *Защитные покрытия на металлах*, К.: Наукова думка, 1994, Вып. 28, с. 37–40.
- [88]. Кіндрачук М.В., *Підвищення експлуатаційних властивостей сталей тормоциклюванням в процесі лазерного легування бором*, *Металознавство та обробка металів*, К.: 1995, № 2, с. 51–53.
- [89]. Кіндрачук М.В., Чернега С.М., Дудка О.І., *Вплив структури на закономірності кавітаційного зношування евтектичних покриттів*, *Фізико-хімічна механіка матеріалів*, 1998, № 2, с. 69–74.
- [90]. Лобода П.І., Онисько Є.А., *Дослідження процесу росту зерна порошкового матеріалу при спіканні в полі температурного градієнта*, *Металознавство та обробка металів*, 2001, № 3, с. 87–92.
- [91]. Dobrzański L.A., *Basics of Material Science Metal Science*, Warsaw: WNT, 2002.
- [92]. Lenik K., Pashechko M., *Development of a new family of wear-resistant eutectic alloys*, In: Works of the Institute of Machine Design and Operation, No 87, The 35th Tribology School, No 27, Publishing House of the Wrocław University of Technology, 2002, p. 196–201.
- [93]. Lenik K., editor., *Anti-wear Eutectic Coatings of the Fe-Mn-C-B System*, Lviv: The National Academy of Science of Ukraine, Institute on Problems of Materials Science, Euro World, 2004.
- [94]. Lenik K., Paszczko M., Paszczko L., *Wear resistance eutectic composite coatings of system Fe-Mn-C-B-Si*, *Problems of Tribology*, 2001, No 3, p. 61–64.
- [95]. Jarzyna W., Augustyniak H., Bocheński H., *Active Piezoelectric Structures in Control Systems*, *Przegląd Elektrochemiczny*, 2010, No 86(4), p. 252–255.
- [96]. Paszczko M., Lenik K., Paszczko L., *Increased durability of machine parts by plasma deposition using eutectic alloys of Fe-Mn-C-B*, In: II Międzynarodowa N-T Konferencja Nowe technologie, metody obróbki i uпрочnienia detali energetycznych установок, 23–28 Sierpnia 2002, Zaporozje-Ałushta, Zaporoski Państwowy Instytut 2002, p. 77–78.

- [97]. Paszczko M., Lenik K., Szewczuk J., *Pidwyszczennia znosostijkosti dyska kopacza korenezbyralnoji maszyny KS-6B nanesenniam ewtektycznych kompozycyjnych pokryttyw systemy Fe-Mn-C-B-Si-Cr*, Problems of Tribology, 2003, No 2, p. 154–157.
- [98]. Pashechko M., Gorecki T., *Surface layer models and self-organisation of the surface with abrasive wear*, In: Zagadnienia dydaktyczne w środowisku systemów technologicznych, Lublin, LTN, 2003, p. 157–162.
- [99]. Paszczko M., Lenik K., Paszczko L., *Pidwyszczennia dowhowiczności detalej maszynymetodom plazmowego naplawlennia z wykorzystanniam ewtektycznych splawiw systemy Fe-Mn-C-B*, Westnik Dwigatelestrojenija, 2002, No 1, p. 127–131.
- [100]. Paszczko M., Popławskij O., *Influence of surface atoms segregation on tribological properties of alloys*, Problems of Tribology, 2001, No 4, p. 115–125.
- [101]. Malec M., Lenik K., Pashechko M., *The possibilities of increasing the lifetime of tools by using modified surface layer*, In: The 7th National Conference on Tool Problems in Plastic Working, Bydgoszcz, 2001, p. 87–93.
- [102]. Pashechko M., Lenik K., *Segregation of atoms of the eutectic alloys Fe-Mn-C-B-Si-Ni-Cr at friction wear*, Wear, No 267 (2009), p. 1301–1304.
- [103]. Pashechko M., Dziedzic K., Barszcz M., *Study of the structure and properties of wear-resistant eutectic Fe-Mn-C-B-Si-Ni-Cr coatings*, Powder Metallurgy and Metal Ceramics, November 2013, Volume 52, Issue 7–8, p. 469–476.
- [104]. Pashechko M., *Wear resistance of eutectic coatings of the Fe-Mn-C-B system alloyed with Si, Ni and Cr*, Materials Science, 2011, Vol. 46, No 5, p. 695–701.
- [105]. Pashechko M., Dziedzic K., Barszcz M., *Study of coatings obtained from alloy Fe-Mn-C-B-Si-Ni-Cr*, Advances in Science and Technology Research Journal, Vol. 10, No 31, 2016, p. 194–198.
- [106]. Pashechko M., Montusiewicz J., *Evaluation of the wear resistance of eutectic coatings of the Fe-Mn-C-B system alloyed by Si, Ni and Cr using multi-criteria analysis*, Materials Science, 2012, Vol. 47, No 6, p. 813–821.
- [107]. Pashechko M., Kindrachuk M., Radionenko O., *The mechanism of friction between surfaces with regular microgrooves under boundary lubrication*,

- [108]. Barszcz M., Paszeczko M., Lenik K., *Self-organization of friction surface of Fe-Mn-C-B coating with increased resistance to abrasion*, Arch. Metall. Mater. 2015, 60, p. 2651–2656.
- [109]. Paszeczko M., Lenik K., Dziedzic K., Barszcz M., *Investigation of changing of chemical and phase composition of the friction surfaces Fe-Mn-C-B-Si-Ni-Cr coating depend on depth*, W: 2nd International Conference on Advanced Functional Materials (ICAFM 2017), Los Angeles, 4-6 August 2017 : conference program – 2017
- [110]. Paszeczko M., *Tribological Behaviour of eutectic coatings obtained by gas metal ARC welding method with use of FE-Mn-C-B-Si-Ni-Cr wire powder*, W: 2nd International Conference on Sustainable Materials Science and Technology (SMST2), 19–21 July 2017.
- [111]. Paszeczko M., Lenik K., Szulżyk-Cieplak J., Duda A., *Powder eutectic materials of Fe-Mn-C-B system for coatings of increased abrasive wear*, W: Powder metallurgy – fundamentals and case studies; [Red:] Dobrzański Leszek A. Rijeka: InTech, 2017, p. 331–348.
- [112]. Paszeczko M., Dziedzic K., Mendyk E., *Study of friction surface Fe-Mn-C-B-Si-Ni-Cr coatings*, W: International Conference Sustainable Materials Science and Technology, 15–17 July 2015, Paris-France: Abstracts Book, 2015, p. 57–57.
- [113]. Paszeczko M., Dziedzic K., Mendyk E., Sobieszek A., *XPS investigation of secondary structures on friction surface Fe-Mn-C-B-Si-Ni-Cr coatings*, W: 4th Nano Today Conference, 6–10.12.2015, Dubaj 2015.
- [114]. Barszcz M., *Wpływ samoorganizacji powierzchni podczas tarcia powłok ze stopu eutektycznego Fe-Mn-C-B na trwałość wybranych elementów maszyn*, rozprawa doktorska, promotor Paszeczko M., Politechnika Lubelska, 2015.
- [115]. Dziedzic K., *Badania struktur wtórnych powstających podczas zużycia ciernego powłok ze stopu eutektycznego Fe-Mn-C-B*, rozprawa doktorska, promotor Paszeczko M., Politechnika Lubelska, 2013.
- [116]. Paszeczko M., Dziedzic K., Mendyk E., Józwiak J., *Chemical and phase composition of the friction surfaces Fe-Mn-C-B-Si-Ni-Cr hardfacing coatings*, journal of tribology-transactions of the asme, 2018, No. 2, Vol. 140.



## Abstract

In this work we propose a new view to natural composite materials – multicomponent eutectic alloys, which may be used for broad variety of applications – manufacturing and recovery of turbine blades, stator vanes, metallurgical furnaces, quick closing equipment, cutting tools etc. These wear resistant materials may be used for manufacturing or modification of heavy duty components, so significant part of current work is devoted to overview and development of efficient coating deposition technologies – plasma and gas spray, laser alloying and surface engineering. We also evaluate the effects of deposition processes parameters on microstructures, mechanical properties and wear resistance of coatings being investigated.

## Streszczenie

W monografii autorzy proponują nowe spojrzenie na materiały kompozytowe – wieloskładnikowe stopy eutektyczne, które mogą być wykorzystywane do różnorodnych zastosowań – produkcja i regeneracja łopatek turbinowych, łopatek stojanów, pieców metalurgicznych, narzędzi skrawających, itp. Te odporne na zużycie materiały mogą być używane do produkcji lub modyfikacji ciężkich komponentów, tak więc znaczna część pracy jest poświęcona przeglądowi i rozwojowi wydajnych technologii nakładania powłok – natryskiwanie plazmowe i gazowe, stopowanie laserowe i zagadnieniom inżynierii powierzchni. Oceniono również wpływ parametrów procesów osadzania na mikrostrukturę, właściwości mechaniczne i odporność na zużycie badanych powłok.

ISBN: 978-83-7947-292-5



9 788379 472925